THE UNIVERSITY
of EDINBURGH

CELL THERAPY FOR

CHRONIC LIVER DISEASE

James A Thomas

Submitted for the degree:
Doctor of Philosophy
University of Edinburgh, 2015

Declaration

This thesis has been composed by myself; work that is the outcome of collaboration is specifically indicated.

The data included in this text have not been submitted for any other degree or qualification.

This thesis does not exceed the word limit of 100 000 words set by the College of Medicine and Veterinary Medicine.

Signed: 

Date: 05/10/2015

Abstract

There is a growing literature of clinical studies of bone marrow (BM) cell therapy for liver cirrhosis. At present, the optimum choice of cell type(s) and the mechanism(s) of effect remain undefined. Cells of the monocyte-macrophage lineage have key roles in the development and resolution of liver fibrosis. Therefore, I tested the therapeutic effects of these cells in the context of experimental murine liver fibrosis.

The effects of unmanipulated, syngeneic macrophages, their specific BM precursors and unfractionated (whole) BM cells were examined in the iterative carbon tetrachloride model of liver fibrosis. BM-derived macrophage (BMM) delivery resulted in early chemokine upregulation with the hepatic recruitment of endogenous macrophages and neutrophils. These cells delivered matrix metalloproteinases-13 and -9 respectively, into the hepatic scar. The effector cell infiltrate was accompanied by increased levels of the anti-inflammatory cytokine IL-10. A reduction in hepatic myofibroblasts was followed by reduced fibrosis detected 4 weeks after macrophage infusion. Serum albumin levels were elevated at this time. Upregulation of the liver progenitor cell mitogen TWEAK preceded expansion of the progenitor cell compartment. BMM delivery increased hepatic expression of cytokines with reparative effects (including colony stimulating factor-1, insulin-like growth factor-1 and vascular endothelial growth factor). In contrast to the effects of differentiated macrophages, liver fibrosis was not significantly improved by the application of macrophage precursors and was exacerbated by whole BM. BMMs did not affect liver fibrosis or regeneration in the 1% DDC model of biliary disease.

These effects were only detected following the intraportal delivery of BM cells. The peripheral (tail) vein administration of BMMs, either singly or repeatedly did not recapitulate the therapeutic phenotype. This was investigated by *in vivo* tracking of BMMs constitutively expressing green fluorescent protein (GFP). The peripheral administration route resulted in the early (1 hour) accumulation of BMMs within the

pulmonary system. This was followed by delayed hepatic engraftment, which was also numerically reduced (<30%) compared with intraportal administration.

Macrophage cell therapy improves clinically relevant parameters in experimental chronic liver injury. Paracrine signalling to endogenous cells amplifies the effect. The benefits from this single, defined cell type suggest clinical potential.

Lay Summary

Chronic liver disease is a major global cause of ill health and death. Unfortunately, effective and safe treatment is not available for many of these patients. Experimental reports have suggested that injecting patients with cells derived from the bone marrow (BM) could improve the most advanced stage of chronic liver disease (termed cirrhosis). Clinical studies have already begun, however, there is limited understanding of the best type(s) of BM derived cell to use and how these cells may help in cirrhosis. Studies in animal models provide an opportunity to determine these factors.

Macrophages are a type of white blood cell (leucocyte) that originates from the BM. These cells have previously been shown to have important roles in liver scarring and healing. The effects of macrophages and also their BM parent cells were tested in the carbon tetrachloride (CCl_4) model of mouse chronic liver disease. CCl_4 causes injury to the bulk of the liver's cells and has similarities with the most common human chronic liver diseases.

The direct injection of donor macrophages into the portal vein that leads directly into the liver was soon followed by the homing of many more of the recipient's own leucocytes from their blood system into the injured liver. Increased amounts of liver proteins that reduce inflammation and promote healing were also detected. The recipient leucocytes that had been recruited into the liver made significant amounts of key scar degrading enzymes. There followed a reduction in liver scarring with improved regeneration. Macrophages, but not their BM parent cells, caused these effects.

Interestingly, injecting macrophages into a peripheral vein that is easily accessed through the skin rather than a deep vein that leads directly to the liver did not lead to the same improvements in liver scarring and regeneration. The peripheral injection

of macrophages resulted in many getting trapped in the lung circulation before arriving at the liver with significantly fewer lodged in the liver in the first 24 hours. These findings suggest that macrophage cell therapy may have potential as a treatment for patients with chronic liver disease.

Acknowledgements

Thanks to Professors Stuart Forbes and John Iredale for their support, enthusiasm and supervision. I would also like to express gratitude to all members of the lab past and present in particular to Davina Wojtacha.

Thank you also to members of the University of Edinburgh Centres for Inflammation Research (Spike Clay, Fiona Rossi), Regenerative Medicine (Kay Samuel, Martin Waterfall) and Reproductive Medicine (Forbes Howie) who helped with this work in particular the Histology Service and Animal Facility technicians.

I would also like to thank the Sir Jules Thorn Trust for funding this project.

Table of Contents

Tables and Figures

List of abbreviations

α-SMA	alpha smooth muscle actin
ALT	alanine aminotransferase
BDL	bile duct ligation
BM	bone marrow
BMM	bone marrow derived macrophage
CCl_4	carbon tetrachloride
CDE	choline deficient ethionine supplemented
cDNA	complementary DNA
CK	cytokeratin
C-P score	Child-Pugh score
CSF-1	colony stimulating factor-1
DAB	diaminobenzidine
DAPI	4',6-diamidino-2-phenylindole
DDC	Diethyl 1, 4-dihydro-2,4,6-trimethyl-3,5-pyridinedicarboxylate
Dlk	delta like kinase
DMEM	Dulbecco's Modified Eagle Medium
DTR	diptheria toxin receptor
ECM	extracellular matrix
EGFP	enhanced green fluorescent protein
FACS	fluorescence-activated cell sorting

Fn14	fibroblast growth factor-inducible 14
FISH	fluorescent in situ hybridization
G-CSF	granulocyte-colony stimulating factor
GM-CSF	granulocyte-macrophage colony stimulating factor
GFP	enhanced green fluorescent protein
HCC	hepatocellular carcinoma
HGF	hepatocyte growth factor
HPV	hepatic portal vein
HSC	haematopoietic stem cell
IGF-1	insulin-like growth factor 1
IL	interleukin
IP	intraperitoneal
IV	intravenous
LPC	liver progenitor cell
MELD	model for end-stage liver disease
M-CSF	macrophage colony stimulating factor
MCP-1	macrophage chemoattractant protein-1
MIP	macrophage inflammatory protein
MMP	matrix metalloproteinase
MNC	mononuclear cell
NOS	nitric oxide synthase
PBC	primary biliary cirrhosis
PBS	phosphate buffered saline

PCK	pancytokeratin
PSC	primary sclerosing cholangitis
PSR	picrosirius red
PT	prothrombin time
SAM	scar associated macrophage
SC	subcutaneous
TV	tail vein
TNF	tumour necrosis factor
TWEAK	tumour necrosis factor-like weak inducer of apoptosis
VEGF	vascular endothelial growth factor

CHAPTER ONE

Introduction

In the United Kingdom, liver disease is currently the fifth most common cause of death. There was a 25% increase in deaths due to liver disease between 2001 and 2009. In contrast, the incidences for the top four causes of mortality are not rising. Over 90% of people who die from liver disease are under 70 years of age. (http://www.statistics.gov.uk/) This therefore represents a significant and growing burden on society in terms of health, productivity and resource demand. Cirrhosis is the most prevalent form of severe liver disease. End stage liver disease with its accompanying complications of liver failure, portal hypertension and hepatocellular carcinoma is the most frequent indication for liver transplantation. There are insufficient donor livers available to cope with the demand. Furthermore, liver transplantation with its attendant mortality and morbidity including the requirement for lifelong immunosuppression is not appropriate for many cirrhotic patients. There is therefore, an urgent need for novel therapies to reduce both the morbidity and mortality from cirrhosis.

Liver fibrosis and ultimately cirrhosis is almost invariably the final common pathway of chronic hepatic injury. Worldwide, chronic viral hepatitis, alcohol excess and non-alcoholic steatohepatitis associated with the metabolic syndrome account for the majority of chronic liver disease. In addition, autoimmune and inherited metabolic aetiologies also contribute to the development of cirrhosis. Specific management of the cause (e.g. antiviral therapy, cessation of alcohol) can limit further tissue damage. The natural history of cirrhosis is relatively slow, usually being measured in years. Given the considerable physiological reserve of the liver, the disease process is typically clinically silent until the advanced stages. Therefore, despite improvements in public health and the screening and treatment of liver diseases, presentation with late stage disease is common. The asymptomatic phase of cirrhosis is considered "compensated". Ongoing damage can eventually result in the clinical manifestations of portal hypertension and liver dysfunction. This "decompensated" phase is characterised by the development of ascites, gastrointestinal bleeding, jaundice and encephalopathy in addition to an increased risk of developing liver cancer.

Longitudinal data indicate that this progression from compensated to decompensated disease is associated with a significant increase in mortality (D'Amico, Garcia-Tsao et al. 2006). Scoring systems such as the Child-Pugh (C-P) score and model for end-stage liver disease (MELD) are used in routine clinical practice and correlate with increasing disease severity and worse outcomes. When assessing the potential utility of novel therapies for cirrhosis, it is important to consider the intrinsically linked processes of liver fibrosis and regeneration in this clinical context.

Liver fibrosis

In the healthy uninjured liver, the production of extracellular matrix (ECM) is balanced by its degradation. Chronic inflammation virtually regardless of aetiology, disrupts this homeostasis effectively resulting in an aberrant wound healing response (Iredale 2007). Damage to hepatocytes and non-parenchymal liver cells (e.g. cholangiocytes and endothelial cells) causes the release of inflammatory factors which interact with a number of cell types including hepatic stellate cells, macrophages and fibroblasts to promote extracellular matrix (ECM) deposition. It is now clear that liver fibrosis is a bi-directional process. Significant resolution of fibrosis is possible in both humans and experimental models. Hepatic stellate cells and macrophages are important mediators of fibrosis regression and therefore represent potential targets for anti-fibrotic therapies.

Extracellular matrix during fibrogenesis

The predominant components of ECM in the normal liver are collagens type I, III, IV, V and VI and glycoproteins such as fibronectin and laminin (Iredale, Thompson et al. 2013). With chronic injury, this is progressively replaced by fibrillar collagen (particularly type I), laminin, proteoglycans and ultimately elastin (Friedman 1993; Pellicoro, Aucott et al. 2012). Histologically, there is capillarisation of the hepatic

sinusoids which has direct effects on hepatocyte function. Subsequently, fibrosis develops within the parenchyma itself. The anatomical distribution may reflect the initial pattern of inflammation e.g. pericentral inflammation and then fibrosis in alcoholic liver disease in contrast to the periportal distribution in chronic viral hepatitis and chronic cholestatic disease (Friedman 1993). With continued injury, vascular structures become linked by scar tissue. Eventually this architectural disruption contributes to the clinical manifestation of portal hypertension. The chronically compromised hepatocytes and non-parenchymal cells situated in the fibrotic liver are unable to execute fully their physiological roles resulting in the clinical features of liver failure. Though incompletely understood, insights into the propensity for tumorigenesis in the cirrhotic liver highlight the biochemical and mechanical effects of fibrosis in conjunction with inflammatory and regenerative mediators promoting genome instability (Zhang and Friedman 2012).

Cellular mediators of fibrosis

Hepatic myofibroblasts are the major source of ECM in injury (Gabele, Brenner et al. 2003). Myofibroblasts may derive from a number of cell populations including fibrocytes (Kisseleva, Uchinami et al. 2006), portal myofibroblasts (Kinnman and Housset 2002) and mesenchymal stem cells (MSCs) (Russo, Alison et al. 2006). However, the main functional source is considered to be via transdifferentiation of hepatic stellate cells (Maher and McGuire 1990; Wells, Kruglov et al. 2004). In the normal liver, quiescent hepatic stellate cells reside in the sub-endothelial Space of Disse. These mesenchymal cells are rich in retinoid and lipid. Injurious stimuli converge on the stellate cell triggering a switch to a myofibroblastic phenotype. This process is modelled by culturing hepatic stellate cells on tissue culture plastic which has allowed a detailed understanding of the signalling processes involved in this activation (Friedman, Rockey et al. 1992). The myofibroblastic phenotype is characterised by the synthesis of α-smooth muscle actin (α-SMA) and collagen. There is accompanying expression of factors that regulate ECM turnover (such as matrix

metalloproteinases (MMPs) and their tissue inhibitors (TIMPs)) as well as vascular reactivity (Friedman, Roll et al. 1985; Rockey 2001). Inflammatory cytokines such as TGF-β (Gressner, Weiskirchen et al. 2002) and PDGF (Pinzani, Gesualdo et al. 1989) promote collagen I expression and proliferation (respectively) of stellate cells. Thus inflammation is critical for the initiation and propagation of scar deposition (Iredale 2007).

Liver macrophages, also known as "Kupffer cells", are largely replenished by monocytes derived from the BM (Klein, Cornejo et al. 2007). Cells from the monocyte-macrophage lineage have key roles in fibrogenesis. Duffield and colleagues used the transgenic diphtheria toxin receptor (DTR) model to achieve the selective ablation of mouse macrophages. The depletion of macrophages during liver injury resulted in less fibrosis indicating that macrophages are important for the generation of liver fibrosis during this inflammatory phase (Duffield, Forbes et al. 2005). Subsequent work by Karlmark and colleagues identified the inflammatory Ly-6C^{hi} monocyte subset as having pro-fibrotic effects, potentially mediated by hepatic stellate cell activation (Karlmark, Weiskirchen et al. 2009).

Molecular mediators of fibrosis

The MMP family of proteins are zinc-dependent proteolytic enzymes that are conventionally categorised according to their main substrate. The degradation of fibrillar collagen by collagenases (such as MMP-13 and MMP-8) results in gelatin products which in turn are cleaved by gelatinases A (MMP-2) and B (MMP-9). The gelatinases are relatively promiscuous in terms of their substrate specificity; in addition to their action on gelatins, there is also collagenase (MMP-2) and elastase (MMPs-2 and -9) activity. Whilst MMPs are responsible for the degradation of ECM constituents, they also play a role in fibrogenesis by contributing to ECM remodelling thereby facilitating scar deposition. MMP-12 (macrophage

metalloelastase) mediates elastin degradation which has been shown to occur even during long term fibrogenesis (Pellicoro, Aucott et al. 2012). Hepatic stellate cells secrete MMP-13 resulting in the local destruction of surrounding ECM with liberation of pro-fibrogenic cytokines such as TGF-β.(Yang, Zeisberg et al. 2003) MMP-2 is expressed by hepatic stellate cells and is an autocrine proliferation and migration factor (Benyon, Hovell et al. 1999). The tissue inhibitors of MMP (TIMPs) are a family of proteins which bind MMPs. Formation of these complexes therefore renders the MMPs physically unavailable to contribute to ECM degradation. Upregulation of myofibroblast derived TIMP-1 disturbs this balance during liver fibrogenesis resulting in net scar deposition (Iredale 1997).

Liver fibrolysis

Liver fibrosis has a reversible component that may become apparent when the injurious stimulus is removed. This is now a well-recognised clinical phenomenon; for example, abstinence in patients with cirrhosis due to alcohol can result in considerable hepatic recompensation and successful antiviral therapy for patients with hepatitis B or C is associated with significant regression of fibrosis (Poynard, McHutchison et al. 2002; Dienstag, Goldin et al. 2003). The mechanisms underlying these effects have been examined in rodent models.

The recovery phase from fibrosis that occurs after injury is accompanied by myofibroblast apoptosis and a decrease in collagen production (Iredale, Benyon et al. 1998). The reduced amount of scar tissue is associated with improvement in the regenerative capacity of the liver (Issa, Zhou et al. 2003; Kallis, Robson et al. 2011). Due to the often asymptomatic nature of liver fibrosis and compensated cirrhosis, patients frequently present with advanced disease. For many such patients, the medical treatments for the various causes of chronic liver disease are either non-existent, not available or inadequate to permit sufficient recovery and prevent eventual liver failure. Therefore targeting these basic processes of fibrogenesis and

fibrolysis represents a rational therapeutic avenue for disease modification in cirrhosis.

Cellular and molecular mediators of fibrolysis

Following the cessation of liver injury, macrophages readily engraft the hepatic scar. This has been examined using the CD11b-DTR mouse model (Duffield, Forbes et al. 2005). In this experimental scenario, depletion of macrophages during the recovery phase after liver injury results in an attenuated reduction in liver fibrosis. This indicates that macrophages have a critical role in the remodelling process. The bone marrow (BM) origin of almost half of these scar associated macrophages (SAMs) highlights the key role of BM cells in the regulation of fibrosis. The mechanisms underpinning this anti-fibrotic role for macrophages during the recovery phase were subsequently examined (Fallowfield, Mizuno et al. 2007). After cessation of injury, increased numbers of macrophages were detected within the scar with concurrently elevated levels of hepatic MMP-13 expression. Further experiments showed that scar associated macrophages (SAMs) were the primary source of this collagenase. DTR mediated macrophage deletion during recovery in CD11b-DTR mice resulted in a marked reduction of MMP-13 positive cells and whole tissue levels of MMP-13 transcript. Furthermore, fibrosis resolution was partially abrogated in transgenic MMP-13 knockout mice relative to wild type. Taken together, these data support a role for macrophage produced MMP-13 as a critical mediator of scar remodelling during recovery. Other macrophage (and non-macrophage) derived MMPs would also be expected to have important roles in fibrosis regression, as indicated by the only partial reduction in fibrolysis in the MMP-13 knockout mice.

In addition to the transient upregulation of MMP-13 soon after the cessation of liver injury, there is also a prolonged increase in MMP-9 expression during the resolution process. Macrophages have been considered the predominant source of MMP-9 in the liver (Knittel, Mehde et al. 1999), however during the recovery phase, MMP-9 expressing neutrophils as well as macrophages have been identified (Higashiyama,

Inagaki et al. 2007). The functional importance of MMP-9 has been demonstrated by adenovirally transferred MMP-9 promoting myofibroblast apoptosis and reducing fibrosis despite ongoing injury.(Roderfeld, Weiskirchen et al. 2006) Mechanistically, part of this action of MMP-9 on myofibroblasts may be mediated by the cleavage of ECM ligands which otherwise provide survival signals through alpha(v)beta(3) integrin (Zhou, Murphy et al. 2004). This conceptually ties in the hepatic influx of circulating, MMP expressing cells associated with the cessation of injury to the observed ECM degradation and reduction in fibrogenic myofibroblasts.

The role of neutrophils has been examined in fibrosis regression following the release of extra-hepatic bile duct ligation (BDL). The recovery phase is characterised by the influx of neutrophils to the liver and increased levels of MMP-8 (neutrophil collagenase) (Harty, Huddleston et al. 2005). Given its activity against collagen I, MMP-8 represents an attractive therapeutic target. Hepatic over-expression of MMP-8 following gene therapy via an adenoviral vector causes significant improvement in fibrosis in both hepatitic (carbon tetrachloride, CCl_4) and cholestatic (BDL) injury models (Siller-Lopez, Sandoval et al. 2004). Macrophage depletion during the recovery period after the release of BDL decreases the chemoattractant signals for neutrophil migration with impairment of fibrolysis (Harty, Papa et al. 2008). The direct deletion of neutrophils also impairs collagenase activity and scar resorption (Harty, Muratore et al. 2010). These data suggest a specific anti-fibrotic role for neutrophils during recovery in this model of sterile liver inflammation and fibrosis.

Bone marrow cells contribute to liver fibrosis and fibrolysis

The analysis of tissue from patients receiving sex mismatched liver transplantation yielded new insights into the BM origin of non-parenchymal liver cells. By using identification of the Y chromosome as a marker of cellular origin, it was shown that the BM supplies a significant proportion of myofibroblasts in liver disease (Forbes, Russo et al. 2004). By testing cell populations that were enriched for either

haematopoietic stem cells (HSCs) or mesenchymal stem cells (MSCs) in murine models of liver fibrosis, it became apparent that the BM MSCs were most likely to differentiate into collagen producing myofibroblasts within the injured liver (Russo, Alison et al. 2006). This was confirmed in subsequent work transplanting human MSCs into immunodeficient mice which were then treated with CCl_4 to induce hepatic fibrosis (di Bonzo, Ferrero et al. 2008). Whilst the MSCs could infrequently adopt a "hepatocyte-like" phenotype, these cells were far more likely to develop a myofibroblastic phenotype and thus have the potential to contribute to fibrogenesis within the injured liver. This has important implications for cell therapy in liver cirrhosis; BM stem cells or their progeny that are of mesenchymal lineage could have deleterious effects by supporting fibrogenic cell populations.

Transplanting enhanced green fluorescent protein (EGFP) expressing BM cells into wild type recipients prior to inducing fibrosis with CCl_4 injections allows the tracking of BM cells (Higashiyama, Inagaki et al. 2007). As per Duffield *et al* (Duffield, Forbes et al. 2005), approximately half of the liver macrophages had a directly traceable BM origin. Early in the recovery phase after liver injury, there are BM derived MMP-13 expressing macrophages and MMP-9 expressing neutrophils within the scar. Interestingly, applying exogenous granulocyte-colony stimulating factor (G-CSF) prior to recovery enhanced the migration of BM cells into the liver and also significantly accelerated fibrolysis after injury (Higashiyama, Inagaki et al. 2007). This suggests that BM cells and their recruitment into the injured liver are feasible therapeutic targets for fibrosis regression.

Liver regeneration

In addition to the range of viral, immune and metabolic insults that can affect the liver, the ongoing requirement to process nutrients and toxins from the environment poses a continuous challenge to the regenerative capacity of the liver. The essential synthetic, metabolic, detoxification and immune functions of the liver must be

executed by a sufficient parenchymal mass in order to maintain the physiological state. Therefore even in health, there is a substantial regenerative burden on the liver. This demand is even greater in the context of chronic liver disease, wherein the regenerative response involves additional complexity.

The primary source of hepatocytes in the healthy (uninjured) liver is mature epithelia. Experimental two thirds partial hepatectomy in this context is followed by full restoration of liver mass by mitotic cell divisions within 10 days. In humans, an analogous situation may occur following tumour resection or living donor transplantation. This efficient mode of regeneration is controlled by a number of cytokines e.g. tumour necrosis factor (TNF) and interleukin (IL)-6 and growth factors e.g. hepatocyte growth factor (HGF) (Fausto, Campbell et al. 2006).

When there is chronic damage to hepatocytes with associated senescence (Marshall, Rushbrook et al. 2005), then this method may not be able to generate sufficient numbers of hepatocytes. In this context, the liver's facultative stem cell compartment is activated. These cells are termed liver progenitor cells (LPCs) or oval cells. LPCs originate from the distal branches of the biliary tree (the Canals of Hering) and are bipotential, differentiating into either biliary epithelia or hepatocytes. Inflammation is considered a key stimulus for LPC proliferation (Knight, Matthews et al. 2005). A number of cytokines have been shown to cause LPC activation including IL-6, interferon γ and members of the TNF superfamily such as TNFα, lymphotoxin and TNF-like weak inducer of apoptosis (TWEAK) (Bird, Lorenzini et al. 2008). TWEAK is of particular interest as it has been identified as a selective mitogen for LPCs (Jakubowski, Ambrose et al. 2005). Its cognate receptor fibroblast growth factor-inducible 14 (Fn14) is a marker of LPCs and is upregulated during the course of LPC activation (Tirnitz-Parker, Viebahn et al. 2010). The process of stem cell expansion and then differentiation into the final lineage is essentially continuous, therefore the selection of stem cell markers is a challenging area. Cytokeratin-19 (CK-19), EpCam

and Fn-14 are amongst the best validated and recognised in the literature (Yovchev, Grozdanov et al. 2008).

Bone marrow and liver regeneration

LPCs possess some of the markers usually seen on BM stem cells such as THY1, and CD34. This resulted in speculation that these cells could derive from the BM. Early reports suggested that the progeny of BM derived stem cells could make a significant contribution to the hepatocyte mass. (Petersen, Bowen et al. 1999; Alison, Poulsom et al. 2000; Theise, Badve et al. 2000; Theise, Nimmakayalu et al. 2000) BM derived (haematopoietic) stem cells are routinely isolated, stored and transplanted in clinical practice. Therefore these findings triggered a large amount of research into this area in the hope that it could yield new therapeutic options which used existing clinical frameworks. Whilst some data support the possibility that BM could differentiate into epithelia, the physiological significance of such a route is likely to be extremely limited, if present at all. Using a variety of cell tracking techniques, many groups have examined the contribution of the BM stem cells to liver regeneration in both experimental models and human tissue from patients that have undergone organ transplantation. These studies have largely found the contribution of BM stem cells to parenchymal regeneration to be minor (Thorgeirsson and Grisham 2006; Vig, Russo et al. 2006).

Substantial, functional parenchymal replacement by BM derived cells has been reported in one particular experimental setting: the FAH deficient mouse (Lagasse, Connors et al. 2000). Subsequent studies definitively proved that this finding was in fact the result of cell fusion between BM derived macrophages and hepatocytes (Wang, Willenbring et al. 2003; Willenbring, Bailey et al. 2004). Whilst this was effectively a successful demonstration of "cellular gene therapy" the donor BM cells did not differentiate into hepatocytes but instead fused with host cells thereby rescuing an otherwise fatal metabolic error. In human clinical studies of cirrhosis it is

unlikely that these fusion cells would have such a strong selection advantage. Though the replacement of damaged hepatocytes with unmodified BM cells is no longer a realistic therapeutic aim, such work has revealed important new insights into the relationship between the liver and BM derived cells.

Though LPCs are not of BM origin they have an intimate spatial association with cells that can originate from the BM such as hepatic stellate cells and macrophages (Lorenzini, Bird et al. 2010). Macrophage depletion has been shown to prevent the activation of LPCs during injury (Olynyk, Yeoh et al. 1998). This may relate to the functional importance of the macrophage mediated delivery of LPC mitogens to the stem cell niche. Macrophages are the dominant source of TWEAK from infiltrating leucocytes in regenerating liver. Furthermore, the exogenous application of recombinant TWEAK causes LPC proliferation *in vivo* (Tirnitz-Parker, Viebahn et al. 2010).

Figure 1.1 summarises these concurrent processes of liver fibrosis and regeneration during chronic injury. Given the roles of macrophages in both liver fibrosis and regeneration, cells from the monocyte-macrophage lineage represent attractive therapeutic candidates for further investigation.

Figure 1.1 Key processes in liver fibrosis and regeneration during chronic liver injury

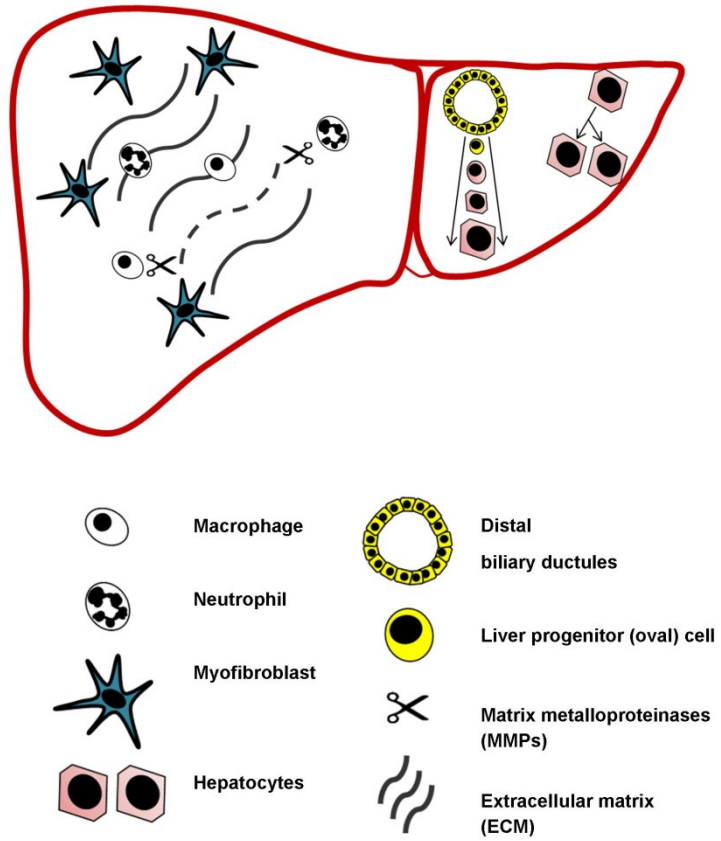

Figure 1.1 Key processes in liver fibrosis and regeneration during chronic liver injury

This figure illustrates the concurrent responses to chronic liver injury. There is expansion of scar producing hepatic myofibroblasts whilst liver macrophages have diverse roles in regulating both scar deposition and resorption. Simultaneously, ongoing tissue injury causes hepatocyte damage and proliferation and also activation of the progenitor cell compartment of the liver. This allows a degree of recovery of liver cell mass and function.

Cell therapy for liver cirrhosis

As described, advancing liver injury places increasing demands on the functional compartments of liver regeneration. Failure to keep pace results in the clinical manifestations of organ failure, such as jaundice and encephalopathy. As liver fibrosis progresses, the capacity for hepatocyte mediated regeneration diminishes whilst structural changes in the liver contribute to portal hypertension and in turn ascites and variceal bleeding. The characteristic abnormal fibrotic architecture with a reduced number of compromised hepatic cells is not an environment conducive to naïve hepatocyte/hepatocyte-like cell engraftment and function. Studies attempting to provide parenchymal support in this manner have been generally unsuccessful and do not address all the clinical problems of cirrhosis.

The structural and functional improvements observed after correction of specific aetiologies e.g. hepatitis B and C virus infection, autoimmune disease, chronic alcohol excess, offer hope to the prospect of clinically successful disease modifying therapy. Disease regression in turn may reduce the predisposition to liver cancer (Hosaka, Suzuki et al. 2013). Therefore the current rationale behind BM cell based therapies is to affect the underlying pathophysiological processes in order to promote fibrolysis and improve regeneration.

Human studies of cell therapy for cirrhosis

The incorrect suggestion that BM cells might significantly and directly supply hepatic parenchyma allied to the existing use of BM stem cells in clinical haematological practice was followed by a wave of studies of BM cell therapy for cirrhosis. These can be categorised in terms of the intended therapeutic cell type.

Haematopoietic stem cells (HSCs) are pluripotent stem cells that comprise a very small fraction of the whole BM. These cells are capable of giving rise to all the major blood cell lineages. BM cell fractions can be enriched for HSCs through sorting using cell surface markers such as CD34 and CD133. The subset of CD34 positive cells that also express CD133 is considered to be further enriched for stem cells (de Wynter, Buck et al. 1998). In addition, CD34-/CD133 positive cells have been identified as having the capacity to form endothelial progenitor cells (Friedrich, Walenta et al. 2006). Cell sorting increases both the cost and complexity of the process; a potential solution is the use of less purified cell fractions. Mononuclear cells (MNCs) can be separated from BM relatively simply by density gradient centrifugation however, CD34 positive cells constitute only 1-2% of this population (Steen, Morkrid et al. 1994) and the proportion of true stem cells within this fraction is even smaller. Nonetheless, it is plausible that an "active" component of this therapy may reside in the non-stem cell fraction or even be the result of interactions between different donor cell types (Thomas 2009).

Autologous candidate cells are initially harvested by either leukapheresis or direct BM aspiration. G-CSF is routinely given prior to leukapheresis in haematological practice to increase HSC yields from peripheral blood. Human studies in which HSCs are extracted from peripheral blood utilise this action of G-CSF in their protocols. The independent actions of G-CSF on the cirrhotic subject must therefore be considered. Animal data support roles for G-CSF in mobilising BM stem cells and also directly stimulating liver regeneration. During regeneration, there is hepatic

production of G-CSF whilst LPCs upregulate expression of the G-CSF receptor, proliferating in response to stimulation by this cytokine (Piscaglia, Shupe et al. 2007).

Distinct from its use in cell therapy protocols, G-CSF itself has been studied as a treatment in cirrhosis. A G-CSF dose finding study in cirrhotics did not demonstrate a consistent improvement in liver function (Lorenzini, Isidori et al. 2008). A small randomised controlled trial of G-CSF therapy in patients with alcoholic steatohepatitis showed early increases in serum HGF, peripheral CD34 positive cell counts and LPC proliferation on paired biopsies taken 7 days apart, but did not show improvement in measures of liver function up to 28 days after treatment (Spahr, Lambert et al. 2008). Subsequently, a randomised control trial of G-CSF treatment in acute on chronic liver failure has shown promising results in this group of very sick patients. In addition to improving blood tests of liver and renal function, clinical indicators such as infection rate and encephalopathy improved. Most strikingly, the 2 month mortality rate was more than halved by G-CSF therapy (17/24 control versus 7/23 with G-CSF). As expected, G-CSF caused an increase in the number of circulating CD34 positive cells; this does not prove direct involvement in the mechanism of effect. The number of patients in this study was small and there was heterogeneity of both cirrhosis aetiology and cause of the acute deterioration. These factors limit the certainty and generalisability of the results. More recently, G-CSF was administered to patients with chronic hepatitis B virus (HBV) infection experiencing an acute deterioration in liver function. In line with the previous report, 3 month mortality was more than halved by G-CSF (13/27 control versus 6/28 with G-CSF) (Duan, Liu et al. 2013). These encouraging findings warrant further investigation and importantly the use of "G-CSF alone" control arms in cell therapy studies.

Mesenchymal stem cells (MSCs) are a heterogeneous population of plastic adherent BM stromal cells characterised by their multi-potentiality (including down osteocytic, chondrocytic and adipocytic lineages) and the presence (and absence) of

specific surface markers (Kolf, Cho et al. 2007). This multipotentiality and their relative ease of accessibility in addition to their immunomodulatory properties (Ryan, Barry et al. 2007) has made MSCs an attractive candidate for cell therapy. As described, the long term stability and potential to differentiate into scar producing myofibroblasts (Russo, Alison et al. 2006; di Bonzo, Ferrero et al. 2008) are important caveats when considering the clinical use of MSC based therapy for cirrhosis (Thomas 2013).

Haematopoietic stem cells

A phase 1 study of autologous CD34 positive cells given to 5 cirrhotic patients was conducted by Gordon and colleagues (Gordon, Levicar et al. 2006). The aetiologies of cirrhosis were alcohol excess, primary sclerosing cholangitis (PSC) and chronic HBV or hepatitis C virus (HCV) infection. CD34 positive cells were mobilised by G-CSF administration and then isolated from the mononuclear cell fraction by magnet based cell sorting. The donor cells were manipulated by adherence to plastic and cultured in media containing a number of cytokines, including stem cell factor, GM-CSF, IL-3, and G-CSF. Between 1 x 10^6 and 2 x 10^8 cells were re-infused via the hepatic artery (n=2) or portal vein (n=3). There were no discernible changes in liver biochemistry or clinical parameters either over the initial 2 month period or on longer term follow up of 12-18 months. However, the primary endpoints of safety and acceptability were achieved (Levicar, Pai et al. 2008). The same group also published a report of 9 patients with cirrhosis due to alcohol excess who had been abstinent for a minimum of 6 months (Pai, Zacharoulis et al. 2008). CD34 positive cells were isolated following G-CSF administration and cultured in similar conditions to their previous study. A mean dose of 2.3 x10^8 cells was injected into the hepatic artery without any detected short or long term complications. Liver chemistry and Child-Pugh score seemed to increase from baseline over the 3 month follow up period though the absence of a control group prevents firm conclusions being drawn.

A multi-disciplinary group of radiologists and surgeons from Dusseldorf, Germany delivered CD133 positive BM cells into the hepatic portal vein (HPV) in non-cirrhotic patients undergoing hepatic resection (Furst, Schulte am Esch et al. 2007). 13 patients underwent pre-operative portal vein embolization as a regenerative stimulus followed by extended right hepatectomy for large hepatic malignancy (primary or secondary). The cell therapy group (n=6) additionally received between 2.4 and 12.3 $x10^6$ autologous CD133 positive cells that had been positively sorted from BM aspirate. Cell recipients had significantly greater increases in radiologically determined liver volume, which allowed earlier tumour resection. One of the treated patients had liver fibrosis due to HCV infection however the majority of these patients did not have chronic liver disease. Nonetheless, it is biologically plausible that such a pro-regenerative effect might also be imparted to the cirrhotic patient.

In a study from the Royan Institute in Iran, 4 patients with decompensated cirrhosis were given between 2.5 and 8 $x10^6$ BM derived CD34 positive cells. These were injected into the hepatic artery (HA) by a radiologically guided procedure (Mohamadnejad, Namiri et al. 2007). 1 of these patients (with autoimmune cirrhosis) experienced worsening renal failure and ultimately died of liver failure. The adverse event was attributed to contrast nephropathy in a cirrhotic patient with pre-existing renal dysfunction and caused the early termination of the study. This represents an important lesson for the research community in terms of the selection of subjects and the route of cell administration in this often frail group of patients.

The effects of partially differentiated CD34 positive cells were studied in 48 cirrhotic patients recruited from hospitals in Cairo, Egypt (Salama, Zekri et al. 2010). 36 of these patients had chronic HCV infection whilst 12 had an autoimmune aetiology. Participants underwent G-CSF mobilisation prior to leukapheresis. CD34 positive cells were isolated, cultured and expanded for a further week in media containing GM-CSF and also growth factors derived from buffalo rat liver extract. The rationale behind the cell culturing process was to begin differentiation towards a hepatocyte

like phenotype. RT-PCR demonstrated that the cells expressed the genes for albumin and also α1-antitrypsin during the protocol. $1x10^9$ cells were infused via the HPV, unless hepatofugal flow was detected in which case the HA was used. Serious adverse events were a single case of post-procedural haemoperitoneum which required blood transfusion and 2 gastrointestinal bleeds which occurred 1 week after cell delivery. One of these haemorrhages was endoscopically controlled however the other was fatal. From baseline, liver biochemistry improved in patients of both HCV and autoimmune aetiology however the lack of a control group limits the appreciation of any therapeutic effect.

This group also conducted a randomised controlled trial of CD34/133 positive cells in patients with HCV cirrhosis.(Salama, Zekri et al.) 90 patients received 5 days of G-CSF treatment prior to BM aspiration from which CD34/ CD133 positive cells were selected. $5x10^7$ cells were re-infused via the HPV. Importantly, the 50 control subjects received control water injections instead of G-CSF. The G-CSF/cell recipients had improvements in liver biochemistry, Child-Pugh score and measures of clinical status which lasted to the end of the 6 month follow up period. Whether these positive effects are attributable to the cells, G-CSF or a combination is undefined. (Thomas 2013)

Mesenchymal stem cells

Reports of MSC delivery to cirrhotic patients have given mixed results. The first published study of MSC therapy in cirrhosis was from the University of Tehran, Iran (Mohamadnejad, Alimoghaddam et al. 2007). 4 patients with decompensated cirrhosis (3 deemed cryptogenic and 1 of autoimmune aetiology) on the liver transplant waiting list received between 1 and 6 x 10^7 MSCs via a peripheral vein. These cells were derived from BM and cultured *in vitro*. 12 months later, all 4 patients were subjectively better as determined by quality of life questionnaire scores whilst 3 had a net reduction in MELD score.

Another study from the Royan Institute used MSCs cultured from BM aspirate which then underwent a hepatocytic differentiation protocol. This process took approximately 2 months. Between 3 and 5 x 10^7 autologous cells were given to 8 cirrhotic patients. The breakdown of their cirrhosis aetiologies was: HBV (n=4), HCV (n=1), cryptogenic (n=2) and chronic alcohol excess (n=1). The cells were injected into the HPV in 6 patients and into a peripheral vein in 2 patients in whom the intraportal route was not technically possible. All 8 cell recipients had improved MELD scores 6 months after treatment (mean score from 17.9 to 10.7) in this uncontrolled study (Kharaziha, Hellstrom et al. 2009).

The largest cell therapy trial to date was performed in the setting of liver failure due to HBV cirrhosis (Peng, Xie et al. 2011). Autologous MSCs were given to 52 patients who consented to cell therapy whilst 105 control subjects were matched for age, sex, liver biochemistry and MELD score. MSCs were derived from BM aspirate and delivered via the HA. 2 weeks after MSC delivery, serum albumin and bilirubin levels were improved. Within another week, prothrombin time (PT) and MELD scores had also significantly improved. These benefits were not sustained beyond 36 weeks after cell infusion. No significant differences in hepatocellular carcinoma (HCC) rate or survival were detected.

Umbilical cord derived MSCs have been used in a study of acute on chronic liver failure due to HBV infection (Shi, Zhang et al. 2012). 24 patients received cells via a peripheral vein on 3 occasions at 4 week intervals. 19 control subjects received saline infusions. Blood test results, MELD score and 12 week survival improved in MSC recipients without apparent side effects.

Mononuclear cells

Terai and co-workers at Yamaguchi University Hospital in Japan recruited 9 cirrhotic patients for an uncontrolled study of MNC therapy. The aetiologies were HBV (n=3), HCV (n=5) and cryptogenic (n=1). Between 2.21 and 8.05 $x10^9$ BM derived unsorted mononuclear cells were injected via a peripheral vein. 2.39% of infused cells were CD45 positive / CD34 positive. Significant improvements from baseline in serum albumin and Child-Pugh score were found up to 6 months after infusion of the MNC fraction (Terai, Ishikawa et al. 2006). 3 of these patients also had pre- and 4 week post-therapy liver biopsies. These demonstrated an increase in immunohistochemical markers of regeneration (α-fetoprotein and proliferating cell nuclear antigen).

Striking improvements were found in 2 abstinent patients with decompensated alcoholic cirrhosis who received 4 or 6.93 $x10^6$ CD34 positive cells per kg within the MNC fraction (Yannaki, Anagnostopoulos et al. 2006). These cells were obtained from leukapheresis product following G-CSF mobilisation and then re-infused via a peripheral venous route. The clinical and biochemical recovery was greatest 1 year after treatment. Without a control group it is not possible to determine benefit categorically. Furthermore, substantial improvement in liver remodelling and function is well recognised following abstinence from alcohol. This highlights the importance of robust, controlled trials to move the field forward.

A randomised controlled trial of autologous MNCs in cirrhosis was undertaken at the Hospital Sao Rafael in Salvador, Brazil (Lyra, Soares et al. 2010). 30 patients with a variety of aetiologies (predominantly alcohol excess, HCV infection and cryptogenic) who were on the liver transplant waiting list were randomised. Half of the subjects received mononuclear BM cells (between 1.6 and 11.2 $x10^8$) via the HA. Though no serious adverse events were detected in the first 3 months, 3 patients in the MNC therapy arm died from complications of cirrhosis at 6, 8 and 10 months whilst 2 died in the control arm (with an additional patient undergoing liver transplantation due to progressive liver failure). Serum albumin levels increased

transiently following MNC infusion with a similarly short term trend of improvement in serum bilirubin. Improvements in Child-Pugh score (but not MELD) reached statistical significance in cell recipients over the first 3 months; the strength of this effect was not maintained to the 12 month time point.

An uncontrolled series from Seoul, South Korea examined 10 patients with HBV cirrhosis who received with $1x10^8$ BM derived MNCs via a peripheral vein (Kim, Park et al. 2010). The greatest improvements in serum albumin and prothrombin time were 6 months after cell infusion. Childs-Pugh score (but not MELD) also improved at 6 months along with subjective features of quality of life. Serial liver biopsies were taken before and 1, 3 and 6 months after therapy. These demonstrated a significant increase in LPC numbers with an accompanying trend towards increased numbers of proliferating hepatocytes 3 months after MNC infusion. This effect did not persist to the 6 month biopsy.

BM derived MNCs were studied as a potential adjunct to the Kasai procedure in a group of paediatric patients with extra-hepatic biliary atresia. This controlled study from New Delhi, India tested the effects of $4 x10^7$ MNC delivered via the HA and/or HPV during surgery. If these vessels were not accessible then superior mesenteric vein radicals or trans-hepatic routes were used (Sharma, Kumar et al. 2011). MNC recipients had improved serum bilirubin, alkaline phosphatase and transaminases within the first post-operative week. The reduction in serum bilirubin was maintained during the following year. MNC therapy conferred fewer episodes of cholangitis and improved survival rates during the year of follow up.

I have collaborated with a group of researchers from Rio de Janeiro, Brazil on a Phase 1 study of BM derived MNCs (Couto, Goldenberg et al. 2011). A novel feature of this study was tracking donor cells *in vivo* by labelling them with $^{99}Tc\text{-}SnCl_2$. Whole body scintigraphy allowed determination of hepatic radiotracer retention following cell injection into the HA. This demonstrated 41% hepatic retention at 3 hours and 32%

by 24 hours after cell delivery. Improvements in serum albumin and bilirubin from baseline were transient; MELD score did not change. An important complication relating to the route of cell delivery was a HA dissection during arteriography prior to cell delivery. There were no deleterious clinical sequelae and the catheter was repositioned to allow cell delivery. Other adverse events included a transient cardiomyopathy, a case of eosinophilic fasciitis and HCC development in one patient.

BM derived MNCs were compared against CD133 positive cells in 6 patients with end stage liver disease (Nikeghbalian, Pournasr et al. 2011). Donor cells were delivered via the HPV. There were no significant differences in liver biochemistry or adverse events. This raises the possibility of clinical equivalence of the much simpler protocol of acquiring the MNC fraction to the costlier and more demanding cell sorting process. However, the fundamental priority is to prove that candidate cells are indeed efficacious and safe in larger randomised controlled trials.

A randomised controlled trial of MNC therapy was undertaken in 58 patients with decompensated cirrhosis due to alcohol excess in Geneva, Switzerland (Spahr, Chalandon et al. 2013). The HA delivery of MNCs acquired from BM aspirate after 5 days of G-CSF priming was tested against standard medical therapy. MELD score and hepatic venous pressure gradient improved over time in both groups but there was no difference between them. Similarly there were no differences detected in histological parameters (of inflammation or LPC number) or serum HGF. The proportion of recidivism in each group was not reported (31% overall), this could confound the results. Furthermore, the substantial degree of improvement in the control arm would make detection of additional benefit from cell therapy potentially difficult indicating the possibility of an underpowered study.

Conclusions from human studies

The early studies of autologous BM cell therapy for cirrhosis were small and uncontrolled. When carried out in carefully selected patient groups and delivered in a controlled manner these have been technically feasible and generally safe. Results have been encouraging but not definitive. Subsequently, a number of controlled trials have shown evidence of benefit thereby justifying further study.

The natural history of untreated chronic liver disease can involve considerable short term variation along an overall downward trend. When the injurious stimulus is lifted, for example successful antiviral therapy or cessation of alcohol, liver function can markedly improve. Therefore patient circumstance and cirrhosis aetiology need to be factored into study design. More, recent trials have examined a single disease aetiology.(Peng, Xie et al. 2011; Spahr, Chalandon et al. 2013) (Salama, Zekri et al. 2010) This permits a clearer assessment of the potential effects of the candidate donor cell type in a defined context. Alternatively, large trials can prospectively subgroup patients according to aetiology in order to distinguish any differential effects. Given the unpredictable episodes of illness that are a feature of decompensated cirrhosis, sufficiently large, well-powered trials may be required to detect therapeutic benefit.

HSC populations seem to be safe as a potential cell therapy, however there is still little mechanistic understanding of their actions in liver disease. A plausible explanation is through paracrine stimulation of the injured liver activating endogenous repair. The purity of the donor cell population will reflect its effectiveness, practicality and cost. If MNC therapy proves to have similar or even superior benefit to more concentrated stem cells, this could facilitate clinical translation. The important caveat concerning MSC use is their potential to adopt a deleterious phenotype (Russo, Alison et al. 2006; di Bonzo, Ferrero et al. 2008). The early direction of MSC differentiation (Kharaziha, Hellstrom et al. 2009) during the cell culture process may allow a degree of control of subsequent cell behaviour *in vivo*. Long term phenotypic stability would need to be robustly proven prior to

routine use. It may be that cirrhosis is not the optimal disease setting for MSC derived cells. As our understanding of the actions of specific cell populations in defined settings increases, it is conceivable that the choice of cell type may ultimately be tailored to a patient's disease stage and aetiology.

Serious complications relating to cell injection into the HA or HPV demonstrate the importance of the administration route and technique (Mohamadnejad, Namiri et al. 2007; Salama, Zekri et al. 2010; Couto, Goldenberg et al. 2011). The advantages of concentrated cell delivery directly to the liver must be balanced against the ease and safety of peripheral venous routes. Insights into the kinetics of donor cells after delivery using techniques such as whole body scintigraphy (Couto, Goldenberg et al. 2011) will help inform this. Transient improvements in liver function have been detected in a number of studies. Repeated cell infusions may be needed to exert clinically relevant benefits and achieve substantial disease modification. This has implications on the selection of delivery route. In terms of trial design, the delivery of inconsistent cell numbers within certain studies limits detection of effect by increasing variation and also hampers comparison between studies through potential dose related effects. Future work will ideally be standardised.

The most important outcome measures are quality of life and survival. These endpoints are affected by the rates of complications, HCC development and need for transplantation. The fluctuating nature of cirrhosis means that narrow windows of data collection could miss important trends. Serial data collection is therefore useful to detect subtle changes. The most convenient are the currently routine blood tests (such as PT and serum albumin, liver biochemistry and creatinine). The Child-Pugh score is simple to calculate and widely used, though limited by subjectivity in the assessment of encephalopathy and ascites. Advantages of the MELD score include its objectivity and routine clinical use in transplant prioritisation as a guide to predicted survival. The well recognised morbidity and mortality of liver biopsy must be weighed against the value of tissue for analysis of both effect and also potential

mechanism. Hepatic venous pressure gradient measurement can be undertaken alongside trans-jugular liver biopsy. This provides important information relating to the risk of complications such as variceal bleeding in addition to prognosis and response to therapy (Albilllos and Garcia-Tsao 2011). Biomarkers such as the panel of serum markers of liver fibrosis (Rosenberg, Voelker et al. 2004) provide validated non-invasive measures of liver fibrosis. Non-invasive tests such as indocyanine green clearance and ^{31}P magnetic reasonance spectroscopy (Lim, Patel et al. 2003) are yet to reflect outcome reliably and gain widespread acceptance. Therefore at present, a panel of surrogate markers is required to provide realistic and achievable goals for clinical trials.

In summary, information from experimental animal work regarding the choice of cell type, route of delivery and the underlying mechanisms of effect emerging from animal work will inform the rational design of human trials. The clinical literature is expanding and the next step is for robust randomised controlled trials to test clinically useful parameters (Thomas 2013).

Table 1.1 Clinical studies of cell therapy for cirrhosis

Infused cell				Trial design	Number of patients	Outcome measures	Benefit?	Adverse events?	Follow up (months)	Year of publication
type	source	number	delivery route							
CD34+	G-CSF mobilised blood	1 x 10^6 - 2 x 10^8	HA or HPV	Uncontrolled case series	5	LFTs	No	No	6-18	2006, 2008(Gordon, Levicar et al. 2006; Levicar, Pai et al. 2008)
CD133+	BM	2.4-12.3 x10^6	HPV	Controlled case series	6 v 7	Liver volumetry, time to surgery	Yes	No	N/A	2007(Furst, Schulte am Esch et al. 2007)
CD34+	BM	5.25x10^6	HA	Uncontrolled case series	4	MELD	No	Yes	6	2007(Mohamadnejad, Namiri et al. 2007)
CD34+	G-CSF mobilised blood	2.3x10^8	HA	Uncontrolled case series	9	CP, LFTs	Yes	No	3	2008(Pai, Zacharoulis et al. 2008)
CD34+	G-CSF mobilised blood	1x10^9	HPV	Uncontrolled case series	48	LFTs	Yes	Yes	12	2010(Salama, Zekri et al. 2010)
CD34+ /CD133+	G-CSF then BM aspirate	5x10^7	HPV	Randomised controlled trial	90 v 50	CP, LFTs, clinical indicators	Yes	No	6	2010(Salama, Zekri et al. 2010)
MSCs	BM	3.1x10^7	Peripheral	Uncontrolled case series	4	MELD	Yes	No	12	2007(Mohamadnejad, Alimoghaddam et al. 2007)
MSCs	BM	3-5x10^7	HPV or peripheral	Uncontrolled case series	8	MELD	Yes	No	6	2009(Kharaziha, Hellstrom et al. 2009)
MSCs	BM	Unclear, derived from 3.4x10^8 MNCs	HA	Controlled case series	52 v 105	LFTs, MELD, survival	Yes	No	12	2011(Peng, Xie et al. 2011)

MNCs	BM	$5.2x10^9$	Peripheral	Uncontrolled case series	9	CP	Yes	No	6	2006(Terai, Ishikawa et al. 2006)
MNCs	G-CSF mobilised blood	4-6.93 $x10^6$ CD34+ cells /kg	Peripheral	Case report	2	CP, MELD	Yes	No	30	2006(Yannaki, Anagnostopoulos et al. 2006)
MNCs	BM	$3.78x10^8$	HA	Randomised controlled trial	15 v 15	CP, MELD, LFTs	Yes	No	12	2010(Lyra, Soares et al. 2010)
MNCs	BM	$1x10^8$/kg	Peripheral	Uncontrolled case series	10	CP, MELD, performance status, liver volumetry, histology	Yes	No	12	2010(Kim, Park et al. 2010)
MNCs	BM	$4.4 x10^7$	HA or HPV	Controlled case series	11 v 15	LFTs, cholangitis episodes, survival	Yes	No	12	2011(Sharma, Kumar et al. 2011)
MNCs	BM	$2–15x10^8$	HA	Uncontrolled case series	8	MELD, LFTs	Yes	Yes	12	2011(Couto, Goldenberg et al. 2011)
CD133+ vs MNCs	BM	$1.3x10^9$ (MNC) $6.4X10^6$ (CD133)	HPV	Controlled case series	3 v 3	MELD, LFTs	No	No	24	2011(Nikeghbalian, Pournasr et al. 2011)
MNCs	G-CSF then BM	$4.8x10^7$ /kg	HA	Randomised controlled trial	28 v 30	MELD, LFTs, histology	No	Yes	3	2013(Spahr, Chalandon et al. 2013)

adapted from *Clinical Studies of Cell Therapy for Liver Cirrhosis*(Thomas 2013)

Animal studies of cell therapy for experimental chronic liver disease

The most widely used animal models of chronic liver disease have involved iterative injury with hepatotoxins such as CCl_4. Candidate cells have been given during the development of advanced fibrosis. Outcome measures have included blood tests of liver function and serum and histological markers of fibrosis, inflammation and regeneration. These experimental models of chronic liver disease have indicated that rather than attempting to transplant hepatocyte-like cells, a more productive therapeutic strategy might be to modulate the underlying pathophysiological processes.

A number of cell types have been examined. As described, MSCs have been considered an attractive candidate for cell therapy due to their accessibility, multipotentiality and immunomodulatory effects. These studies have given conflicting results; some have shown a reduction in liver fibrosis following MSC delivery whereas other groups have not been able to reproduce this (Zhao, Lei et al. 2005; Carvalho, Quintanilha et al. 2008; di Bonzo, Ferrero et al. 2008). Considering the risk of contributing to myofibroblast like cells (Russo, Alison et al. 2006) given current limitations in characterisation and purification, MSCs may not be ideal cell populations to treat cirrhosis. One study of MSC therapy published in 2012, examined the effects of different routes of cell delivery (Wang, Lian et al. 2012). Interestingly, the portal vein but not tail vein administration of MSCs caused improvement in liver fibrosis, liver biochemistry and serum albumin. The reasons behind this were not explored though the authors suggested that this could relate to the effective cell dose reaching the target organ in sufficient concentration.

Sakaida and colleagues have used a Liv-8 depleted BM fraction to reduce hepatic fibrosis induced by repetitive CCl_4 in mice (Sakaida, Terai et al. 2004). It was suggested that the BM derived donor cells might be transdifferentiating into hepatocytes however a more likely mechanism may relate to the observed

upregulation of MMP-9 expression and localisation of MMP-9 expressing donor cells within the scar. HCC is an important complication of cirrhosis with few effective treatment options available for the majority of patients. The same group from Yamaguchi University Hospital, Japan have also tested BM cells in a model of murine liver fibrosis and carcinogenesis (Maeda, Takami et al. 2012). In line with human data, the improvement in fibrosis was accompanied by suppressed rates of liver cancer formation. Importantly, no cancers were derived from donor (GFP positive) elements.

The delivery of exogenous endothelial progenitor cells has also conferred anti-fibrotic and pro-regenerative effects in rat liver fibrosis (Nakamura, Torimura et al. 2007). This was associated with increased expression of certain MMPs (-2, -9 and -13) and cytokines (such as HGF and VEGF (vascular endothelial growth factor)). Human CD34 cells injected into immunodeficient fibrotic rats also caused increased expression of MMPs-2, -9 and -13 with a reduction in myofibroblast number and fibrosis. There was also evidence of improved hepatocyte regeneration with upregulation of restorative cytokines (HGF and VEGF) (Nakamura, Tsutsumi et al. 2012) .

The delivery of unfractionated BM cells via the tail vein to mice with liver fibrosis has recently been shown to reduce hepatic scar (Suh, Kim et al. 2012). Approximately 75% of the infused BM cells were of myeloid lineage (CD11b, Gr-1 positive) and up to 20% possessed the macrophage marker F4/80. The anti-fibrotic effect required donor cell IL-10 expression however the donor cell populations were not fractionated in this set of experiments. Therefore it is not certain which subset of BM cells, or indeed interaction between cell populations, is responsible for the phenotype.

The adoptive transfer of dendritic cells during fibrosis regression after cessation of liver injury has been shown to accelerate fibrolysis (Jiao, Sastre et al. 2012). Levels of MMP-9 but not MMP-13 were elevated; donor cell derived MMP-9 contributed to the

observed phenotype. Of note, different groups have noted apparently divergent effects of dendritic cells in liver fibrosis (Connolly, Bedrosian et al. 2010). There is not widespread agreement regarding the characterisation of dendritic cells, therefore examination of biologically distinct cell types may explain the disparate findings. Furthermore, the derivation of the transferred cells involved priming donor mice by injection with a melanoma cell line prior to spleen harvest. Splenic cells were then fractionated based on cell surface marker profile to obtain the donor dendritic cell population. This adds to our understanding of the processes underlying fibrosis and its regression. However, the complexity and manipulation required to acquire the donor cells make this unlikely to be an easily practicable therapy for patients. As with studies of whole BM, various MNC fractions and impure HSC and MSC populations, difficulties defining consistent cell populations hamper translation of such findings. The use of mixed cell populations also limits the understanding of mechanisms of action (Houlihan and Newsome 2008). Therefore the identification of defined single cell types with beneficial effects is more likely to inform rational and predictable therapy.

Macrophages have a broad repertoire of context dependant immune, inflammatory, trophic and regulatory actions (Mantovani, Sica et al. 2004). As described, endogenous macrophages mediate hepatic scar remodelling through local MMP expression (Duffield, Forbes et al. 2005; Fallowfield, Mizuno et al. 2007). BM precursors differentiate into macrophages under the control of colony stimulating factor-1 (CSF-1) acting through its receptor (CSF-1R). CSF-1 also controls macrophage proliferation, viability and phenotypic fate (Pollard 2009). The delivery of exogenous CSF-1 stimulates macrophage infiltration, improving fibrosis and function in models of renal (Menke, Iwata et al. 2009) and cardiac (Morimoto, Takahashi et al. 2007) injury. Though LPCs are not of BM origin (Vig, Russo et al. 2006; Lorenzini, Bird et al. 2010) their activation is influenced by a number of paracrine signals that represent potential targets for BM derived cell therapy (Jakubowski, Ambrose et al. 2005; Bird, Lorenzini et al. 2008). Based on these

findings, we hypothesised that cells from the monocyte-macrophage lineage could have utility as a cell therapy in experimental chronic liver disease.

Given this, the experimental aims were to:

1) To study the therapeutic potential of exogenous unmanipulated BM derived cells, in particular those of the monocyte-macrophage lineage, delivered during chronic liver injury due to repeated CCl_4 injury.

2) On identification of a beneficial phenotype following BMM delivery, further experiments were to determine potentially mechanistic changes in mediators of liver fibrosis and regeneration.

3) To test the effects of BMM therapy in a cholestatic (DDC) model of chronic liver disease.

4) To determine the effectiveness of different routes of cell injection.

CHAPTER TWO

Materials and Methods

Donor cell preparation and characterisation

Femurs and tibias were removed from euthanised age-matched, syngeneic male mice. These were washed in 70% ethanol. BM cells were then extracted and a single cell suspension prepared by passing the cells through a 40 μm filter (BD Falcon).

The *Tg*(*Csf1r-Gfp)Hume* (*MacGreen*) mouse was used in order to isolate macrophage precursors from the BM (Sasmono, Oceandy et al. 2003). MacGreen mice used were of the balb-c mouse strain background. EGFP expressing cells were gated using fluorescence-activated cell sorting (FACS, FACSVantage, Becton and Dickinson). These cells will be termed "macrophage precursor cells" in this thesis.

BM derived macrophages (BMMs) were prepared as previously described (Duffield, Erwig et al. 2000). DME (Dulbecco's Modified Eagle)/F12 Glutamax medium was conditioned with 10% fetal calf serum, 100 U/ml penicillin and 100 μg/ml streptomycin. Murine fibrosarcoma cells (L929) which secrete CSF-1 were cultured in T162 flasks in 25 ml of the DME medium. The supernatant was harvested 3 days after confluency and then filtered, aliquoted and stored at -80°C. This L929 medium was subsequently added to the DME media to make 20% L929 medium. BM extracted from each femur or tibia was cultured in 40ml of 20% L929 medium in a 90 ml teflon pot. These were matured for 7 days; 25% of the medium was replaced on alternate days during the process. Diff-Quik staining was performed on cytospin samples to characterise the resultant cells. Macrophage surface marker expression was analysed by flow cytometry (FACSCalibur, Becton and Dickinson). Cells were stained using the following pre-conjugated antibodies: F4/80, CD11b (eBiosciences), Ly-6G (Biolegend), Ly-6C, CD3 and CD19 (BD Pharmingen) with the appropriate isotype controls.

The traditional categorisation of macrophage phenotypes has been into the classical or alternatively activated states. In order to characterise unstimulated (naïve) BMMs

in this context, BMMs were polarised for the purposes of phenotypic comparison, Classically activated (M1) macrophages were generated by overnight stimulation with lipopolysaccharide (Sigma, 50 ng/ml) and interferon-γ (Peprotech, 20 ng/ml). Alternatively activated (M2) macrophages were produced by stimulation with IL-4 and IL-13 (both Peprotech, 20 ng/ml) (Mantovani, Sica et al. 2004).

To test the effect of nonviable, physically disrupted BMMs, these were sonicated using a Bandelin sonicator (Bandelin) - twice for 10 seconds at a 50% power setting.

Recipient disease models

Wild type rodents were supplied by Harlan (UK). Rodents were housed in a sterile animal facility with a 12 hour dark/light cycle and free access to food and water. All animal experiments were carried out under procedural and ethical guidelines of the British Home Office.

Preliminary work in collaboration with Dr Caroline Pope tested the effects of twice weekly intraperitoneal (IP) injection of 1mg/kg CCl_4 (dissolved in sterile olive oil) given to adult female Sprague-Dawley rats over 12 weeks. Rats were euthanised after 8, 10 and 12 weeks of injury. Upon confirmation of safe administration and the histological progression of liver fibrosis with increasing CCl_4 exposure (appendix two) subsequent work focused on murine liver fibrosis as detailed below. Advanced liver fibrosis was induced in adult female mice by either iterative intraperitoneal CCl_4 injection or administration of the diethyl 1, 4-dihydro-2, 4, 6-trimethyl-3,5-pyridinedicarboxylate (DDC) diet.

1) Carbon tetrachloride injection

   Twice weekly intraperitoneal (IP) injection of 0.75 ml/kg CCl_4 dissolved in sterile olive oil was given over a 10 week period. One day after the 12th CCl_4 injection (6 weeks), mice from the same cohort were randomly allocated to receive either cell or control medium injections via the HPV. To examine the early effects of cell delivery, separate experiments were undertaken with mouse groups being euthanised at 10 minutes, 1, 6 and 12 hours and 1, 3 and 7 days after cell/control medium delivery.

In order to determine the effects of different CCl_4 dose and experimental duration in addition to an alternative route of cell delivery, further experiments were performed using:

i) 12 weeks of twice weekly IP 0.4 ml/kg CCl_4 dissolved in sterile olive oil with cell/control delivery 1 day after the 16^{th} CCl_4 injection (8 weeks)

ii) delivery of cells/control medium via the tail vein

iii) repeated administration of cells/control medium via the tail vein (4 doses over the final 4 weeks of injury); each cell/control medium injection was performed 1 day after the preceding CCl_4 injection.

Transgenic mice were used to allow donor cell tracking and selection of specific subpopulations of BM cells. Recipient mice were of the same strain as donors to ensure syngeneic cell transfer. C57Bl/6 (wild type), CBA/Ca (for constitutive GFP expression (Pratt, Sharp et al. 2000)) and balb-c (for conditionally enhanced GFP expressing macrophage precursor cells (Sasmono, Oceandy et al. 2003)) strains were used.

2) Diethyl 1, 4-dihydro-2,4,6-trimethyl-3,5-pyridinedicarboxylate (DDC) diet

S129 S2 mice were fed a diet with 1% DDC (by weight) *ad libitum* for 5 weeks. After 3 weeks of injury they received either cell or control medium injections via the HPV. The mice then continued on the DDC diet until euthanisation at 5 weeks.

C57Bl/6 mice were used for most experiments. As donor and recipient mice were syngeneic, additional strains were required for certain experiments: CBA/Ca mice were used for GFP positive donor BMM tracking and balb-c mice for macrophage precursor selection. S129 S2 mice were used for the DDC model as this toxic diet was tolerated by this strain but had proved deleterious in others when used in our group (personal communication, Dr Luke Boulter).

Cell delivery

Donor cells from age and strain-matched mice were suspended in 100 μl of DME medium. Cells were administered via either the hepatic portal vein (HPV) or tail vein (TV):

1) The HPV was accessed by midline laparotomy using aseptic technique. Anaesthesia was induced using 1 mg/kg medetomidine and 76 mg/kg ketamine (IP). 22.5 mcg/kg buprenorphine (SC) was given as analgesia. Careful identification of the HPV and injection of cell suspension/control medium under direct vision was promptly followed by haemostasis using sterile Surgicel (Ethicon). Following surgical closure of the abdomen, anaesthesia was reversed with 1 mg/kg atipamezole given subcutaneously (SC).
2) The TV was identified in unanaesthetised, restrained mice and injected under direct vision.

Tissue harvest and preservation

Rodents were venesected at euthanisation. Liver, spleen, lungs and kidneys were removed and split for freezing or fixation. Organ pieces were snap frozen either alone or in Tissue-Tek OCT Compound (Sakura Finetek) in a sterile container on 100% ethanol in dry ice until the OCT had set. Further samples were fixed in buffered formalin (10 ml 37% formalin in 100ml PBS) or methacarn (70 ml methanol, 20 ml chloroform and 10 ml acetic acid). Fixed tissue was then dehydrated and stored in 70% ethanol prior to embedding in paraffin. 3 μm thick sections were cut for immunohistochemistry.

Collagen staining and immunohistochemistry

Prior to staining, tissue sections were dewaxed in xylene for 10 minutes at room temperature and then rehydrated sequentially through 100%, 75% and 60% ethanol (5 minutes each step). Sections were then rehydrated in water for 10 minutes.

For picrosirius red (PSR) staining, sections were immersed in picrosirius red solution (Sigma, UK) and incubated for 60 minutes. Slides were then washed in water before sequentially dehydrating in alcohol (50 to 100%) and finally xylene before mounting in Pertex hard medium.

For immunostaining, sections were dewaxed and rehydrated as described. If required, an antigen retrieval step was performed (table 2.1). Sections were then washed in phosphate buffered saline (PBS) prior to quenching of endogenous peroxidases by incubation in 1% hydrogen peroxide solution for 10 minutes. Sections were washed with PBS and mounted into Sequenza racks. An avidin/biotin blocking kit (DAKO) was used to block endogenous activity (15 minute incubations with PBS washes). Species specific serum (20%) was used to block non-specific binding of the secondary antibody by incubation for 30 minutes. Following this, sections were incubated with the primary antibody made up in antibody diluent (DAKO) (as per table 2.1) for 60 minutes at room temperature. Appropriate isotype controls were used for each primary antibody. After a further set of PBS washes, sections were incubated with biotinylated secondary antibody (1:400 dilution) for 30 minutes. Vector RTU reagent was then applied (30 minute incubation) following which slides were developed for 3 minutes using 3, 3'-diaminobenzidine (Dako) and then counterstained for 10 seconds with Harris' haematoxylin. Slides were then washed in water before sequentially dehydrating in alcohol (50 to 100%) and finally xylene before mounting in Pertex hard medium.

Table 2.1 Commercial antibodies used for immunohistochemistry

Epitope	Primary antibody supplier	Antigen retrieval	Primary antibody dilution	Secondary antibody	Secondary antibody supplier	Dilution for DAB
MMP-9	Abcam	0.01M Sodium Citrate pH 6	1:500	Swine anti-rabbit biotinylated	Vector	1/400
Collagen 1	Southern Biotech	0.01M Sodium Citrate pH 6	1:100	Rabbit anti-goat biotinylated	Vector	1/300
Delta like kinase (Dlk)	Abcam	0.01M Sodium Citrate pH 6	1:150	Goat anti-rabbit biotinylated	Vector	1/500
α-smooth muscle actin (α-SMA)	Sigma	0.01M Sodium Citrate pH 6	1:2000	Rabbit anti-mouse	Vector	1/500
Pancyto-keratin (PCK)	Dako	0.01M Sodium Citrate pH 6, then proteinase K solution (125mcg/ml)	1:200	Goat anti-rabbit biotinylated	Vector	1/500
Ki67	Novo Castro	Tris-EDTA pH 9	1:500	Swine anti-rabbit biotinylated	Vector	1/500
MMP-13	Abcam	Tris-EDTA pH 9	1:800	Rabbit anti-sheep biotinylated	Vector	1/500
GFP	Abcam	Tris-EDTA pH 9	1:500	Rabbit anti-chicken /turkey biotinylated	Invitrogen	1/1000
F4/80	Abcam	-	1:50	Rabbit anti-rat biotinylated	Vector	1/400
Ly-6G	BD Pharmingen	-	1:100	Rabbit anti-rat biotinylated	Vector	1/400

Dual staining was used to determine the cellular source of MMP-9 in liver sections. Frozen sections were stained with MMP-9 and F4/80 or Ly-6G, which were detected with Alexa Fluor 488, 546 and 555 (Invitrogen) respectively. These slides were then mounted using Vectashield with DAPI (Vector Laboratories).

TUNEL staining (Promega) was performed on formalin fixed liver tissue as per the manufacturer's instructions. Briefly, following dewaxing, rehydration and permeabilisation using 20 μg/ml proteinase K, sections were incubated with the manufacturer's equilibration buffer with recombinant terminal deoxynucleotidyl transferase and a nucleotide mix. A DAPI nuclear stain in Vectashield mounting medium was used prior to fluorescent visualisation of apoptotic cells. Dual staining for α-SMA was visualised with streptavidin-Alexa Fluor 555 (Invitrogen).

Male cells were detected by Y chromosome fluorescent in situ hybridization (FISH) using FITC-labelled Y-chromosome paint (Star-FISH; Cambio), as previously described (Russo, Alison et al. 2006). Briefly, following dewaxing with xylene and rehydration through graded alcohols to water, liver sections were incubated in 1 M sodium thiocyanate at 80°C for 10 minutes. Following PBS washes, sections underwent proteolytic digestion (0.4% pepsin in 0.1 M HCl at 37°C) for 10 minutes before quenching with glycine (0.2% vol/wt). After further PBS washes, sections were postfixed in paraformaldehyde solution and then dehydrated through graded alcohols before air drying. The manufacturer's Y chromosome paint mix was applied to the sections which were then sealed under a coverslip with rubber cement and heated to 60°C for 10 minutes. The slides were then allowed to hybridise overnight at 37°C. The next day, the coverslips were removed and the slides rinsed in 0.5xSSC and then PBS before mounting in Vectashield with DAPI (Vector Laboratories). Appropriate male and female control liver tissue was included in each run.

Assessment of tissue sections

Stained slides were blinded and randomised prior to microscopy and photographing for quantification. Prior publications from our group that had used histological quantification of liver sections to examine these parameters used 10 images at x200 magnification (Fallowfield, Mizuno et al. 2007) and at least 10 images at x100 magnification (Duffield, Forbes et al. 2005). In order to facilitate identification of cells when counting, the higher x200 magnification was chosen. For comparison, a similar study of cell therapy for liver fibrosis by a different group had used only 6 images at x200 magnification (Nakamura, Torimura et al. 2007). The accuracy of the results increases with the number of images examined, however this must be balanced against the need for a practicable and efficient method. Use of a rolling mean of quantification scores had shown that achieving a minimum of 20 serial, non-overlapping fields at x200 magnification covered at least as large an area of liver tissue as in this recent literature whilst producing accurate data; therefore this method was adopted.

Male donor cells were detected by FISH for the Y chromosome. As not all male cells in a tissue section will have an exposed nucleus, the amount of Y chromosome probe binding will underrepresent the number of male cells. Therefore a correction coefficient was determined using male liver tissue. The proportion of non-parenchymal cells in male sections that bound the probe was established (54%). This allowed adjustment of subsequent counts to determine the total number of male donor cells present within female liver sections.

In order to quantify the number of F4/80, Ly-6G, GFP, MMP-9 and MMP-13 expressing cells, the number of positively stained cells per high power field was counted using Image J software (National Institutes of Health). Proliferating hepatocytes were identified as parenchymal cells with hepatocytic morphology and Ki67 positive nuclei (Nakamura, Torimura et al. 2007).

Pancytokeratin (PCK) has been validated as a marker of murine LPCs (Kofman, Morgan et al. 2005). Though considered sensitive for progenitor cells, this antigen is not specific as PCK is also a marker of biliary epithelia. As per Oben et al (Oben, Roskams et al. 2003) and Kofman et al (Kofman, Morgan et al. 2005), the consensus in the field is that LPCs can be more selectively detected by considering the location and morphology of these cells in addition to their expression of cytokeratin. These and subsequent studies (e.g. (Van Hul, Lanthier et al. 2011), (Bird, Lu et al. 2013)) defined LPCs as also being small oval/cuboidal cells with a high nuclear to cytoplasmic ratio, importantly, cells with hepatocyte like morphology and low nuclear to cytoplasmic ratio and also small cells directly abutting a lumen (considered bile duct cells) were excluded. This could potentially result in missing LPCs which are indistinguishable from the bile duct due to the two dimensional nature of histological sections however this method prevents incorrectly including cholangiocytes. Furthermore, the majority of LPCs are clearly distinct from the bile duct and so would be counted. To date, a fully sensitive and specific LPC marker has not been identified therefore this method combining cell marker, topography and morphology represents the current standard in the literature.

In order to quantify the amount of α-SMA, collagen I and PSR staining, the photomicrographs were processed using image analysis software (Adobe Photoshop). This produced a measurement of the area of staining; the percentage staining was calculated by using the total field area as the denominator. To allow for differences in staining intensity between different batches, all sections from the same experimental group were stained together under the same conditions. In order to compare across experimental groups, these measurements are expressed relative to matched control recipient samples from the same time point.

Protein measurement

Frozen whole liver samples (approximately 0.1cm^3) were placed in 300 μl of Tissue Protein Extraction Reagent (TPER) (Pierce). The sample was then disrupted by repeated passage through a 19 gauge needle, sonicated and centrifuged (at 12 000 rpm) for 10 minutes. The supernatant was then removed to determine the protein concentration by modified Bradford assay (Bradford 1976). 5 μl of protein extract was added to 150 μl of Bradford Reagent (Sigma) and 155 μl of distilled water. Bovine serum albumin (Sigma) was diluted to generate reference standards. Absorbance was measured at 595nm using a Biotek Synergy HT microplate reader (Biotek).

Multiplex cytokine assays for KC, MCP-1 (macrophage chemoattractant protein-1), MIP-1α (macrophage inflammatory protein-1α), MIP-2, IL-6, IL-10, TNFα, VEGF and CSF-1 were performed using the Bio-Plex Pro Magnetic Cytokine Assay kit on the Bio-Plex 200 Suspension Array system and Bio-Plex Pro Wash Station (Bio-Rad) in collaboration with Dr Tim Gordon-Walker. Cytokine assays were performed according to the manufacturer's instructions. Test samples were diluted to a concentration of 10 mg/ml, eight standards in addition to blank wells (to determine background fluorescence) were used; all measurements were in duplicate. Per well, 50 μl of sample was incubated with magnetic beads (conjugated to the capture antibody of interest) for 30 minutes at room temperature. Samples were then washed 3 times in 100 μl of Bio-Rad Wash buffer (Bio-Rad). The biotinylated detection antibody was then added to samples and incubated for 30 minutes at room temperature. After a further wash step (3 times in 100μl of Bio-Rad Wash buffer (Bio-Rad)), the samples were incubated with the streptavidin-conjugated phycoerythrin reporter for 10 minutes at room temperature. The samples were again washed as previously before resuspension in Bio-Rad Assay buffer (Bio-Rad). This mixture was then analysed on the Bio-Plex 200 Suspension Array system using Bio-Plex Manager 3.0 software (Bio-Rad) and the concentration of each target protein calculated against

the standard curve. Final protein concentrations are expressed relative to matched control samples from the same time point.

Serum biochemistry measurements were performed independently by the Specialist Assay Service run by Dr Forbes Howie (Centre for Reproductive Medicine) using the Roche Cobas Fara Centrifugal Analyser. Commercial kits for serum albumin (Randox Laboratories Ltd) and ALT and bilirubin (Alpha Laboratories Ltd) were used. Successful venesection requires aspiration of blood at the time of euthanisation but before cardiac death. In addition to this relatively narrow window for venesection, the small calibre of needle required to cannulate murine vessels can cause sample haemolysis. Therefore adequate samples were not obtained from all subjects.

Hydroxyproline assay

Snap frozen liver samples (approximately 200 mg) were weighed and homogenised prior to hydrolysing in 2N sodium hydroxide at 120°C for 20 minutes. The hydrolysed samples were then mixed with acetate-citrate buffered chloramine T reagent (0.056M) and allowed to oxidise at room temperature for 25 minutes. Ehrlich's aldehyde reagent was then added prior to incubation at 65°C for 20 minutes. Absorbance was measured at 550 nm using a spectrophotometer and hydroxyproline content expressed as μg/g liver (Reddy and Enwemeka 1996).

Quantification of mRNA levels by Real Time Reverse-Transcription Polymerase Chain Reaction

RNA was extracted from whole liver tissue using RNA extraction kits (RNeasy mini kit, Qiagen) according to the manufacturer's instructions. Briefly, approximately 30 mg of frozen liver tissue was added to 600 μl of buffer RLT (with 10 μl/ml β-mercaptoethanol added) disrupted and then homogenised using the QIAshredder microfuge column (Qiagen). The lysate was centrifuged at high speed for 3 minutes

and the resulting supernatant was mixed with an equal volume of 70% ethanol before transferring to an RNeasy spin column (Qiagen) to centrifuge for 15 seconds at 10 000 rpm. The column was then washed firstly by the addition of 700 μl of RW1 buffer and centrifugation for 15 seconds at 10 000 rpm. 500 μl of RPE buffer was then used to wash the column by further centrifugation for 15 seconds at 10 000 rpm. This was then repeated with another 500 μl of RPE buffer for a longer centrifugation of 2 minutes. The RNA was then eluted from the column by adding 50 μl of RNase-free water directly to the column membrane and centrifuging for 1 minute at 10 000 rpm. The resulting concentration of RNA was measured using a NanoDrop (Thermo Fisher).

Complementary DNA was reverse transcribed from 1 μg of RNA using the Superscript II kit (Invitrogen) according to the manufacturer's instructions. Briefly, per sample, 0.8 μl DNAse I solution, 1 μl 10x DNAse reaction buffer and DNAse/RNAse free water were added to 1 μg of RNA to make a total volume of 8.2 μl. After 15 minutes at room temperature, 0.8 μl of 25 nM EDTA solution was added prior to heating to 65°C for 10 minutes. Each 20 μl reaction also included 2 μg (in 2 μl) of random hexamers, 4 μl of 5xRT buffer, 0.5 μl of 10mM dNTP mix, 2 μl of 0.1 M DTT, 0.5 μl of Superscript II, 0.5 μl of RNAse inhibitor and 1.5 μl of DNAse/RNAse free water. The reaction was carried out at 37°C for 60 minutes before inactivation and storage.

Primers for MMPs-2, 9, 12 and 13, Fizz-1, IL-10, inducible nitric oxide synthase (iNOS), MCP-1, mannose receptor, TNF-α and Ym-1 were designed using primer express software (table 2-2). Predesigned, validated primer sets for macrophage inflammatory protein (MIP)-1α, MIP-2, KC, MMP-8, HGF, insulin-like growth factor-1 (IGF-1), CK-19 and TWEAK were purchased from Qiagen (UK). A predesigned, validated eukaryotic 18S primer/probe set (Applied Biosystems) was used as the internal control.

Equal amounts of cDNA from each sample were combined and diluted 1:9 in DNAse/RNAse free water to generate a standard which was then serially diluted 1:1 to produce 7 reference standards. Test samples of cDNA were diluted 1:100 for analysis. 10 µl of reaction mixture per well of the optical plate contained 4 µl of diluted cDNA, 5 µl of SYBR Green Master Mix (Qiagen) and 1 µl of primer mix. All reactions were performed in triplicate. The reaction conditions were 1 cycle of 95°C for 20 seconds to activate DNA polymerase and then 40 cycles of denaturation (95°C for 3 seconds) and annealing/extension (60°C for 30 seconds) on an ABI 7500 Fast Real Time PCR system (Applied Biosystems). Where primer probe sequences were used (table 2.2), TaqMan Express qPCR Supermix (Invitrogen) was used as per manufacturer's instructions. Gene expression was internally controlled by measuring expression of ribosomal 18S in the same sample. These standardised results are expressed relative to matched experimental control samples from the same time point.

Table 2.2 Primer sequences designed using primer express software

Gene	Orientation	Sequence
MMP-2	forward	5′-AACTACGATGACCGGAAGTG-3′
	reverse	5′-TGGCATGGCCGAACTCA-3′
	probe	5′-TCTGTCCTGACCAAGGATATAGCCTATTCCTCG-3
MMP-9	forward	5′-CGAACTTCGACACTGACAAGAAGT-3′
	reverse	5′-GCACGCTGGAATGATCTAAGC-3′
	probe	5′-TCTGTCCAGACCAAGGGTACAGCCTGTTC-3′
MMP-12	forward	5′-GAAACCCCCATCCTTGACAA-3′
	reverse	5′-TTCCACCAGAAGAACCAGTCTTTAA-3′
	probe	5′-AGTCCATCAACTTTCTGTCACCAAAGC-3′
MMP-13	forward	5′-GGGCTCTGAATGGTTATGACATTC-3′
	reverse	5′-AGCGCTCAGTCTCTTCACCTCTT-3′
	probe	5′-AAGGTTATCCCAGAAAAATATCTGACCTGGGATTC-3′
Fizz-1	forward	5′-TACTTGCAACTGCCTGTGCTTACT-3′
	reverse	5′-TATCAAAGCTGGGTTCTCCACCTC-3′
IL-10	forward	5′-TGCAGGACTTTAAGGGTTACTTGG-3′
	reverse	5′-CAGGGAATTCAAATGCTCCTTG-3′
iNOS	forward	5′-CTATCTCCATTCTACTACTACCAGATCGA -3′
	reverse	5′-CCTGGGCCTCAGCTTCTCAT-3′

Mannose receptor	forward	5′-CATCTGGCTTCTCCTGCTTCT-3′
	reverse	5′-TTGCCGTCTGAACTGAGATGG-3′
MCP-1	forward	5′-CTTCTGGGCCTGCTGTTCA-3′
	reverse	5′-CCAGCCTACTCATTGGGATCA-3′
TNF-α	forward	5′-CGCTCTTCTGTCTACTGAACTT-3′
	reverse	5′-GATGAGAGGGAGGCCATT-3′
Ym-1	forward	5′-TCACAGGTCTGGCAATTCTTCTG-3′

Statistical Analysis

Statistical support for data analysis was received from Justin Scott (statistician, University of Queensland): parametric data were analysed by 2 tailed Student's t test whilst Mann-Whitney U test was used for non-parametric data and data are presented as mean ± standard error of the mean, unless otherwise stated. These calculations were conducted using Prism by GraphPad Software Inc. Statistical analysis was performed on absolute values.

As explained in "Assessment of tissue sections", inter-experimental variables in particular tissue staining intensity were controlled for by comparing samples with matched controls stained in the same run. Therefore measurements of effect in a treatment group were only directly analysed against the matched controls from the same experiment. In order to represent temporal trends between different experiments graphically, measurements from each experiment are expressed relative to the specific time-matched control. Mathematically, each data point within an individual experiment (treatment and control) was divided by the mean value of the control group thereby expressing the treatment effect as a ratio of its matched control and preserving the relative distributions therefore including error bars.

CHAPTER THREE

Characterisation and selection of candidate donor bone marrow cell populations

Introduction

As described, a number of groups have found potential benefits of BM cell therapy for liver disease in human subjects and also murine models. In order to inform the rational design of clinical studies, the aim of this project was to determine which cell types might have beneficial effects in experimental models and to explore the underlying mechanism(s).

Given the lack of clarity regarding the precise cell populations used in the literature, a hierarchical approach was taken to allow the accurate delineation of candidate donor BM derived cells in a logical manner. Considering the theoretical basis for macrophages having potential as cell therapy (Sakaida, Terai et al. 2004; Duffield, Forbes et al. 2005), BM was fractionated by lineage. Candidate cells included whole BM, those BM cells with the capacity to differentiate into macrophages ("macrophage precursor cells") and the differentiated macrophages (BMMs) themselves. By using clearly defined cell types and examining their effects when applied to experimental models, I aimed to investigate their utility as therapeutic agents. Well characterised BM cell populations were used in order to improve mechanistic understanding and facilitate subsequent translation to the clinic.

The aim of this chapter is to describe the different outcomes of the candidate donor cells types on CCl_4 liver injury.

Characterisation of candidate bone marrow cell types

Whole (unfractionated) bone marrow contains heterogeneous populations of cells. These include HSCs, myelopoietic and erythropoietic cells and stromal cells (including MSCs, endothelial cells and their progenitors and fibroblasts) in addition to lymphocytes, plasma cells, megakaryocytes and reticular cells (Yang, Busche et al. 2013). As previously discussed, some of these cells e.g. MSCs (Russo, Alison et al. 2006; di Bonzo, Ferrero et al. 2008) and fibroblasts, could have fibrogenic effects and thus be deleterious in the therapeutic context. A subset of the BM is comprised of cells with the potential to differentiate into macrophages. The differentiation of BM progenitors into macrophages is controlled by the lineage restricted growth factor, CSF-1. CSF-1 (also known as macrophage colony stimulating factor (M-CSF)) promotes macrophage differentiation through binding to the cell surface receptor (CSF-1R). CSF-1R is encoded by the *c-fms* gene. Sasmono and colleagues developed transgenic mice with an EGFP reporter gene under the control of the *c-fms* promoter (termed MacGreen mice). This allows detection of BM cells with the capacity to respond to CSF-1 stimulation and therefore develop into macrophages in the correct circumstances. Flow cytometric analysis of MacGreen mouse BM shows that EGFP co-localises with CD11b indicating that transgene expression is confined to myeloid cells. Approximately 50% of EGFP positive BM cells express F4/80 or CSF-1R protein (Sasmono, Oceandy et al. 2003).

Interestingly, subsequent work by the same group showed that EGFP expression was not restricted to macrophages. Neutrophils (marked by the Ly-6G antigen) also expressed the EGFP reporter indicating transcription of the CSF-1R gene. Neutrophils have previously been shown to undergo a lineage switch to cells with the morphological, cytochemical and phenotypic characteristics of macrophages under the influence of CSF-1 (Araki, Katayama et al. 2004). Of particular relevance, Sasmono and colleagues went on to demonstrate that the 7 day *in vitro* culture of murine neutrophils with CSF-1 results in their transdifferentiation into mature F4/80 positive macrophages (Sasmono, Ehrnsperger et al. 2007). FACS was used to separate

the EGFP expressing cells from the BM of MacGreen mice (figure 3.1A) thereby selecting potential macrophage precursor cells. There appear to be two populations of EGFP expressing BM cells in figure 3.1A. Whilst these EGFP positive cells all have the potential to differentiate into macrophages upon stimulation with CSF-1, this may reflect differential CSF-1R promoter activity between granulocytes and mononuclear cells.

In contrast to the potential macrophage precursor cells fluorescently sorted from the BM of MacGreen mice, differentiated BMMs were cultured in non-adherent conditions for 7 days. BMMs produced in this way are recognised as naïve (unstimulated) macrophages. The photomicrograph of the BMM cytospin Diff-Quik stain shows that the majority of these cells were morphologically homogenous (figure 3.1B). Further characterisation by flow cytometry demonstrated that BMMs expressed the conventional macrophage markers of F4/80 and CD11b (Hume 2006) without significant contamination by Ly-6C positive monocytes, Ly-6G positive neutrophils, CD3 positive T lymphocytes or CD19 positive B lymphocytes (figure 3.1C). The gene expression of a panel of phenotypic activation markers was measured in order to consider unstimulated BMMs in the traditional paradigm of the classically (M1) and alternatively (M2) activated macrophage (Mosser and Edwards 2008) (figure 3.2A). These results are from collaboration with Stephen Hartland and Marielle Van Deemter. In comparison with macrophages deliberately stimulated to develop the polarised M1 and M2 phenotypes, naïve BMMs do not fit clearly into either classification (figure 3.2B). Donor BMMs expressed a number of factors with potentially anti-fibrotic, chemotactic, anti-inflammatory and pro-regenerative activity (table 3.1).

Figure 3.1 Characterisation of candidate donor cells

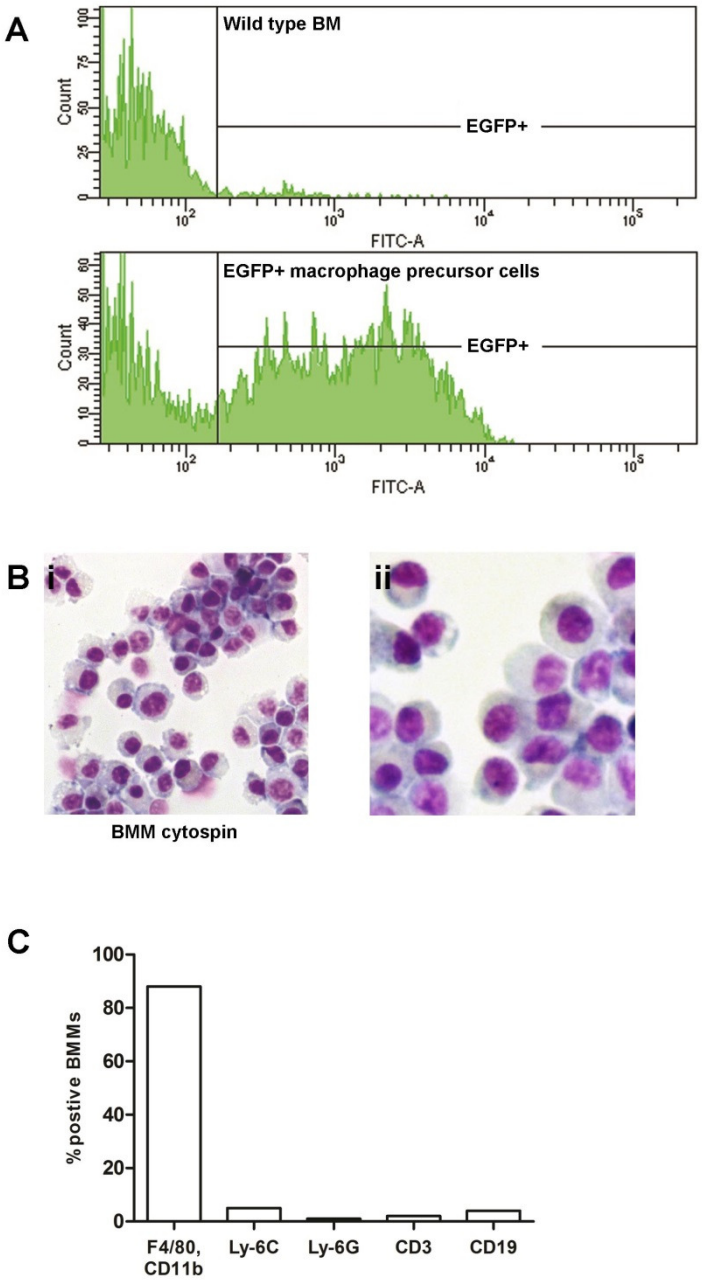

Figure 3.1 Characterisation of candidate donor cells

D

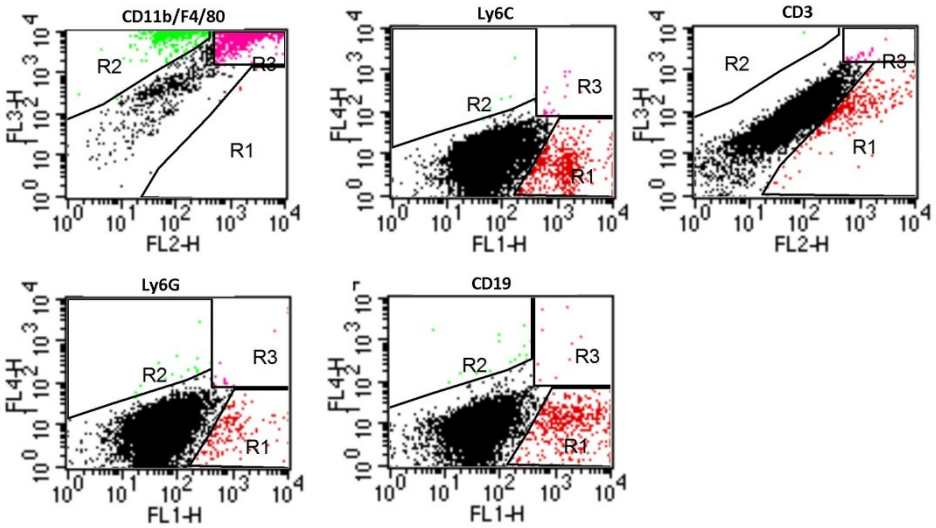

BMM flow cytometry plots

Figure 3.1 Characterisation of candidate donor cells

(**A**) MacGreen mouse BM cells expressing the CSF-1 receptor/EGFP transgene are potential macrophage precursors. These cells were positively selected by FACS (denoted "EGFP+ macrophage precursor cells").

(**B i**) Macrophages were differentiated from whole BM cultured for 1 week in CSF-1 conditioned media. Diff-Quik staining of cytospins of these cells demonstrates that they are mononuclear with the characteristic staining profile of violet nuclei with light blue cytoplasm. Original magnification, x200. **B ii** shows a cytospin under higher effective magnification (x400) allowing clearer visualisation of the morphological heterogeneity.

(**C**) Flow cytometric analysis demonstrated that BMMs possessed the typical macrophage markers F4/80 and CD11b. The donor BMMs were relatively pure; markers of other leukocyte populations (monocytes, neutrophils and T and B cells) were minimally detected. This histogram was derived from the data in figure D.

(**D**) Original flow cytometry plots determining BMM surface marker expression. CD11b - F4/80 co-positive cells were in gate R3, positive cells in the single fluorochrome assessments were gated as R1. Flow cytometry was done in conjunction with Kay Samuel (CRM).

Figure 3.2 Donor BMMs are phenotypically intermediate between classically and alternatively activated macrophages

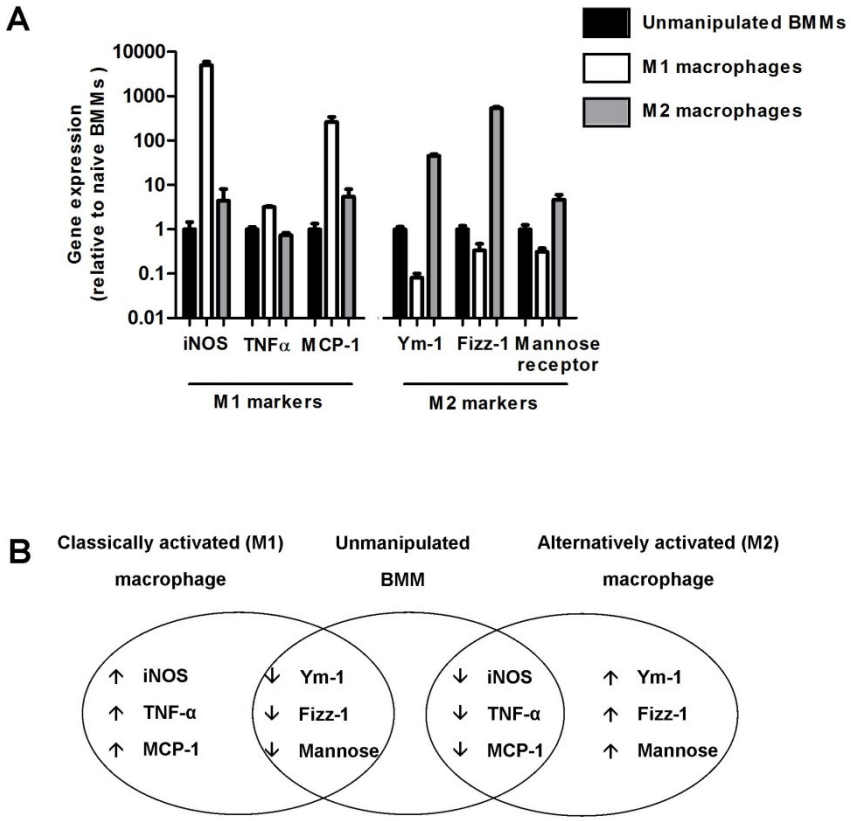

Figure 3.2 Donor BMMs are phenotypically intermediate between classically and alternatively activated macrophages

(**A, B**) BMMs were stimulated by *in vitro* incubation with lipopolysaccharide and interferon-γ or IL-4 and IL-13 to polarise them to the traditional classically (M1) or alternatively (M2) activated phenotype respectively. Unstimulated (naïve) BMMs were then examined in this context. Gene expression analysis of classical and alternative macrophage activation markers demonstrated that BMMs did not conform to either phenotype in this regard. These figures are descriptive therefore no statistical analysis was performed; n=3 per group. Data in collaboration with Stephen Hartland and Marielle Van Deemter.

Table 3.1 Pre-injection BMMs expressed anti-inflammatory, anti-fibrotic, pro-regenerative and chemotactic mediators

Gene	BMM gene expression (relative to untreated fibrotic liver)	BMM Mean +/- SEM	BMM N	Control liver Mean +/- SEM	Control liver N	P value (S = Student's t test, MW = Mann-Whitney test)
IL-10	2.2	6.5 +/- 1.5	5	2.9 +/- 2.4	5	0.15 (MW)
MMP-13	38.4	14.6 +/- 3.0	5	0.4 +/- 0.04	5	<0.01 (S)
TWEAK	20.7	17.6 +/- 2.8	5	0.8 +/- 0.1	5	<0.01 (S)
MCP-1	75.6	19.4 +/- 4.1	5	0.3 +/- 0.03	5	<0.01 (S)
MIP-1α	668.9	42.7 +/-10.1	5	0.1+/- 0.004	5	<0.01 (S)
MIP-2	77.6	20.3 +/- 3.2	5	0.3 +/- 0.2	5	<0.01 (MW)
KC	0.4	1.7 +/- 0.3	5	4.2 +/- 0.9	5	0.04 (S)

Cells of the monocyte-macrophage lineage have differential effects on liver fibrosis

1 x 10^6 candidate donor BM derived cells were delivered via the HPV 6 weeks into a 10 week CCl_4 injury protocol. Mice were then euthanised and tissue harvested for analysis. The schematic below demonstrates the time course of the experiment (figure 3.3).

Figure 3.3 Schematic of CCl_4 experimental protocol testing candidate donor BM cells

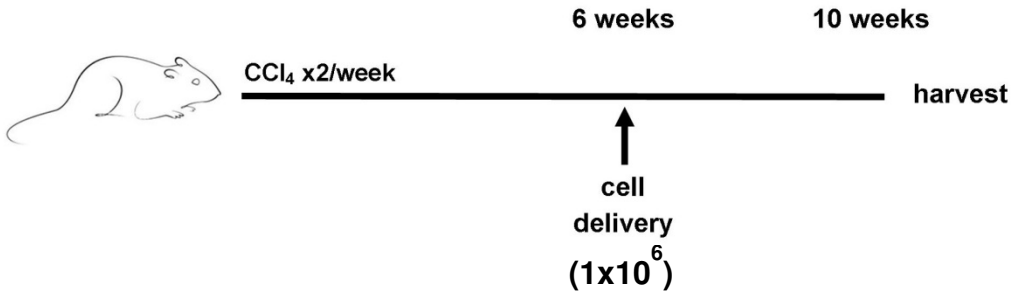

4 weeks after the injection of 1 x 10^6 whole BM cells, there was an increase in liver fibrosis measured by PSR quantification. Whole BM cell recipient mice had 161% more fibrosis than controls ($P < .05$, figure 3.4A, B). In contrast to this pro-fibrogenic effect, injecting 1 x 10^6 macrophage precursor cells did not significantly change the amount of fibrosis ($P = .21$, figure 3.4A, B). The same number of BMMs however resulted in a significant reduction in fibrosis (67% of control, $P < .05$, figure 3.4A, B).

Figure 3.4 BM derived cell populations have differential effects on liver fibrosis

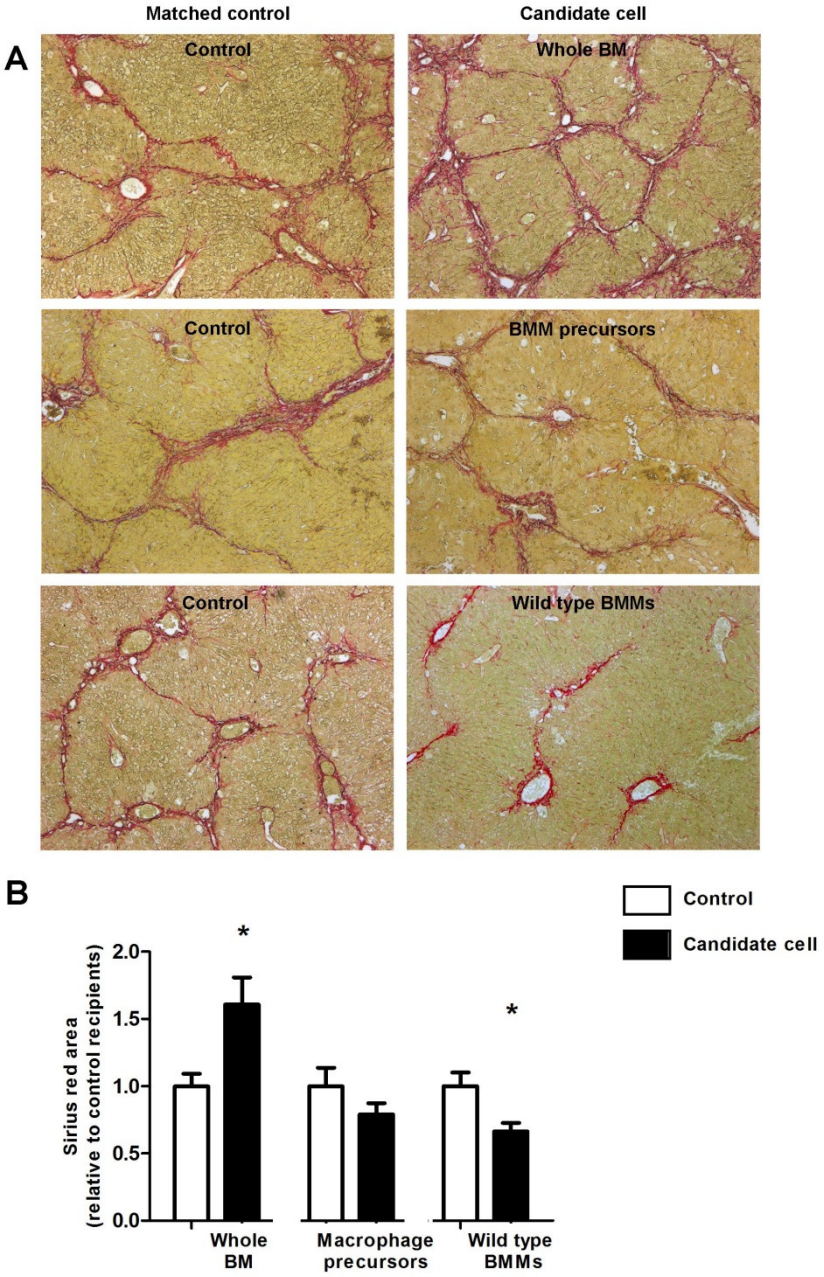

Figure 3.4 BM derived cell populations have differential effects on liver fibrosis

Advanced liver fibrosis was induced in adult female mice by the chronic administration of twice weekly IP CCl_4.

(**A**) Photomicrographs show PSR staining for fibrillar collagens 4 weeks after the intraportal delivery of 1 x 10^6 syngeneic whole (unfractionated) BM, macrophage precursor cells or wild type BMMs (right sided column). Age and strain-matched mice within each cohort received an equal volume of control medium (left sided column). As stated in the Methods, macrophage precursor cells were obtained from the BM of MacGreen mice on a balb-c background therefore these cells were delivered to fibrotic balb-c recipients. Whole BM and BMMs were obtained from C57Bl/6 mice and therefore delivered to C57Bl/6 mice. Original magnification, x80.

(**B**) Morphometric analysis of PSR staining revealed that the application of whole BM increased the amount of fibrosis. BM macrophage precursor cells did not significantly change the amount of fibrosis. Treatment with differentiated BMMs caused a reduction in liver scarring. (* $P < .05$ compared with control recipients; n=6-7 per group). These histograms are derived from the data in table 3.2 below. Within each separate experiment, all values are expressed as a ratio of the mean of the internal control group. This allows a graphical comparison of the magnitude of treatment effect between experiments.

Table 3.2 BM derived cell populations have differential effects on liver fibrosis

Candidate cell type	Whole BM	Macrophage precursor cells	BMMs
Control PSR % Mean +/- SEM	4.9 +/- 0.5	9.7 +/- 1.3	7.2 +/- 0.7
Control N	6	6	7
Candidate cell PSR % Mean +/- SEM	7.9 +/- 1.0	7.7 +/- 0.8	4.8 +/- 0.4
Candidate cell N	6	7	6
P value (S = Student's t test)	0.02 (S)	0.21 (S)	0.02 (S)

BMM delivery improves liver fibrosis and serum albumin levels

Given the reduction in PSR staining following the injection of BMMs, subsequent experiments focused on specifically examining this phenotype with regard to its translational potential. Additional methods of scar quantification were employed to confirm the magnitude of effect from BMM delivery. Hydroxyproline is a post-translational product of the hydroxylation of the amino acid proline and a key component of collagen (Reddy and Enwemeka 1996). Hydroxyproline assay carried out on approximately 200mg pieces of liver demonstrated a similar magnitude decrease in liver collagen following BMM therapy (368.2 ±41.0 v 558.8 ±94.6 μg/g liver, $P = .05$, figure 3.5A). Specific immunostaining for collagen I was quantified using image analysis, this also confirmed a comparable improvement in BMM recipients (73% of control, $P < .01$, figure 3.5B, C). These data support the PSR morphometric analysis (figure 3.4) detecting an approximately 1/3 reduction in liver fibrosis following BMM delivery.

Figure 3.5 BMM therapy causes a reduction in liver fibrosis

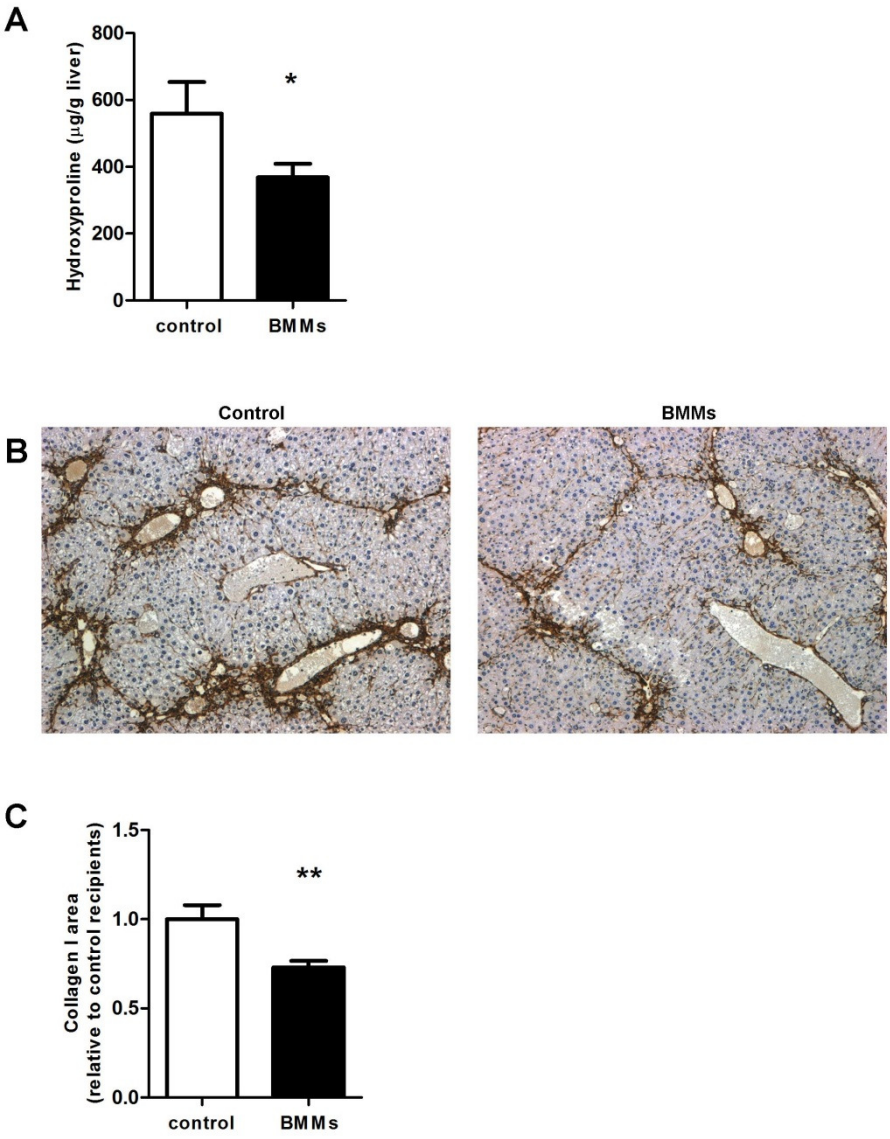

Figure 3.5 BMM therapy causes a reduction in liver fibrosis

Following identification of the anti-fibrotic effect of BMMs, further experiments using alternative measures of scar quantification were undertaken to confirm the magnitude of this effect. Advanced liver fibrosis was induced in adult female C57Bl/6 mice by administration of twice weekly IP CCl_4. The reduction in liver fibrosis 4 weeks after the intraportal delivery of 1 x 10^6 BMMs was confirmed by (**A**) hydroxyproline assay and (**B**) collagen I immunostaining (original magnification, x80) with (**C**) morphometric analysis and quantification. (* $P \leq .05$, ** $P < .01$ by 1 tailed analysis compared with control recipients; n=6-7 per group). This histogram is derived from the data in table 3.3 below; all values are expressed as a ratio of the mean of the internal control group.

Table 3.3 BMM therapy causes a reduction in liver fibrosis

Assay	Hydroxyproline content (µg/g)	Collagen 1 staining (%)
Control Mean +/- SEM	558.8 +/- 94.6	11.6 +/- 0.9
Control N	7	7
BMMs Mean +/- SEM	368.2 +/- 41	8.5 +/- 0.4
BMMs N	6	6
P value (S = Student's test, 1 tailed)	0.05(S)	<0.01(S)

In addition to determining the impact of the candidate BM derived donor cells on liver fibrosis, serum was also taken at the time of euthanisation 4 weeks after cell injection to measure albumin and bilirubin levels. These tests are routinely used as indicators of "liver function" in the clinical setting.

It is important to note that there is group to group variability between cohorts of CCl_4 treated mice. This is likely to be mostly attributable to differences between mouse strains. In addition, there may well be minor variations in housing conditions, composition and delivery of CCl_4 and potentially host factors even within an inbred strain. This was addressed by using inbred strains of mice housed in the same rooms within one animal facility and only directly comparing the effects of intervention against control within the same mouse cohort (as opposed to between).

Neither the delivery of whole BM (36.0 ± 0.6 v 36.5 ± 0.5 g/L) nor macrophage precursor cells (42.2 ± 3.3 v 39.4 ± 0.5 g/L) significantly affected serum albumin levels. However, BMM therapy resulted in an increase in serum albumin from 39.9 ± 0.9 g/L in the control group to 46 ± 2.6 g/L post treatment (figure 3.6A). Albumin is synthesised by the liver. Low serum levels can indicate reduced hepatic synthetic function therefore serum albumin is a marker of liver regeneration. Serum albumin in also an acute phase marker, therefore laparotomy at the time of HPV cell injection could also affect this. For reference, normal adult murine albumin is ~40 g/L (Fernandez, Pena et al. 2010). Mice that received iterative CCl_4 but did not undergo surgery had a mean serum albumin of 39.5 g/L (figure 5.4C). This suggests that the CCl_4 induced injury was not sufficiently severe to cause liver decompensation with associated low serum albumin levels. Furthermore, if surgery did cause a reduction in serum albumin in this context, then this effect was transient as it was not apparent 4 weeks later at the time of harvest. Though baseline albumin levels were not significantly suppressed, the additional increase in serum albumin following BMM therapy suggests a pro-regenerative stimulus. This is consistent with work examining the peripheral delivery of BMMs to normal (uninjured) mice. (Bird, Lu et

al. 2013) In this setting, in the absence of surgery or liver injury, BMM injection caused LPC expansion via TWEAK signalling and increased serum albumin levels indicating enhanced liver function.

Serum bilirubin measurements were obtained following the application of whole BM and differentiated BMMs. Consistent with the increase in fibrosis following BM delivery, there was a significant rise in serum bilirubin (7. 7 ± 0. 9 v 11.8 ± 1.5 μmol/L) in the whole BM recipients. Serum bilirubin levels were not elevated in either the control or BMM treatment groups (figure 3.6B).

The results of these serum measurements in conjunction with the improvement in liver fibrosis indicated a potentially beneficial phenotype following BMM delivery. Therefore, subsequent experiments focused on exploring the nature of these effects and the underlying mechanisms. The following results chapters detail this work.

Figure 3.6 Effects of BM derived cells on serum biochemical markers of liver function 4 weeks after cell injection

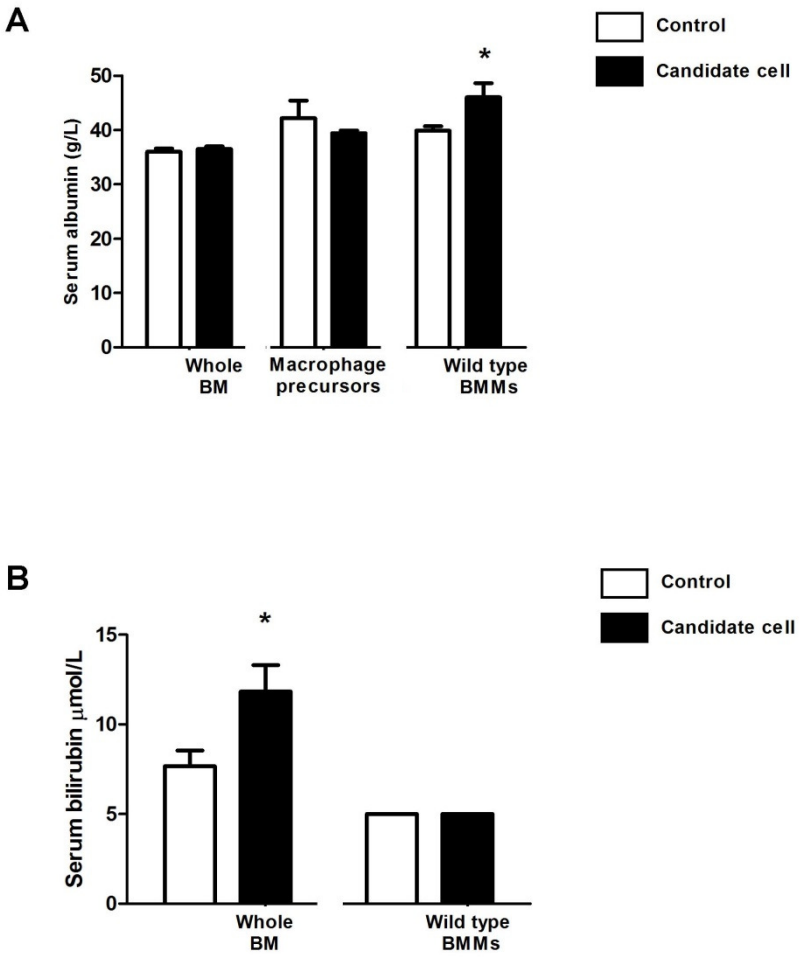

Figure 3.6 Effects of BM derived cells on serum biochemical markers of liver function 4 weeks after cell injection

Advanced liver fibrosis was induced in adult female mice by the chronic administration of twice weekly IP CCl_4. Whole BM and BMM cell experiments were carried out in C57Bl/6 mice, macrophage precursor cell experiments were in balb-c mice. 1 x 10^6 cells were injected via the HPV. Serum taken 4 weeks afterwards was analysed to determine the effect on biochemical markers of liver function.

(**A**) Serum albumin levels did not significantly change following the delivery of 1 x 10^6 whole BM or macrophage precursor cells. In contrast, BMM therapy resulted in a significant increase in albumin levels.

(**B**) Serum bilirubin levels rose just above the normal range after the application of whole BM cells. When testing the effects of BMM therapy, no sample in either the control or treatment group had a measurable serum bilirubin above the 5 μmol/L assay detection level (graphically represented as 5 μmol/L without error bars). Serum samples from the macrophage precursor cell experiment were not available for bilirubin measurement. (* $P \leq .05$, compared with control recipients; n=6-8 per group).

Tables 3.4 Effects of BM derived cells on serum biochemical markers of liver function 4 weeks after cell injection

Candidate cell type	Whole BM	Macrophage precursor cells	BMMs
Control Serum albumin (g/L) Mean +/- SEM	36 +/- 0.6	42.2 +/- 3.2	39.9 +/- 0.9
Control N	6	6	7
Candidate cell Serum albumin (g/L) Mean +/- SEM	36.5 +/- 0.5	39.4 +/- 0.5	46.0 +/- 2.6
Candidate cell N	6	5	8
P value (S = Student's test, MW = Mann-Whitney test)	0.62 (MW)	0.46 (S)	0.05 (S)

	Control serum bilirubin (µmol/L)	Whole BM serum bilirubin (µmol/L))
Mean +/- SEM	7.7 +/- 0.9	11.8 +/- 1.5
N	6	6
P value (S = Student's test)	0.04 (S)	

CHAPTER FOUR

Cellular and molecular events underlying BMM therapy

Introduction

The previous chapter describes the therapeutic changes caused by the application of BMMs in contrast to their specific BM precursors and unfractionated (whole) BM. I went on to examine the underlying cellular and molecular processes following BMM delivery. With regard to clinical translation, a robust approach is to have a clear characterisation of the donor cells to be given and also their *in vivo* effects based on experimental models. These data can then inform the rational design of clinical studies to test efficacy in cirrhotic patients.

These studies involved analysing the phenotype of donor BMMs, tracking their passage in recipient liver and measuring the effects on mediators of liver fibrosis, inflammation and regeneration. Interestingly, it became apparent that whilst the changes detected in the host liver were initiated by the delivery and engraftment of a relatively small number of donor BMMs, this also involved a paracrine interaction with host cells to mediate these whole organ effects.

This work was carried out in the well characterised CCl_4 model of liver injury and fibrosis. To determine whether BMM therapy had utility in a predominantly cholestatic model of liver injury, I also tested its effects in mice fed the 1% DDC diet.

Key changes occur relatively early following BMM therapy

Following identification of the improvement in liver fibrosis and serum albumin 4 weeks after BMM delivery, tissue from this time point was examined to determine the cellular and molecular changes underpinning these effects.

α-SMA positive myofibroblasts are considered to be the predominant source of ECM synthesis during fibrogenesis. There is an increase in the number of scar producing myofibroblasts during chronic liver injury. Conversely, apoptosis of myofibroblasts is a critical early event during the resolution of fibrosis (Iredale, Benyon et al. 1998). Therefore, the area of α-SMA staining was measured using image analysis software. This did not show a statistically significant reduction in myofibroblasts 4 weeks after BMM delivery (figure 4.1A, B). As described, MMPs (in particular MMP-13 and MMP-9) are known to be key mediators of matrix degradation in the liver. Therefore gene expression of these enzymes was also measured at this time point. This showed no significant change in either MMP-13 or MMP-9 expression (figure 4.1C, D).

In order to detect a pro-regenerative stimulus to the recipient liver as a potential explanation for the increase in serum albumin, I investigated both the hepatocyte and LPC compartments. Quantification of Ki67 positive hepatocytes as a marker of cellular proliferation (Gerlach, Sakkab et al. 1997) did not reveal a significant increase following BMM delivery at this 4 week time point (figure 4.2A, B). Similarly, quantification of PCK positive LPCs did not show any difference at this stage (figures 4.2C, D).

The transfer of male donor BMMs into female mice allows detection of donor cells by FISH for the Y chromosome. Interestingly, by 4 weeks, donor BMMs were not detected in the recipient liver (figure 4.3C). Therefore the next set of experiments was designed to examine the early changes occurring after BMM delivery in order to detect the key events responsible for the observed phenotype (figure 4.2E).

Figure 4.1 No difference in mediators of fibrosis detected 4 weeks after BMM therapy

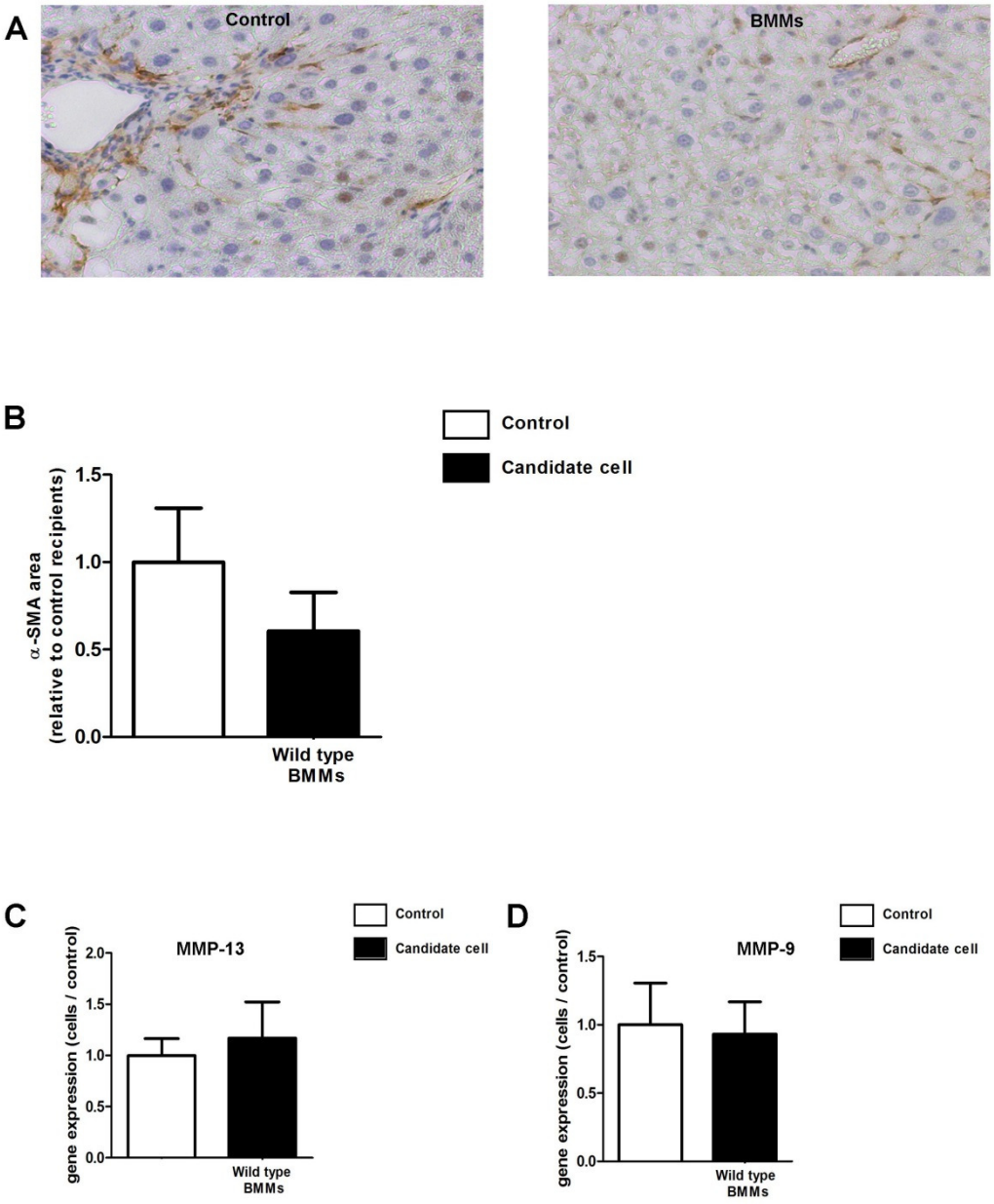

Figure 4.1 No difference in mediators of fibrosis detected 4 weeks after BMM therapy

Advanced liver fibrosis was induced in adult female C57Bl/6 mice by the chronic administration of twice weekly IP CCl_4.

(**A**) Photomicrographs show α-SMA staining for myofibroblasts 4 weeks after BMM delivery. Original magnification, x200.

(**B**) Morphometric analysis demonstrates that there was not a statistically significant reduction in α-SMA staining in the BMM recipient group at this time point.

(**C, D**) Gene expression of the fibrolytic enzymes MMP-13 and MMP-9 was not elevated 4 weeks after BMM therapy (compared with control recipients; n=7-8 per group).

These histograms are derived from the data in table 4.1 below; all values are expressed as a ratio of the mean of the internal control group.

Table 4.1 No difference in mediators of fibrosis detected 4 weeks after BMM therapy

	Control	BMMs
α-SMA % Mean +/- SEM	3.5 +/- 1.1	2.1 +/- 0.8
α-SMA % N	8	8
P value (Mann-Whitney test)	0.14	
MMP-13 gene expression Mean +/- SEM	8.0 +/- 1.3	9.4 +/- 2.8
MMP-13 gene expression N	7	8
P value (Student's t test)	0.68	
MMP-9 gene expression Mean +/- SEM	6.3 +/- 2.2	5.9 +/- 1.5
MMP-9 gene expression N	7	8
P value (Mann-Whitney test)	0.73	

Figure 4.2 No difference in mediators of regeneration detected 4 weeks after BMM therapy

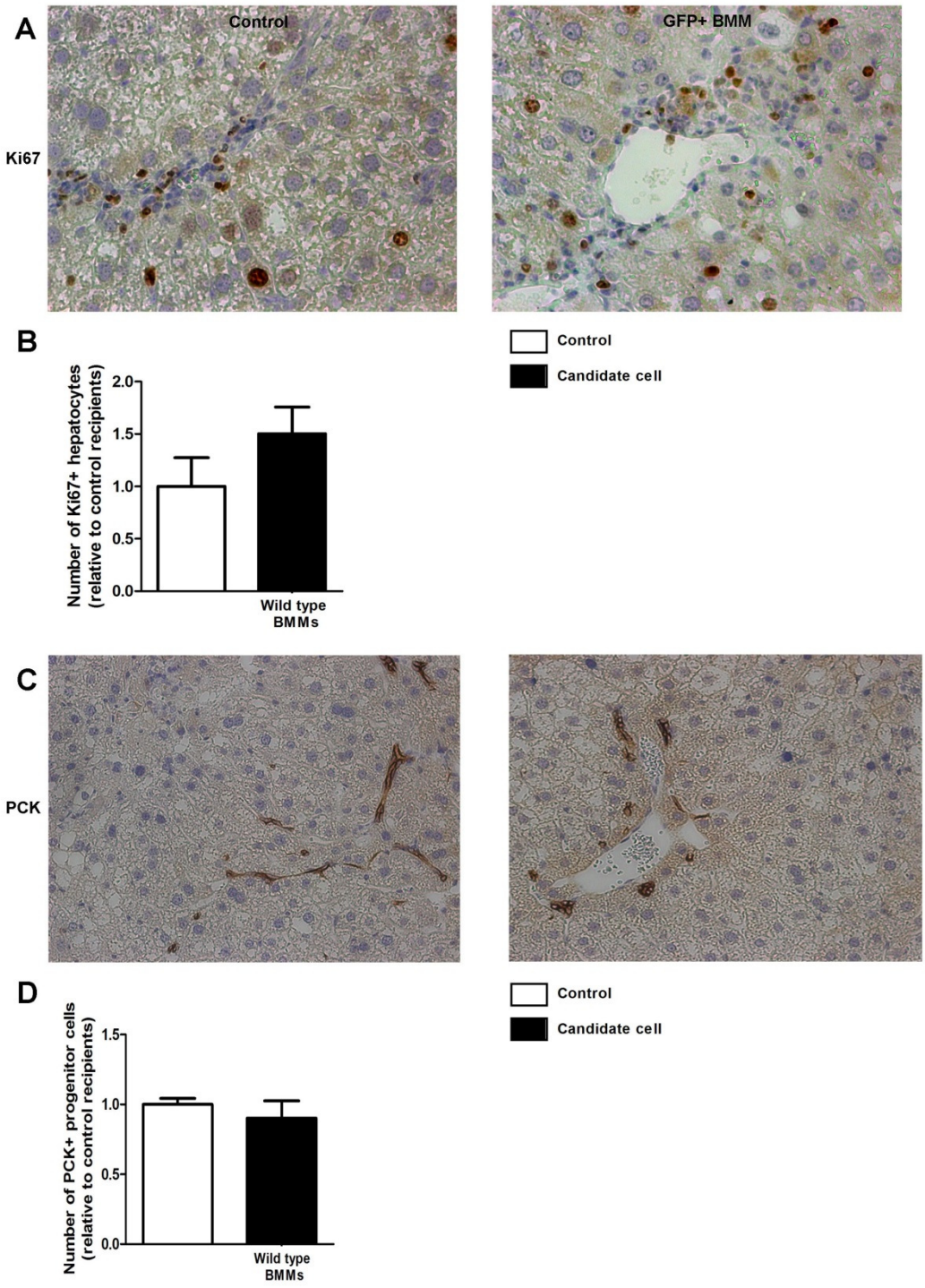

Figure 4.2 No difference in mediators of regeneration detected 4 weeks after BMM therapy

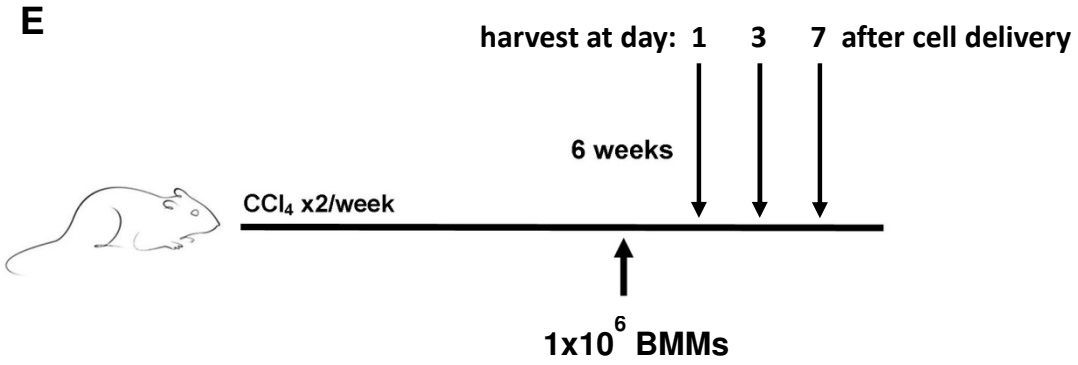

Figure 4.2 No difference in mediators of regeneration detected 4 weeks after BMM therapy

Advanced liver fibrosis was induced in adult female C57Bl/6 mice by the chronic administration of twice weekly IP CCl_4.

(**A**) Photomicrographs show Ki67 staining to identify proliferating hepatocytes 4 weeks after BMM delivery. Original magnification, x200.

(**B**) Cell counting demonstrates that there was not a significant increase in the number of Ki67 positive hepatocytes in the BMM recipient group.

(**C**) Photomicrographs show PCK staining to identify LPCs 4 weeks after BMM delivery. Original magnification, x200.

(**D**) Cell counting demonstrates that there was not a significant increase in the number of PCK positive oval cells in the BMM recipient group (compared with control recipients; n=7-8 per group).

These histograms are derived from the data in table 4.2 below; all values are expressed as a ratio of the mean of the internal control group.

(**E**) Given that potentially mechanistic changes were not detected 4 weeks after BMM injection, subsequent experiments examined the early effects of BMM delivery. This schematic illustrates the experimental protocol testing the effects of $1x10^6$ BMMs injected via the HPV within the first week. Mice were harvested 1, 3 and 7 days after BMM injection.

Table 4.2 No difference in mediators of regeneration detected 4 weeks after BMM therapy

	Control	BMMs
Ki67+ hepatocytes / x200 field Mean +/- SEM	1.4 +/- 0.4	2.0 +/- 0.3
Ki67+ hepatocytes / x200 field N	8	7
P value (Student's t test)	0.21	
PCK+ LPCs / x200 field Mean +/- SEM	3.9 +/- 0.2	3.5 +/- 0.5
PCK+ LPCs / x200 field N	7	7
P value (Student's t test)	0.48	

BMMs transiently engraft in the fibrotic liver

In previous reports of successful cell therapy in experimental models (Sakaida, Terai et al. 2004; Nakamura, Torimura et al. 2007), the donor cells have been considered to have direct effects on liver remodelling and also to transdifferentiate into cell types that might assist liver function (e.g. hepatocyte-like cells or vascular endothelium). I therefore sought to track the donor BMMs in the recipient liver.

Engraftment of donor BMMs was assessed using 2 independent cell tracking techniques. Sex mismatch bone marrow transplantation (male BM to female recipient) has been used as a means of tracking BM cells in the female liver (Duffield, Forbes et al. 2005; Russo, Alison et al. 2006). Y chromosome FISH of control wild type female and male liver sections confirmed that the Y chromosome probe is specific, not blinding to female tissue (figure 4.3A). Therefore the presence of the Y chromosome (detectable by FISH) indicates a donor cell in these experiments. Importantly, the nucleus will not always be detected in the tissue section when quantifying engraftment by this method. Therefore, as described in the methods chapter, a correction coefficient was calculated to improve the accuracy of the estimate of the number of engrafted cells.

The second tracking technique involved delivering donor BMMs that constitutively express GFP (Pratt, Sharp et al. 2000). This allowed subsequent immunohistochemical or fluorescent detection of donor cells.

The majority of identified donor BMMs detected by either method were located either within the hepatic scar or closely apposed to it (figure 4.3B). 1 day after the delivery of 1 x 10^6 BMMs, the mean number of engrafted donor BMMs was 6.9 per x200 magnification field by GFP immunostaining. Quantification of male donor BMMs using Y chromosome FISH revealed 6.5 donor BMMs per x200 magnification field at this time point. From day 1, this figure decreased to 5.3 within the first week. Extensive examination of sections from the 4 week time point demonstrated that

donor BMMs were no longer detected in recipient livers (figure 4.3C). Hepatic macrophages are known to turnover rapidly (Crofton, Diesselhoff-den Dulk et al. 1978), so the longevity of donor BMMs is in keeping with expectations of host hepatic macrophages in this regard. The transience of donor BMM engraftment supported the hypothesis that the important mechanistic events resulting in the observed phenotype might occur relatively soon after cell delivery.

Figure 4.3 BMMs transiently engraft the fibrotic liver

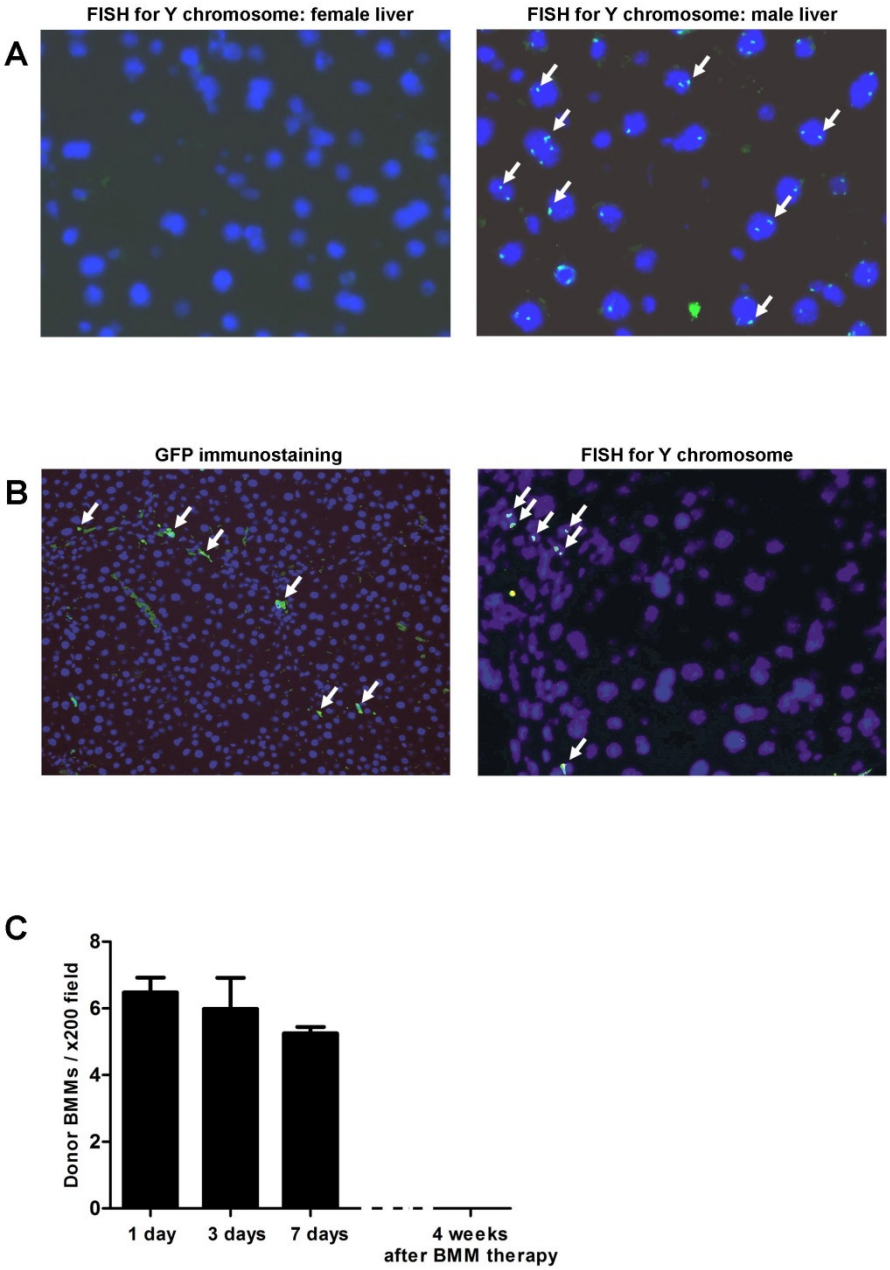

Figure 4.3 BMMs transiently engraft the fibrotic liver

Advanced liver fibrosis was induced in adult female mice by the chronic administration of twice weekly IP CCl_4. Donor BMMs engraft transiently in the liver.

(A) Y chromosome FISH is specific for only detecting male cells. Original magnification, x320.

(B) Syngeneic donor cells were tracked by treating wild type fibrotic CBA mice with GFP positive BMMs (arrowed). Original magnification x200. In addition, syngeneic male donor cells (arrowed) were detected within injured female C57Bl/6 liver using FISH for the Y chromosome. Original magnification, x320.

(C) Quantification of donor BMM engraftment by Y chromosome FISH demonstrated a reduction in number during the first 7 days after BMM delivery. No donor cells were detected 4 weeks after infusion (n=3 per time point).

Early reduction in myofibroblasts following BMM delivery

The area of α-SMA staining in the BMM treatment group decreased within the first week (figure 4.4A) falling to 40% of control recipients 7 days after BMM therapy ($P < .05$, figure 4.4B). As described, the decrease in myofibroblasts was no longer statistically significant 1 month after intervention ($P = .29$) suggesting that the peak anti-fibrotic effect upon the myofibroblast population occurs relatively soon after BMM delivery. Double staining for TUNEL with α-SMA revealed that scar associated myofibroblasts underwent apoptosis during this reduction (figure 4.4C).

Given the major contribution of hepatic myofibroblasts to ECM deposition during liver injury, this marked reduction in the amount of scar producing cells is likely to be responsible for a significant component of the observed anti-fibrotic phenotype.

Whilst not the focus of this body of work, the increase in fibrosis following the delivery of whole BM is of biological and translational interest. α-SMA staining of BM recipients 4 weeks after cell delivery did not show a statistically significant increase in myofibroblasts (figure 4.5A, B). Given previous studies demonstrating a BM origin for hepatic myofibroblasts (Russo, Alison et al. 2006), FISH for the Y chromosome was performed to determine whether donor cells of BM origin had engrafted in the fibrotic recipient liver. No male cells were detected at this 4 week time point. This does not exclude the engraftment of BM cells (e.g. MSCs) that could differentiate into myofibroblastic cells as they may not have persisted for the 4 week period. In addition, the absolute number of such cells within the total of $1x10^6$ whole BM cells would be low presenting a practical limitation in terms of detection. Alternatively, there may be early paracrine influences from BM cell populations which produce this pro-fibrotic phenotype in the host liver.

Figure 4.4 BMM therapy causes a reduction in hepatic myofibroblasts

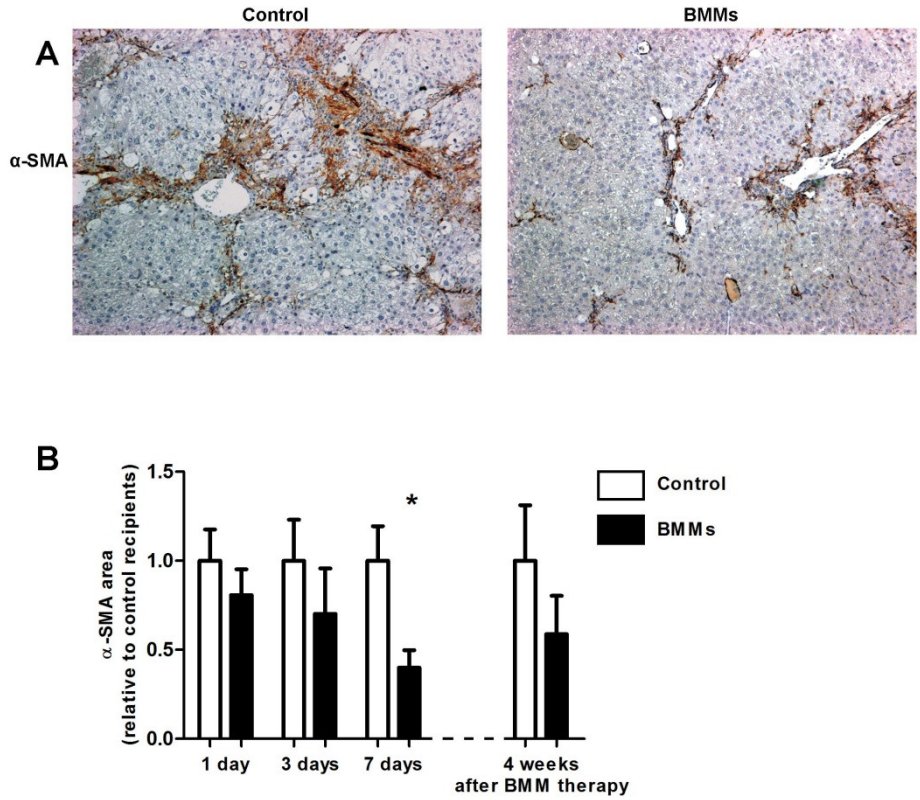

Figure 4.4 BMM therapy causes a reduction in hepatic myofibroblasts

Advanced liver fibrosis was induced in adult female C57Bl/6 mice by the chronic administration of twice weekly IP CCl_4. BMM delivery causes a reduction in the amount of hepatic myofibroblasts.

(**A**) Photomicrographs demonstrate the reduction in α-SMA positive myofibroblasts 7 days after BMM delivery. Original magnification, x80.

(**B**) Morphometric analysis of α-SMA immunostaining revealed that myofibroblast numbers decreased within 7 days of BMM treatment, this effect did not persist to 4 weeks after infusion. This histogram is derived from the data in table 4.3 below; all values are expressed as a ratio of the mean of the internal control group. This allows relative comparison of BMM effect between experiments at different time points.

(**C**) Dual staining for TUNEL (green) and α-SMA (red) demonstrated the presence of apoptotic myofibroblasts 3 days after BMM delivery. (* $P < .05$ compared with control recipients per time point; n=5-8 per group).

Table 4.3 BMM therapy causes a reduction in hepatic myofibroblasts

	Control	BMMs
α-SMA % 1 day after injection Mean +/- SEM	3.3 +/- 0.6	2.7 +/- 0.5
α-SMA % 1 day after injection N	6	6
P value (Student's t test)	0.41	
α-SMA % 3 days after injection Mean +/- SEM	1.1 +/- 0.3	0.8 +/- 0.3
α-SMA % 3 days after injection N	5	6
P value (Student's t test)	0.44	
α-SMA % 7 days after injection Mean +/- SEM	2.7 +/- 0.5	1.1 +/- 0.3
α-SMA % 7 days after injection N	6	5
P value (Student's t test)	0.03	

Figure 4.5 Unfractionated (whole) BM cell delivery does not significantly increase the amount of hepatic myofibroblasts

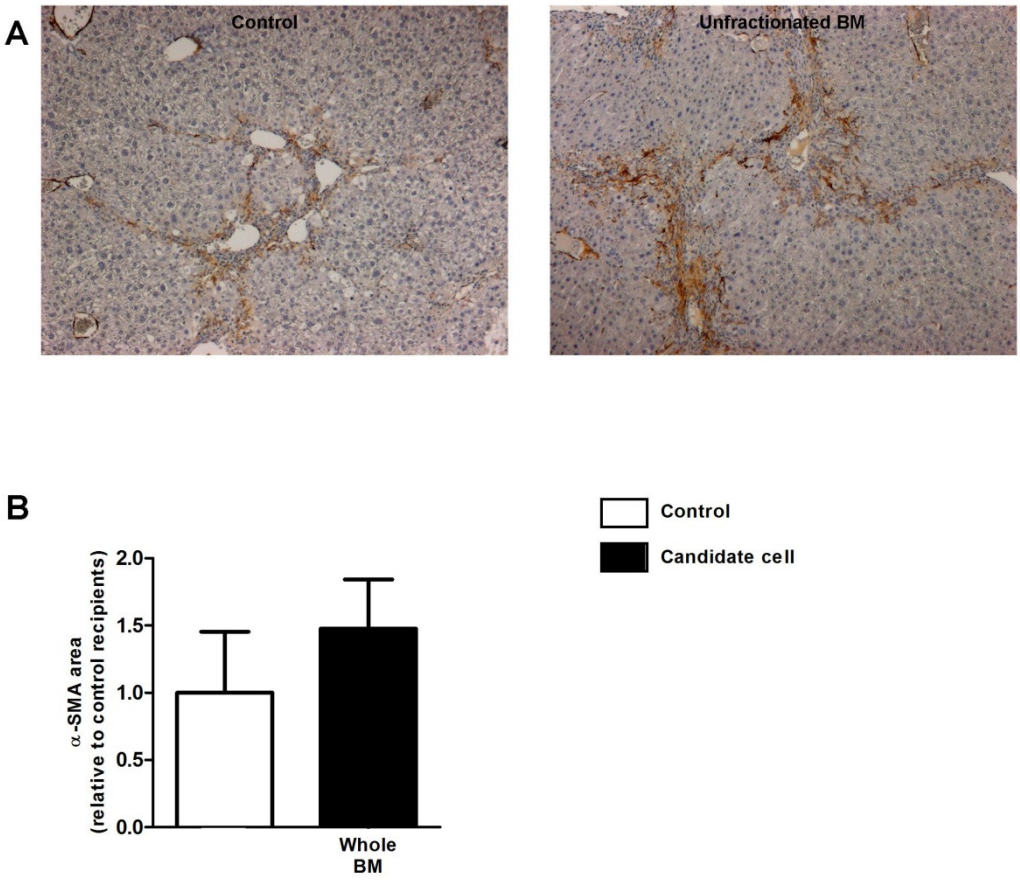

Figure 4.5 Unfractionated (whole) BM cell delivery does not significantly increase the amount of hepatic myofibroblasts

Advanced liver fibrosis was induced in adult female C57Bl/6 mice by the chronic administration of twice weekly IP CCl_4.

(**A**) Photomicrographs demonstrate similar amounts of α-SMA positive myofibroblasts 4 weeks after whole BM delivery. Original magnification, x80.

(**B**) Morphometric analysis of α-SMA immunostaining revealed that there was not a significant increase in the amount of hepatic myofibroblasts. (n=6 per group). This histogram is derived from the data in table 4.4 below; all values are expressed as a ratio of the mean of the internal control group.

Table 4.4 Unfractionated (whole) BM cell delivery does not significantly increase the amount of hepatic myofibroblasts

Sample 4 weeks after injection	Control (α-SMA %)	BM (α-SMA %)
Mean +/- SEM	0.7 +/- 0.3	1.1 +/- 0.3
N	6	6
P value (Mann-Whitney test)	0.23	

Upregulation of matrix metalloproteinase expression following BMM therapy

A key component of fibrosis resolution is the degradation of ECM mediated by the MMP family of enzymes. Therefore I examined the expression of MMPs in whole liver tissue during the first week after BMM delivery.

Within 1 day of BMM therapy, whole liver gene expression of MMP-9 was elevated by 510% above control recipients ($P < .05$). In parallel with this was a group-wide trend towards increases in MMP-13 ($P = .21$), MMP-8 (neutrophil collagenase, $P = .17$) and MMP-12 (macrophage metalloelastase, $P = .08$) (figure 4.6A). Interestingly, this was not a universal phenomenon across the MMPs. MMP-2 has been shown to have pro-fibrotic actions potentially mediated by supporting HSC proliferation (Preaux, Mallat et al. 1999). In contrast to MMPs -8, -9 and -13, there was a non-significant reduction in MMP-2 expression at all measured time points in the first week following BMM delivery (figure 4.6A).

Given the magnitude of MMP-9 upregulation, the next line of investigation was to determine the origin of MMP-9. Hepatic macrophages have previously been identified as the predominant cellular source of MMP-9 in the fibrotic liver (Knittel, Mehde et al. 1999). Therefore I explored the possibility of the donor BMMs being responsible for this increase in MMP-9 expression. As male donor BMMs were given to female mice, combining MMP-9 immunostaining with FISH for the Y chromosome allowed this hypothesis to be tested. Control male tissue confirmed that male (Y chromosome positive) MMP-9 producing cells were detectable (figure 4.6B). Interestingly, donor cells in the BMM recipients' livers did not show co-localisation of these signals indicating that the donor BMMs were not expressing MMP-9 *in vivo* (figure 4.6C). Further dual staining for MMP-9 and the macrophage marker F4/80 demonstrated that these signals were also topographically distinct (figure 4.7A). The lobulated nuclei of the MMP-9 positive cells in this panel gave an indication as to

their identity. Staining for the neutrophil marker Ly-6G with MMP-9 showed that hepatic neutrophils were in fact responsible for production of this enzyme and were mostly located within the scar or closely associated areas (figure 4.7B i, ii).

As previously described, hepatic macrophages within or closely apposed to the scar (SAMs) are a critical source of MMP-13. This is functionally important during the resolution of fibrosis on cessation of injury (Fallowfield, Mizuno et al. 2007). Serial section analysis of MMP-13 and F4/80 staining confirms that a subset of SAMs in BMM recipients produced MMP-13 (figure 4.7C).

Figure 4.6 MMP-9 expression is upregulated in BMM recipients but is not produced by donor macrophages

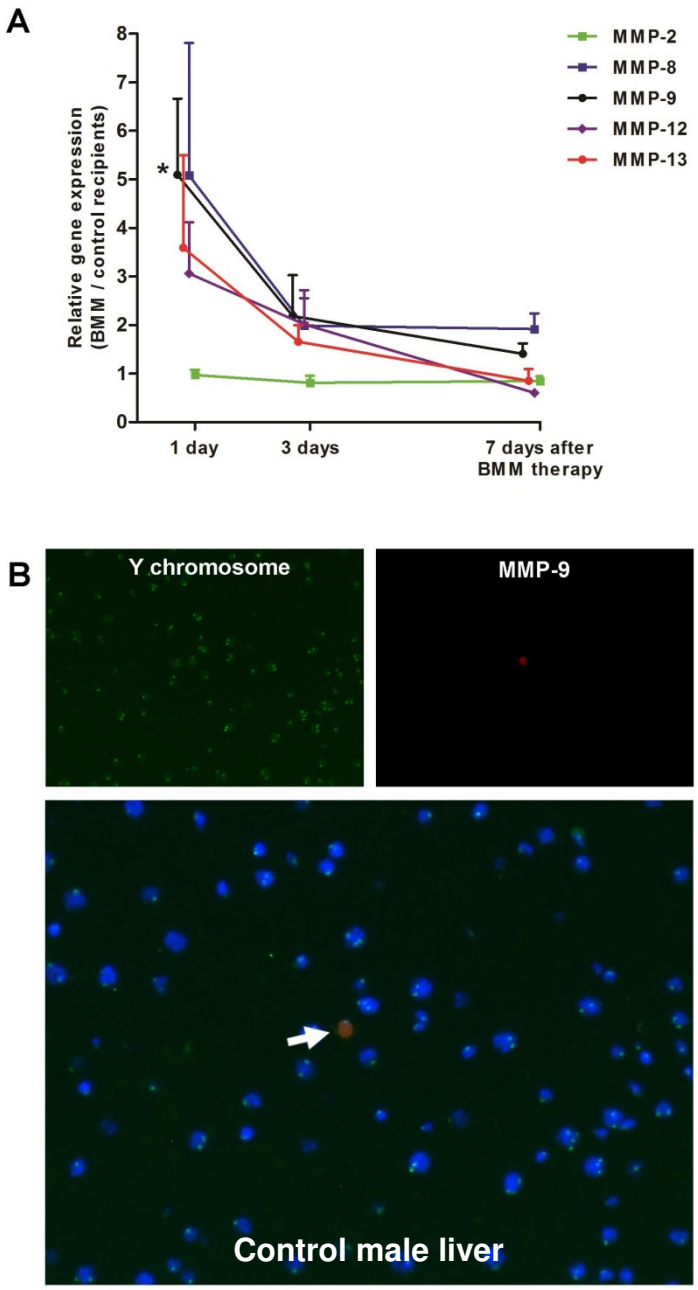

Figure 4.6 MMP-9 expression is upregulated in BMM recipients but is not produced by donor macrophages

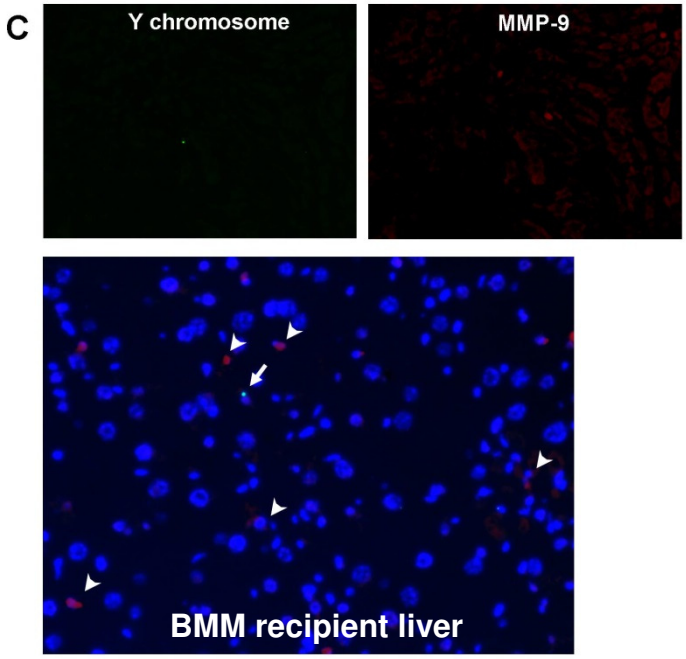

Figure 4.6 MMP-9 expression is upregulated in BMM recipients but is not produced by donor macrophages

Advanced liver fibrosis was induced in adult female C57Bl/6 mice by the chronic administration of twice weekly IP CCl_4.

(**A**) Whole liver gene expression of MMP-9 was significantly elevated in BMM recipients within 1 day of delivery. Gene expression levels of MMPs-8, -12 and -13 were not significantly increased. By day 3, these levels had reduced (* $P < .05$, ** $P < .01$ compared with control recipients per time point; n=5-6 per group). This graph is derived from the data in tables 4.5 below; all values are expressed as a ratio of the mean of the internal control group.

(**B**) The Y chromosome probe (green) co-localised with MMP-9 (red) in control male liver indicating successful co-staining of male MMP-9 expressing cells (arrow). Following injection of male BMMs into female recipients however, (**C**) male donor BMMs (arrow) did not express MMP-9 (arrowheads) in liver. Original magnification, x400.

Table 4.5 MMP-9 expression is upregulated in BMM recipients but is not produced by donor macrophages

MMP gene expression								
Time after injection	1 day			3 days			7 days	
Sample	Control	BMMs		Control	BMMs		Control	BMMs
MMP-2 Mean +/- SEM	12.9 +/- 1.7	12.6 +/- 1.4		9.0 +/- 2.4	7.3 +/- 1.3		10.1 +/-2.4	8.6 +/- 1.0
MMP-2 N	6	6		5	6		6	5
P value	0.87 (S)			0.79 (MW)			0.59 (S)	
MMP-8 Mean +/- SEM	4.0 +/- 1.7	20.1 +/- 10.8		4.6 +/- 0.7	9.2 +/- 2.6		4.8 +/- 1.4	9.2 +/- 1.6
MMP-8 N	6	6		5	6		6	5
P value	0.17 (S)			0.15 (S)			0.06 (S)	
MMP-9 Mean +/- SEM	1.6 +/- 0.6	8.0 +/- 2.5		2.3 +/- 0.5	5.0 +/- 1.9		3.7 +/- 0.9	5.2 +/- 0.8
MMP-9 N	6	6		5	6		6	5
P value	<0.01 (MW)			0.17 (S)			0.22 (S)	
MMP-13 Mean +/- SEM	2.2 +/- 0.3	7.8 +/- 4.2		2.6 +/- 0.3	4.3 +/- 0.9		13.8 +/- 2.7	11.8 +/- 3.3
MMP-13 N	6	6		5	6		6	5
P value	0.21 (S)			0.08 (MW)			0.6 (S)	

(S = Student's test,
MW = Mann-Whitney test)

Figure 4.7 Identification of the cellular sources of MMP-9 and MMP-13 in BMM recipients

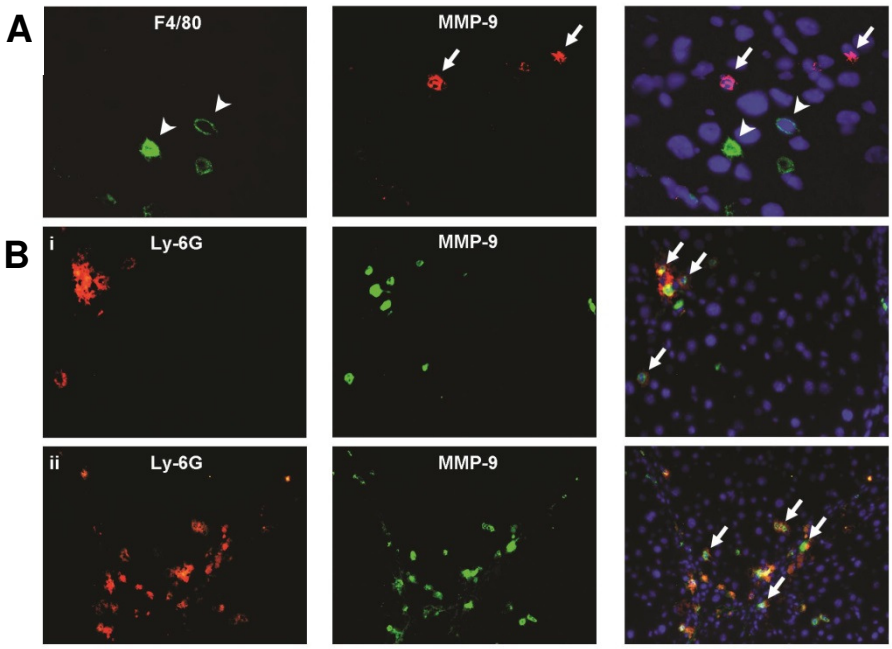

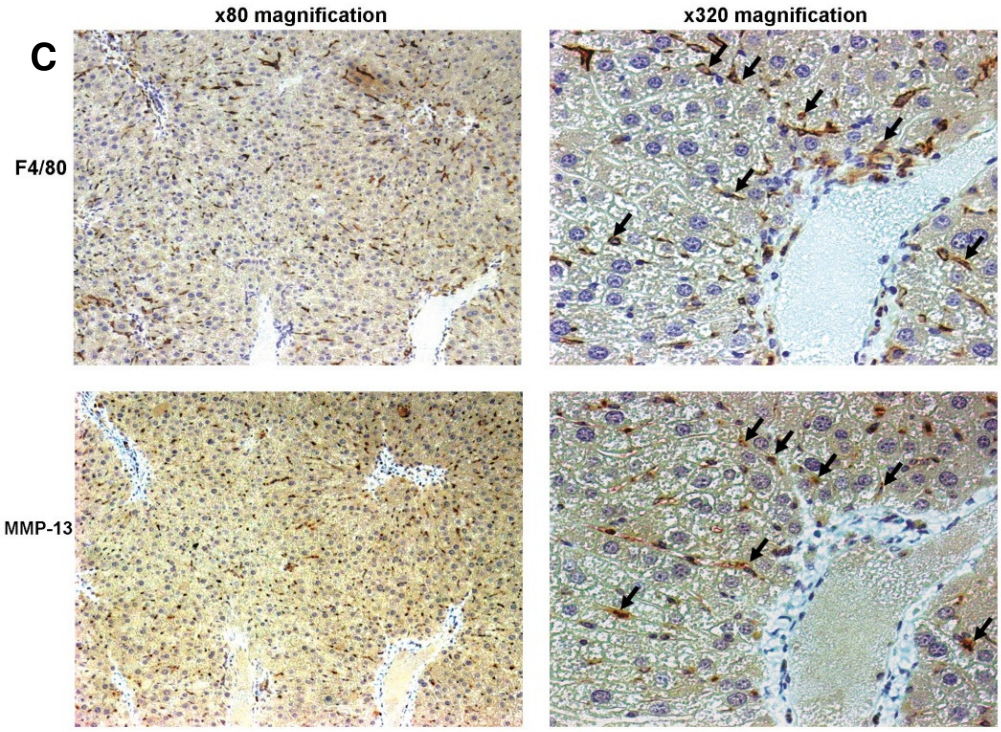

Figure 4.7 Identification of the cellular sources of MMP-9 and MMP-13 in BMM recipients

Advanced liver fibrosis was induced in adult female C57Bl/6 mice by the chronic administration of twice weekly IP CCl_4.

(**A**) Dual staining for MMP-9 (red) and F4/80 (green) demonstrates that hepatic macrophages (arrowheads) did not express MMP-9 (arrows) in BMM recipients. Original magnification, x1000.

(**B i**) Co-localisation (arrows) of the neutrophil marker Ly-6G (red) with MMP-9 staining (green) indicates that hepatic neutrophils were expressing MMP-9 in BMM recipients. Original magnification, x320. (**B ii**) The x200 magnification demonstrates that most of these scar associated neutrophils produced MMP-9.

(C) Immunostaining of serial liver sections demonstrates that a subset of scar associated F4/80 positive macrophages produced MMP-13 (arrowed). Original magnification, x80 and x320.

To characterise further the increased expression of MMPs following BMM delivery, recipient livers were immunostained for MMP-9 and MMP-13. Examination of these sections revealed that the cells producing these ECM degrading enzymes were predominantly located in or closely around the scar (figure 4.8A). Quantification of positively stained cells demonstrated an increase in the numbers of MMP-9 and MMP-13 expressing cells within 1 day of donor macrophage delivery (figure 4.8B).

This early increase in hepatic MMP-9 following BMM delivery precedes the reduction in myofibroblasts at the 7 day time point. The contribution of upregulated MMP-9 levels to the reduction in myofibroblasts has been shown *in vitro* by the finding that the application of recombinant MMP-9 to cultured HSCs results in their apoptosis, possibly through dissolution of ECM-integrin mediated survival signals to HSCs (Zhou, Murphy et al. 2004). This is consistent with the observed apoptosis of myofibroblasts (figure 4.4C) detected in conjunction with falling numbers of myofibroblasts following BMM therapy (figure 4.4B).

Figure 4.8 Increased numbers of MMP-9 and MMP-13 positive cells following BMM therapy

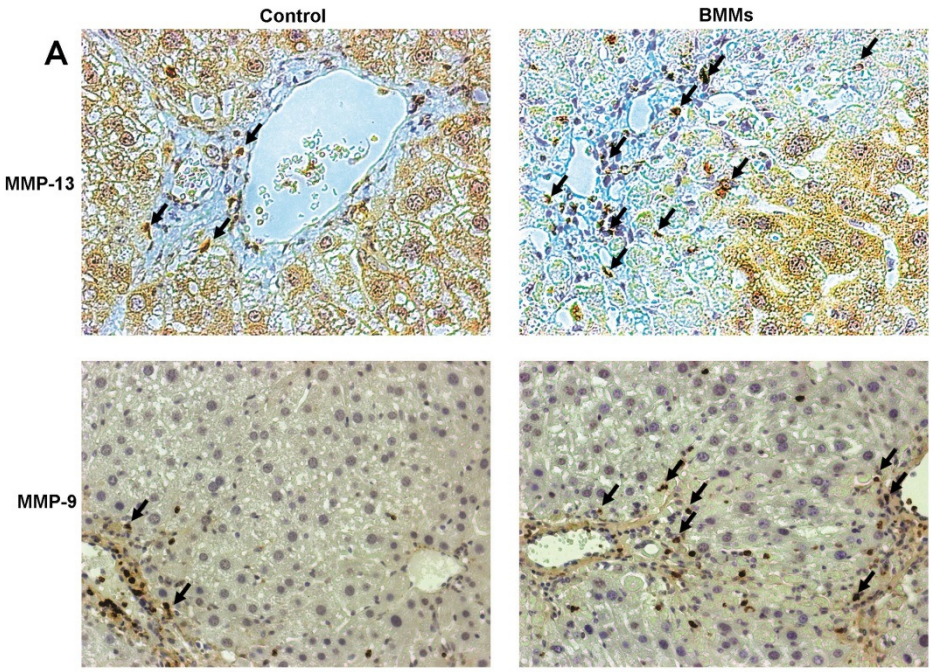

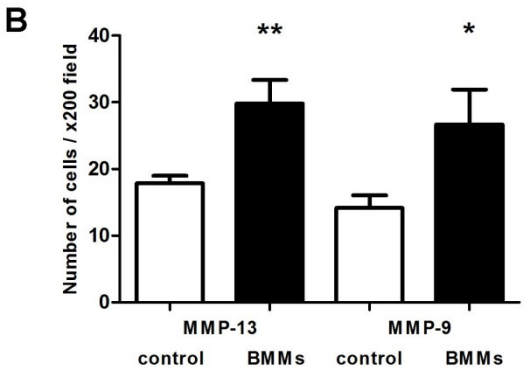

Figure 4.8 Increased numbers of MMP-9 and MMP-13 positive cells following BMM therapy

Advanced liver fibrosis was induced in adult female C57Bl/6 mice by the chronic administration of twice weekly IP CCl_4.

(**A**) Immunohistochemical analysis of liver sections 1 day after BMM delivery revealed infiltration of MMP-13 and MMP-9 positive cells (arrowed). Original magnification, x320 and x200 respectively.

(**B**) The numbers of MMP-13 and -9 expressing cells were significantly elevated in BMM recipients (* $P < .05$, ** $P < .01$, compared with control recipients per time point; n=6 per group). Absolute data is shown in table 4.6 below.

Table 4.6 Increased numbers of MMP-9 and MMP-13 positive cells following BMM therapy

	MMP-13+ cells			MMP-9+ cells	
Sample	Control	BMMs		Control	BMMs
Mean +/- SEM	17.9 +/- 1.1	29.8 +/- 3.5		14.2 +/- 1.9	26.7 +/- 5.2
N	6	6		6	6
P value	0.01 (S)			0.03 (MW)	

(S = Student's test,
MW = Mann-Whitney test)

Host macrophages and neutrophils are recruited to the liver by BMM therapy

The increased whole liver expression of predominantly neutrophil mediated MMP-9 and macrophage mediated MMP-13 could be due to a phenotypic switch amongst the resident hepatic leucocyte populations or recruitment of these cells to the liver. I therefore examined the absolute numbers of neutrophils and macrophages in recipient livers following BMM delivery. Within 1 day of BMM delivery, there was a marked change in the cellular composition of the fibrotic liver. F4/80 immunostaining and quantification revealed a 44% increase in macrophage number ($P < .05$, figures 4.9A, B). The absolute increase in macrophages in BMM treated mice (from 53 to 76, i.e. an additional 23 per x200 field) significantly exceeds the number of donor BMMs (mean <7) in the same area of tissue. This suggests that the majority of these macrophages could be recruited to the liver as opposed to being of donor origin. Ly-6G immunostaining showed a 242% increase in hepatic neutrophil numbers ($P < .01$, figures 4.9A, B) at this time point.

Analysis of candidate chemokines in recipient livers was undertaken in order to investigate the mechanism of neutrophil and macrophage recruitment. Whole liver extract was assayed to determine the concentration of these proteins during the first 7 days after BMM delivery. In keeping with the early increase in neutrophil and macrophage numbers, samples from the 1 day time point revealed that BMM recipients had significantly higher levels of chemokines expressed by the donor BMMs (figures 3.2C, 4.10C). The macrophage chemoattractant MCP-1 (CCL2) was upregulated to 160% ($P < .001$) whilst MIP-1α (CCL3) was 137% of control ($P < .05$). The neutrophil chemoattractants KC (CXCL1) and MIP-2 (CXCL2) were also markedly elevated (242%, $P < .001$ and 842%, $P < .01$ respectively). Macrophages and neutrophils can have a number of inflammatory actions in certain contexts. Therefore I also measured the whole liver protein levels of anti- and pro-inflammatory cytokines to gauge the hepatic environment in this regard at the time of cell

recruitment. Importantly, IL-10 protein levels were considerably elevated to 346% in BMM recipients ($P < .05$), whilst pro-inflammatory mediators such as TNF-α and IL-6 were unchanged (figure 4.10F). The CCl_4 model involves significant liver inflammation following toxic injury. Consequently ALT levels are high with a significant degree of variability. 4 weeks after BMM therapy, serum ALT levels were approximately 80% of control levels. However, the standard deviation of these results was substantial and this was not a statistically significant reduction (figure 4.9D).

Therefore, BMM therapy in the context of ongoing liver injury switches the hepatic milieu towards an anti-inflammatory cytokine environment whilst recruiting host macrophages and neutrophils into this altered setting.

Figure 4.9 Host macrophages and neutrophils are recruited to the liver following BMM delivery

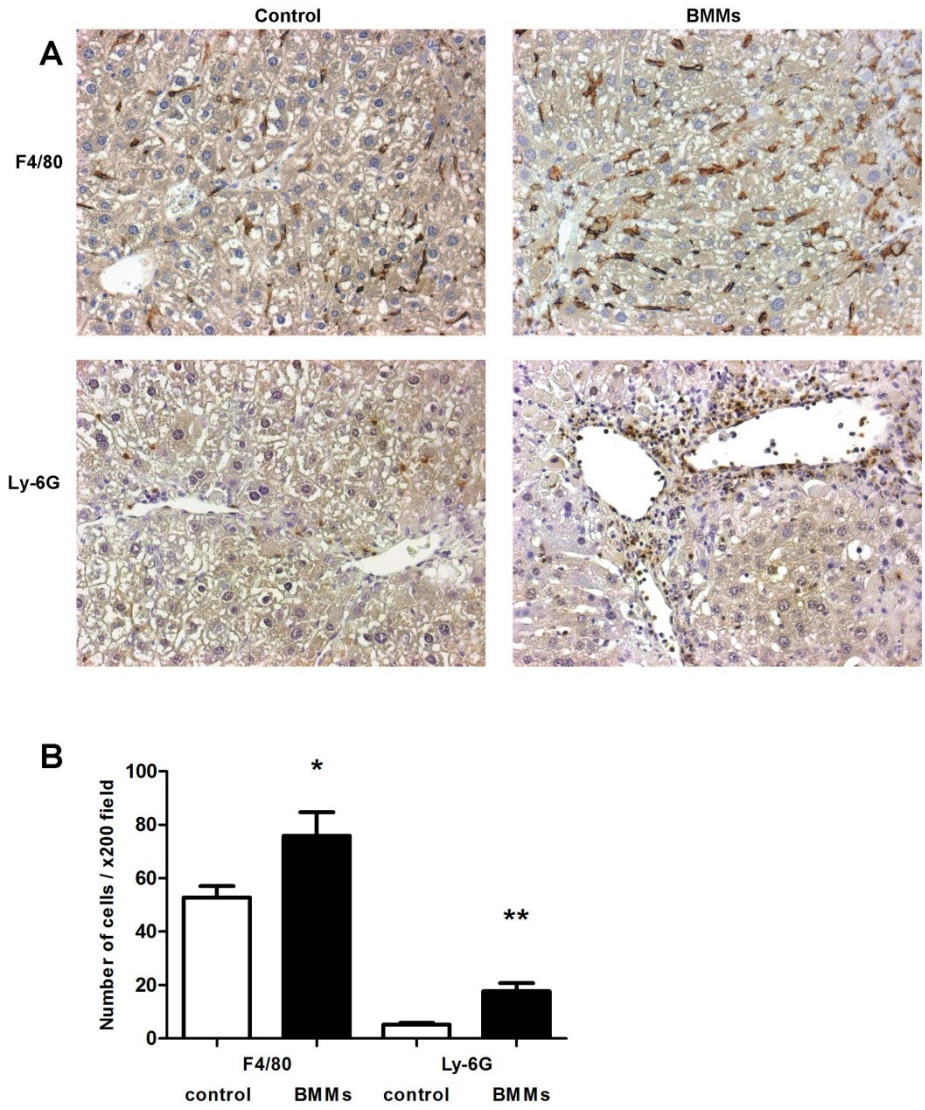

Figure 4.9 Host macrophages and neutrophils are recruited to the liver following BMM delivery

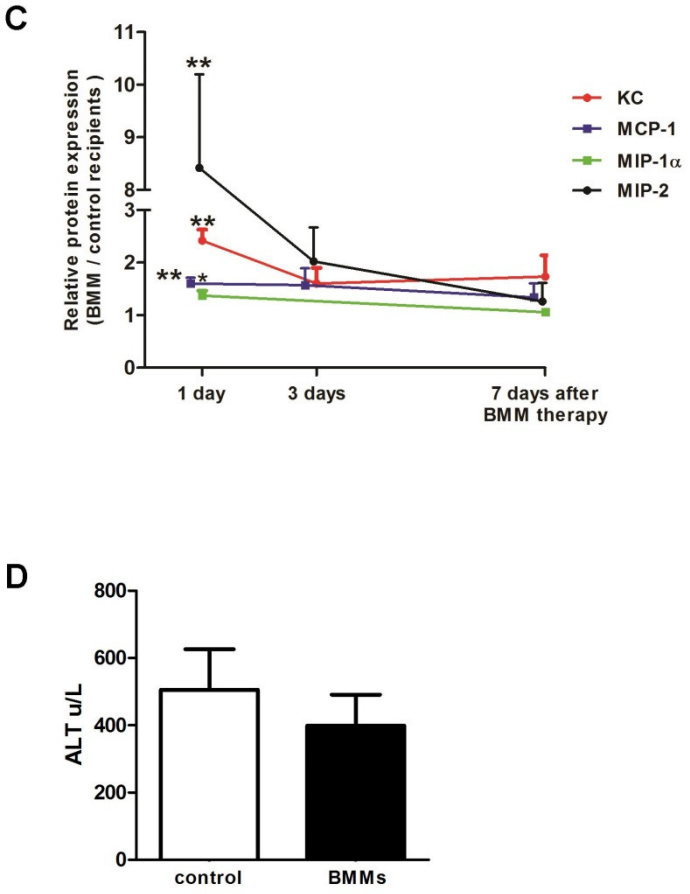

Figure 4.9 Host macrophages and neutrophils are recruited to the liver following BMM delivery

Advanced liver fibrosis was induced in adult female C57Bl/6 mice by the chronic administration of twice weekly IP CCl_4.

(**A**) Immunohistochemical analysis of liver specimens harvested 1 day after BMM delivery revealed that macrophages and neutrophils were recruited to the fibrotic liver. Original magnification, x200.

(**B**) The extent of cell influx was greater in BMM recipients than control. Absolute data in table 4.7.

(**C**) Whole liver protein levels of macrophage and neutrophil chemokines (MCP-1, MIP-1α, MIP-2 and KC) were significantly elevated within 1 day of BMM delivery. By day 3, these levels were returning towards baseline. This graph is derived from the data in table 4.7 below; all values are expressed as a ratio of the mean of the internal control group. This allows relative comparison of BMM effect between experiments at different time points. Insufficient measurements of MIP-1 α levels above the minimum detection level from the day 3 time point precluded analysis (data in collaboration with Dr Tim Gordon-Walker).

(**D**) Serum ALT measured 4 weeks after BMM therapy was not significantly reduced compared to controls. (* $P < .05$, ** $P < .01$ compared with control recipients per time point; n=5-8 per group). Absolute data in table 4.7.

Tables 4.7 Host macrophages and neutrophils are recruited to the liver following BMM delivery

	F4/80+ cells			Ly-6G+ cells	
Sample (1 day after injection)	Control	BMMs		Control	BMMs
Mean +/- SEM	52.9 +/- 4.2	75.9 +/- 8.9		5.2 +/- 0.7	17.8 +/- 2.9
P value	0.04			<0.01	

Cytokine protein levels							
Time after injection	1 day		3 days		7 days		
Sample	Control	BMMs	Control	BMMs	Control	BMMs	
KC Mean +/- SEM	210.5 +/- 19.7	509.3 +/- 43.3	206.4 +/- 43.5	331.0 +/- 61.6	137.7 +/- 15.6	238.7 +/- 56.1	
KC N	5	6	5	6	6	5	
P value	<0.01		0.15		0.09		
MCP-1 Mean +/- SEM	233.6 +/- 8.3	374.6 +/- 25.1	225.5 +/- 8.5	347.5 +/- 70.6	238.7 +/- 12.7	319.4 +/- 64.0	
MCP-1 N	5	6	5	6	6	5	
P value	<0.01		0.15		0.21		
MIP-1α Mean +/- SEM	193.0 +/- 14.6	264.8 +/- 18.3	n/a	n/a	201.7 +/- 9.5	213.4 +/- 9.5	
MIP-1α N	5	6	n/a	n/a	6	5	
P value	0.02		n/a		0.41		
MIP-2 Mean +/- SEM	154.9 +/- 70.7	1304.0 +/- 275.1	90.3 +/- 18.9	182.8 +/- 58.4	292.7 +/- 82.7	369.3 +/- 103.7	
MIP-2 N	5	6	5	6	6	5	
P value	<0.01		0.20		0.57		

	Control serum ALT (u/L)	Whole BMMs serum ALT (u/L)
Mean +/- SEM	505.7 +/- 120.7	399.2 +/- 91.7
N	7	6
P value	0.51	

Student's test used to analyse these data.

BMM therapy stimulates regeneration of the injured liver

Chronic liver injury with accompanying fibrosis results in activation of the regenerative compartments of the liver. With advancing fibrosis, progenitor cell mediated regeneration becomes increasingly important in addition to hepatocyte proliferation.

Serum albumin was increased in BMM recipients 4 weeks after cell delivery (46.0 ±2.6 g/l v 39.9 ±0.9 g/l, $P = .05$, figure 3.6A). Proliferating hepatocytes were identified based on their expression of the Ki67 antigen. There was not a statistically significant increase in hepatocyte proliferation after BMM therapy ($P = .21$, figures 4.10A, B), however the consistently higher average count amongst BMM recipient groups at all time points suggests that there may be an underlying trend towards an increase. In line with this, there was also a trend towards an increase in the expression of the hepatocyte mitogen HGF (figure 4.10D). In keeping with human cirrhosis, increased numbers of LPCs were present in this model. 3 days after BMM delivery, whole tissue mRNA levels of the LPC marker CK-19 were increased by 55% over control recipients (1.55 ±0.1 v 1.00 ±0.2, $P= .05$, figure 4.10C). By day 7, there was a histologically evident peri-portal expansion of PCK and Dlk positive LPCs in BMM recipients. The number of LPCs increased by 40% over control ($P < .05$, figures 4.10A, C). Consistent with this upregulation of LPC numbers, gene expression of the LPC markers EpCam and Fn14 were consistently albeit non-significantly increased at days 3 and 7 after BMM therapy (figure 4.10C). Donor BMMs used here express high levels of the LPC mitogen TWEAK relative to recipient liver (table 3.1). 3 days after BMM therapy, at a time when hepatic macrophage numbers were increased, whole liver TWEAK mRNA levels were significantly elevated to 216% of control ($P < .05$, figure 4.10E).

There was no increase in the level of the cytokines IL-6 and TNF-α which are also associated with LPC proliferation (Bird, Lorenzini et al. 2008) (figure 4.10F). IGF-1 mRNA levels were significantly increased 3 and 7 days after BMM delivery ($P < .05$

and .001 respectively, figure 4.10E). CSF-1 protein levels increased to 165% of control 1 day after BMM delivery ($P < .01$, figure 4.10F) before decreasing over the first week. VEGF protein levels in contrast, increased in the BMM recipients over this period, reaching 127% of control at day 7 ($P < .05$, figure 4.10F). In addition to the upregulation of these reparative factors, increased TWEAK expression and the subsequently expanded LPC compartment are also implicated in the improved hepatic function in BMM treated mice.

Figure 4.10 Improved regenerative indices following BMM therapy

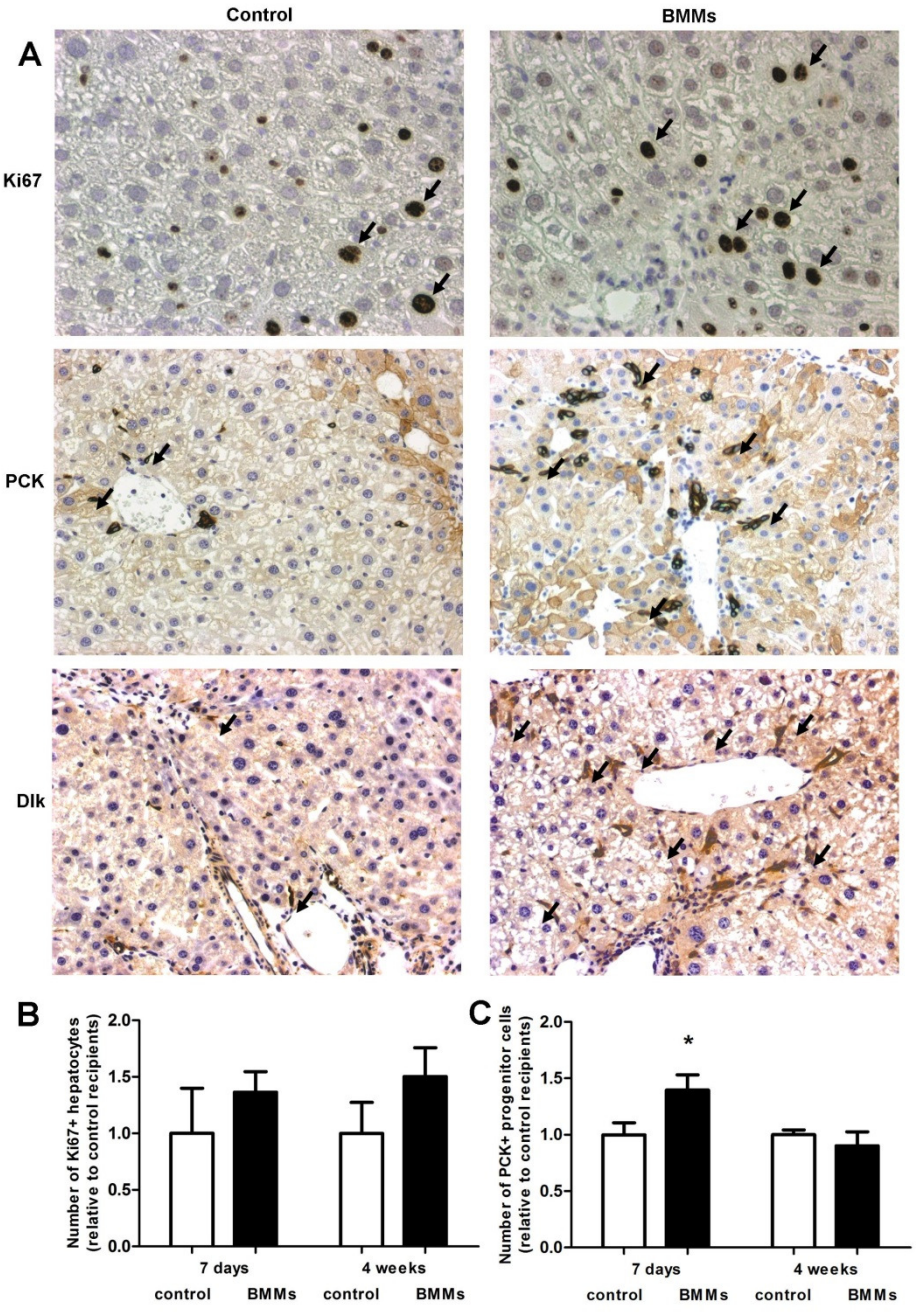

Figure 4.10 Improved regenerative indices following BMM therapy

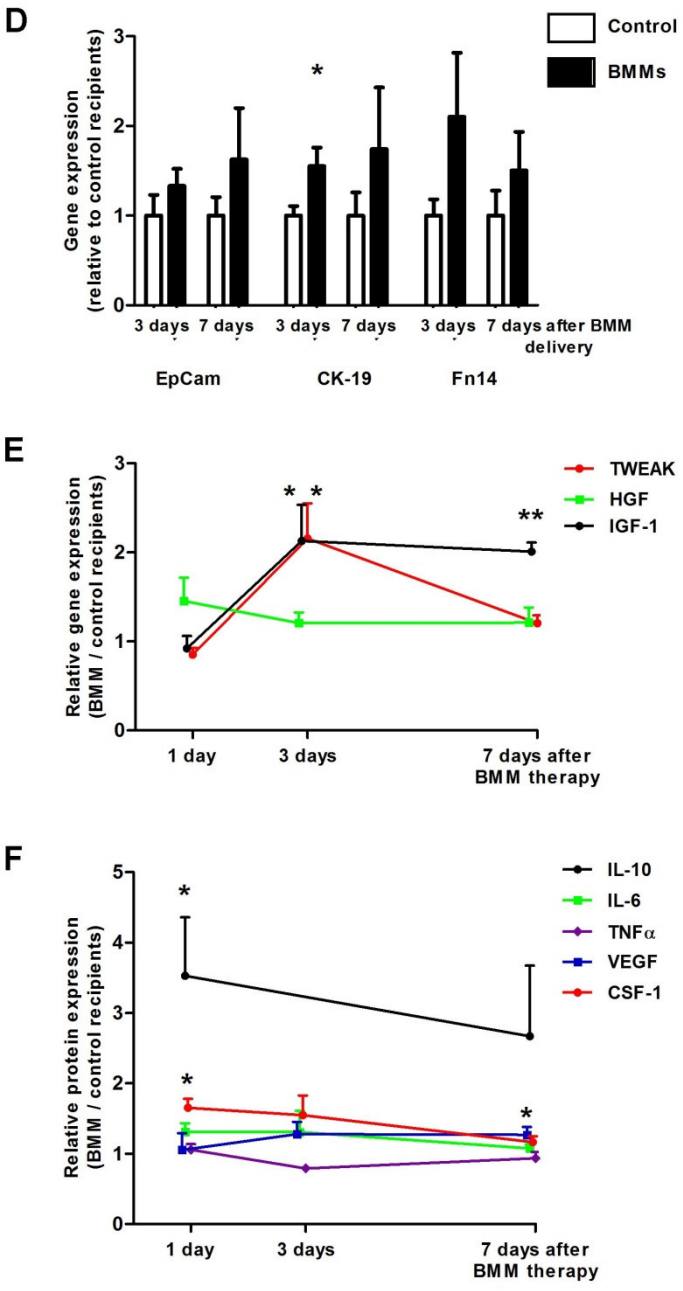

Figure 4.10 Improved regenerative indices following BMM therapy

Advanced liver fibrosis was induced in adult female C57Bl/6 mice by the chronic administration of twice weekly IP CCl_4. BMM delivery activated regenerative pathways.

(**A**) Photomicrographs show Ki67, PCK and Dlk immunostaining of liver tissue 7 days after BMM therapy. Original magnification, x200.

(**B**) The number of Ki67 positive hepatocytes did not increase to a statistically significantly level after BMM therapy. Graphs B-F are derived from data in table G; all values are expressed as a ratio of the mean of the internal control group. This allows relative comparison of BMM effect between experiments at different points.

(**C**) Increased numbers of PCK positive LPCs were detected 7 days after BMM infusion. This expansion was not maintained at 4 weeks.

(**D**) Gene expression of a panel of LPC markers showed a consistent increase following BMM therapy, CK-19 expression 3 days after BMM therapy reaching statistical significance. (**E**) Gene expression of HGF was not significantly elevated in BMM recipients. The liver progenitor cell mitogen TWEAK was upregulated 3 days after BMM delivery. IGF-1 mRNA was increased 3 and 7 days after BMM treatment.

(**F**) Whole liver protein levels of IL-10 and CSF-1 were elevated 1 day after BMM delivery, whilst IL-6 and TNF-α were unchanged. VEGF protein levels increased after BMM therapy reaching significance at day 7 (data in collaboration with Dr Tim Gordon-Walker) (* $P \leq .05$, ** $P < .01$ compared with control recipients per time point; n=5-8 per group). Insufficient measurements of IL-10 levels above the minimum detection level from the day 3 time point precluded analysis.

Graphs are derived from the data in table 4.8 below; all values are expressed as a ratio of the mean of the internal control group.

Tables 4.8 Improved regenerative indices following BMM therapy

7 days after BMM injection	Ki67+ hepatocytes / x200 field			PCK+ LPCs / x200 field	
Sample	Control	BMMs		Control	BMMs
Mean +/- SEM	1.9 +/- 0.7	2.6 +/- 0.3		9.6 +/- 1.0	13.4 +/- 1.3
N	6	6		6	5
P value (Mann-Whitney test)	0.17			0.03	

LPC marker gene expression					
Time after injection	3 day			7 days	
Sample	Control	BMMs		Control	BMMs
EpCam Mean +/- SEM	6.6 +/- 1.5	8.9 +/- 1.3		7.6 +/- 1.6	12.4 +/- 4.4
EpCam N	5	6		6	5
P value	0.29 (Student's t test)			0.33 (Mann-Whitney test)	
CK-19 Mean +/- SEM	5.7 +/- 0.6	8.9 +/- 1.2		8.4 +/- 2.2	14.6 +/- 5.8
CK-19 N	5	6		6	5
P value	0.05 (Student's t test)			0.31 (Student's t test)	
Fn14 Mean +/- SEM	2.5 +/- 0.5	5.3 +/- 1.8		6.8 +/- 1.9	10.3 +/- 2.9
Fn14 N	5	6		6	5
P value	0.21 (Student's t test)			0.25 (Mann-Whitney test)	

Tables 4.8 Improved regenerative indices following BMM therapy

Cytokine gene expression								
Time after injection	1 day			3 day			7 days	
Sample	Control	BMMs		Control	BMMs		Control	BMMs
TWEAK Mean +/- SEM	8.2 +/- 0.5	7.0 +/- 0.6		8.2 +/- 0.9	17.8 +/- 3.3		12.0 +/- 1.9	14.4 +/- 1.0
TWEAK N	6	6		5	6		6	5
P value (Student's t test)	0.15			0.03			0.32	
HGF Mean +/- SEM	15.2 +/- 1.4	22.1 +/- 4.0		6.2 +/- 0.7	7.4 +/- 0.7		8.7 +/- 1.8	10.5 +/- 1.5
HGF N	6	6		5	6		6	5
P value (Student's t test)	0.13			0.25			0.48	
IGF Mean +/- SEM	15.9 +/- 3.0	14.7 +/- 2.2		16.2 +/- 1.9	34.5 +/- 6.5		15.2 +/- 1.8	30.4 +/- 1.5
IGF N	6	6		5	6		6	5
P value (Student's t test)	0.75			0.04			<0.01	

Tables 4.8 Improved regenerative indices following BMM therapy

Cytokine protein expression							
Time after injection	1 day			3 day		7 days	
Sample	Control	BMMs		Control	BMMs	Control	BMMs
IL-10 Median +/- SEM	79.9 +/- 37.2	276.3 +/-66.5		n/a	n/a	25.9 +/-12.0	41.2 +/-17.4
IL-10 N	6	6		n/a	n/a	6	5
P value (Mann-Whitney test)	0.04			n/a		0.35	
IL-6 Mean +/- SEM	67.0 +/- 4.7	88.1 +/- 8.0		65.4 +/- 2.9	85.4 +/- 19.8	59.7 +/- 5.1	64.3 +/- 3.4
IL-6 N	5	6		5	6	6	5
P value (Student's t test)	0.06			0.39		0.49	
TNF-α Mean +/- SEM	2756 +/- 207.7	2608 +/- 108		2689 +/- 90.8	3400 +/- 821.3	2419 +/- 228.2	2579 +/- 110.7
TNF-α N	5	6		5	6	6	5
P value (Student's t test)	0.52			0.46		0.57	
VEGF Mean +/- SEM	284.3 +/- 23.0	299.8 +/- 67.2		213.7 +/- 24.8	273.5 +/- 37.1	200.7 +/- 9.7	255.0 +/- 22.0
VEGF N	5	6		5	6	6	5
P value (Student's t test)	0.85			0.23		0.04	
CSF-1 Mean +/- SEM	563.1 +/- 39.1	930.3 +/- 71.7		559.5 +/- 62.5	865.5 +/- 156.7	650.3 +/- 42.6	757.7 +/- 52.6
CSF-1 N	5	6		5	6	6	5
P value (Student's t test)	<0.01			0.13		0.14	

Macrophage viability is required for therapeutic effect

I examined the effect of dead BMMs in this model in order to test whether macrophage viability and in turn the capacity for hepatic engraftment and subsequent biological actions (e.g. expression of mediators such as IL-10, TWEAK and the chemokines listed in figure 3.2C) was required to generate the therapeutic phenotype. This was achieved by sonicating the same dose of cells (1×10^6) such that no intact BMMs remained. Injection of this macrophage debris into the HPV did not lead to a significant change in the amount of fibrosis or serum albumin (figure 4.11A, B, C).

Figure 4.11 Dead BMMs do not recapitulate the phenotype resulting from therapy with viable BMMs

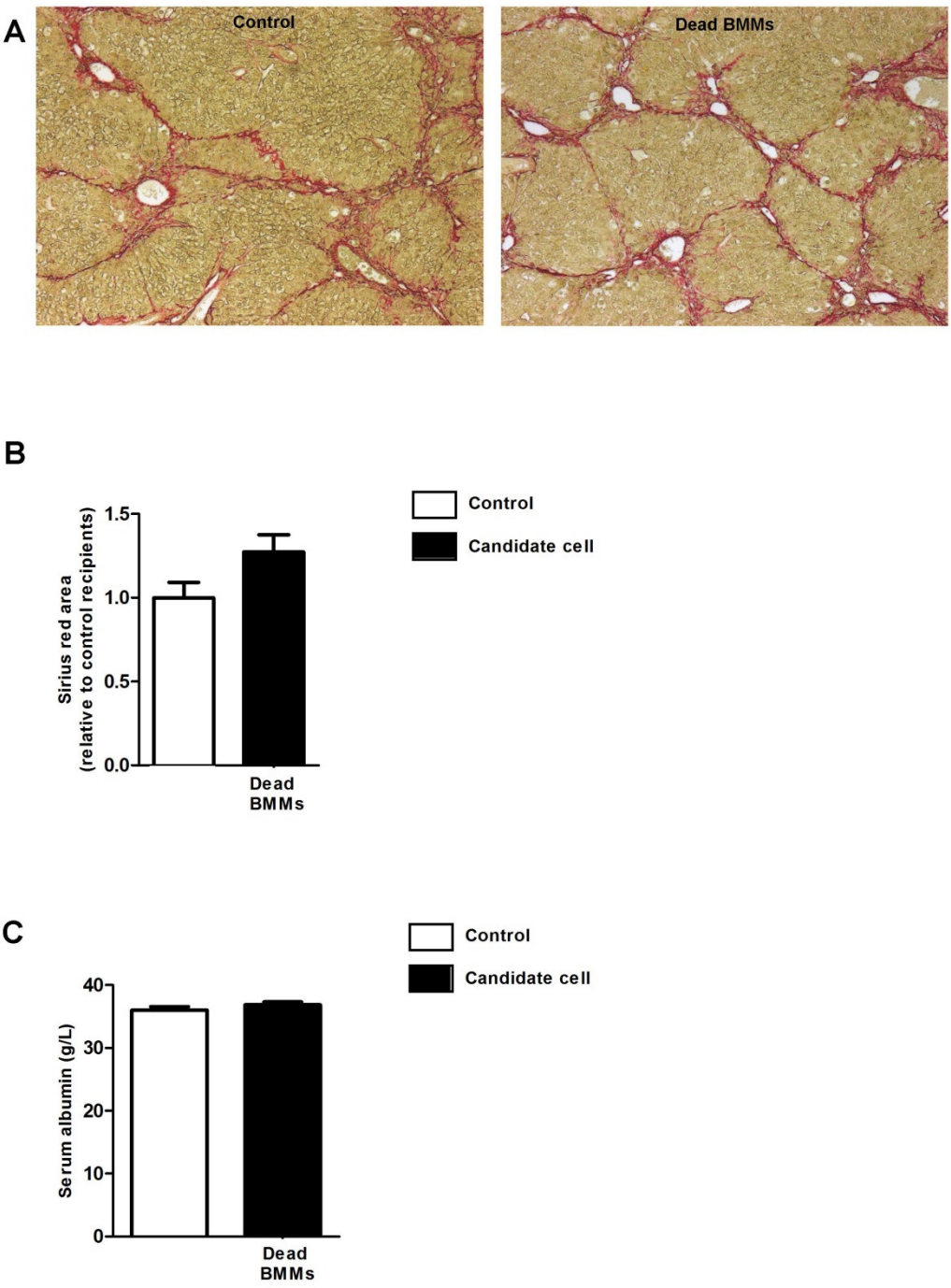

Figure 4.11 Dead BMMs do not recapitulate the phenotype of viable BMMs

Advanced liver fibrosis was induced in adult female C57Bl/6 mice by the chronic administration of twice weekly IP CCl_4.

(**A**) The injection of 1 x 10^6 sonicated BMMs into the HPV did not improve liver fibrosis. Photomicrographs show PSR staining for hepatic collagens 4 weeks after dead BMMs were delivered to syngeneic fibrotic mice (right sided column). Age and strain-matched mice from the same cohort received an equal volume of control medium (left column). Original magnification, x80.

(**B**) Morphometric analysis demonstrated a non-significant trend (P = .08) towards an increased amount of fibrosis following the application of dead BMMs. This histogram is derived from the data in table 4.9 below; all values are expressed as a ratio of the mean of the internal control group.

(**C**) Serum albumin levels were not changed by the delivery of non-viable BMMs (n=6-7 per group).

Table 4.9 Dead BMMs do not recapitulate the phenotype of viable BMMs

Sample	Control	Dead BMMs
PSR % Mean +/- SEM	4.9 +/- 0.5	6.2 +/- 0.5
PSR % N	6	7
P value (Student's t test)	0.09	
serum albumin (g/L) Mean +/- SEM	36+/- 0.6	36.9 +/- 0.5
serum albumin (g/L) N	6	7
P value (Student's t test)	0.26	

BMMs do not improve fibrosis or regeneration in the cholestatic 1% DDC diet model

An important categorisation of the common aetiologies of human cirrhosis is that some disease processes predominantly involved parenchymal (hepatocyte) damage such as viral hepatitis and alcohol induced injury whilst some are cholestatic such as PSC and primary biliary cirrhosis (PBC). Though less prevalent, these cholangitic diseases are significantly different in terms of injury pattern and therefore the precise fibrotic and regenerative pathways involved. In order to determine the effects of BMM therapy in a cholestatic model, I delivered 1 x 10^6 donor BMMs 3 weeks into a 5 week 1% DDC diet protocol. The DDC diet causes cholangiopathy with biliary fibrosis and an accompanying progenitor cell response (Fickert, Stoger et al. 2007; Boulter, Govaere et al. 2012). The figure below (figure 4.11) illustrates the experimental time course.

Figure 4.12 Schematic of DDC diet experimental protocol

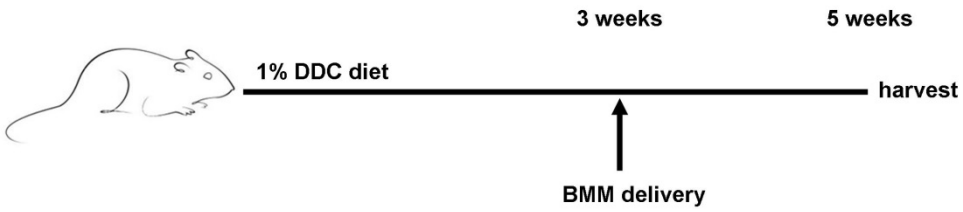

There were no differences detected in PSR staining, PCK positive progenitor cell numbers or serum albumin following BMM delivery (figure 4.12). Previous work in our group (personal communication with Dr Luke Boulter) had shown that extended

periods on this diet led to a reduction in weight with an increased risk of mortality. Therefore in line with guidance from the Home Office veterinary surgeons, the protocol was designed in the light of this to prevent a high rate of death before the intended end of the experiment. It is possible that injecting BMMs after 3 weeks of injury, with a further 2 weeks before harvesting the mice, may not have been the optimal timeframe to detect any changes.

Another plausible explanation as to why BMM therapy may be of limited value in cholangiopathy relates to structural aspects of this disease model. Digital reconstruction of the cellular relationships in this model has shown that LPCs are surrounded by a dense layer of myofibroblasts and collagen I effectively limiting macrophage access and therefore influence. This has important implications upon the direction of LPC fate specification. The spatial relationships in a more hepatocytic model (the CDE diet) demonstrate a greater number of macrophages with fewer myofibroblasts and collagen I around the LPC niche (Boulter, Govaere et al. 2012). Thus it is conceivable that macrophage based therapy may be of limited efficacy in the context of cholestatic disease.

Figure 4.13 BMMs did not improve fibrosis or regeneration in the DDC model

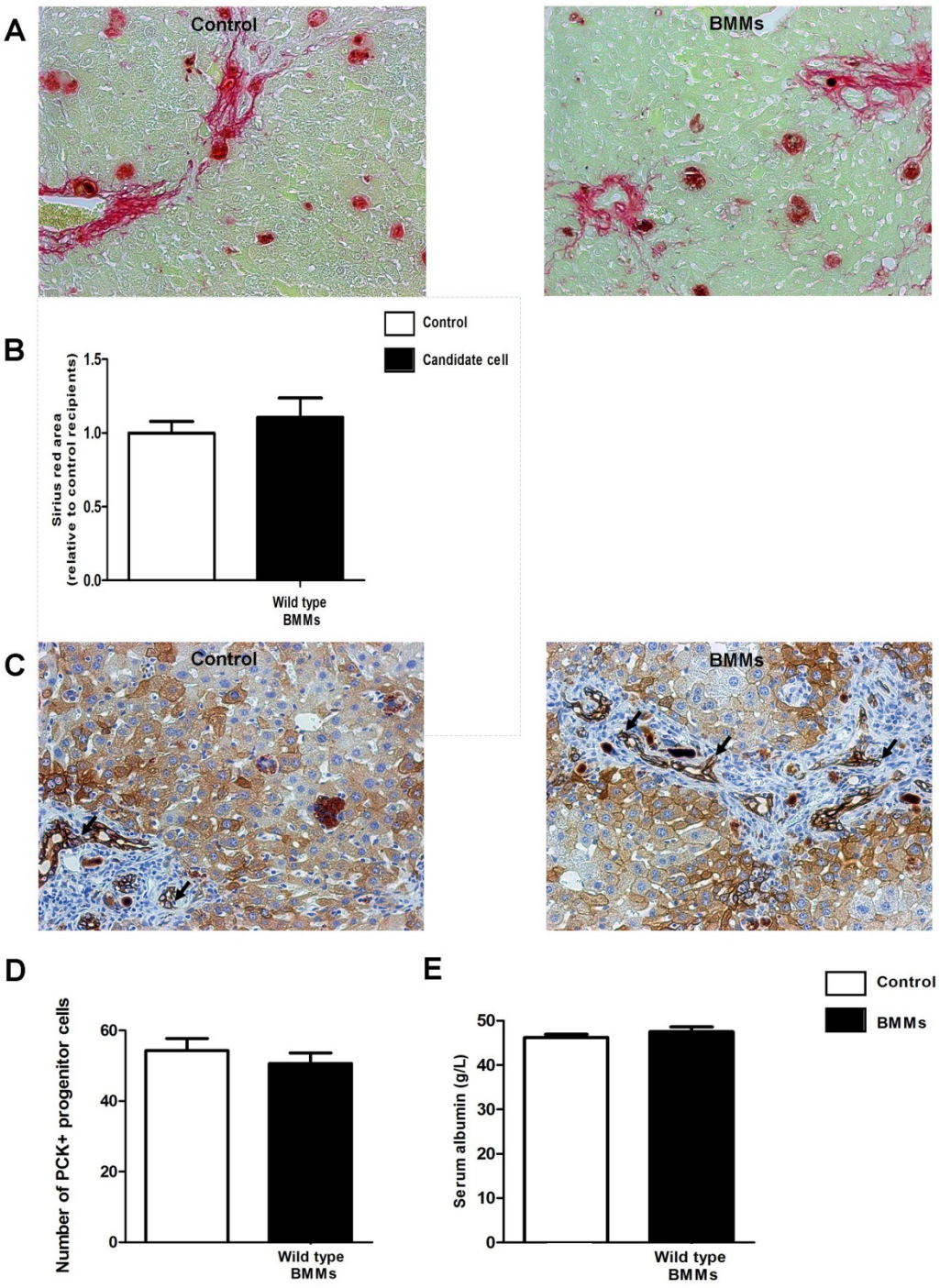

Figure 4.13 BMMs did not improve fibrosis or regeneration in the DDC model

The injection of 1 x 10^6 syngeneic BMMs into the HPV during the DDC diet injury model in S129 S2 mice did not lead to apparent improvements in disease phenotype.

(**A**) Photomicrographs show PSR staining for hepatic collagens 2 weeks after BMMs were delivered to syngeneic fibrotic mice (right sided image). Age and strain-matched mice from the same cohort received an equal volume of control medium (left image). Original magnification, x200.

(**B**) Morphometric analysis did not show any difference in liver fibrosis.

(**C**) Photomicrographs show PCK immunostaining of LPCs (arrowed) following BMM delivery. Original magnification, x200.

(**D**) Quantification of LPC number did not show any difference 2 weeks after BMM delivery.

(**E**) Serum albumin levels were not changed by the delivery of BMMs in the DDC model (n=6-9 per group).

Histograms are derived from the data in table 4.10 ; all values are expressed as a ratio of the mean of the internal control group.

Table 4.10 BMMs did not improve fibrosis or regeneration in the DDC model

Sample	Control	BMMs
PSR % Mean +/- SEM	6.4 +/- 0.5	7.1 +/- 0.8
PSR % N	9	6
P value (Student's t test)	0.48	
PCK+ LPCs/ x200 field Mean +/- SEM	2.7 +/- 0.2	2.6 +/- 0.1
PCK+ LPCs/ x200 field N	9	6
P value (Student's t test)	0.52	
serum albumin (g/L) Mean +/- SEM	46.2 +/- 0.7	47.5 +/- 1.0
serum albumin (g/L) N	9	6
P value (Student's t test)	0.33	

Discussion

From a translational perspective, the deleterious effect of unfractionated (whole) BM on liver fibrosis is particularly noteworthy. This could be due to components of the BM such as MSCs that have pro-fibrogenic actions in specific circumstances (Russo, Alison et al. 2006; di Bonzo, Ferrero et al. 2008). Interestingly, exogenous CSF-1R positive macrophage precursors did not significantly improve liver fibrosis. This population contains Gr-1^{hi} (Ly-6C^{hi}) monocytes (Sasmono, Ehrnsperger et al. 2007) that have pro-fibrogenic actions during liver injury (Karlmark, Weiskirchen et al. 2009). Therefore this mixed cell population might have competing effects on net fibrosis.

Following culture in CSF-1 conditioned medium, CSF-1R positive macrophage precursors within BM differentiate into macrophages (Sasmono, Ehrnsperger et al. 2007). The BMMs used here were cultured in non-adherent conditions and possessed neither the typical M1 nor M2 profiles. They expressed a number of factors with effects on cell recruitment as well as inflammation and repair. Though donor BMM engraftment was transient, their effects persisted and were amplified by paracrine signalling to host cell populations. The net effect on the injured liver was a reduction in fibrosis and improvement in regeneration beyond the lifespan of the donor cells.

BMM therapy caused the recruitment of MMP producing host cells into the hepatic scar. MCP-1 and MIP-1α are members of the CC chemokine subfamily that bind to the CCR2 and CCR1/5 receptors of monocytes respectively. These interactions contribute to the navigation of monocytes into target tissues during their maturation into macrophages (Mantovani, Sica et al. 2004). The delivery of MCP-1 and MIP-1α expressing BMMs to injured mice caused upregulation of hepatic MCP-1 and MIP-1α and the recruitment of endogenous macrophages. These increased numbers of SAMs expressed MMP-13 which has proteolytic actions on fibrillar collagens and gelatin, as well as activating other MMPs (including MMP-9) (Fallowfield, Mizuno et al. 2007).

Donor BMMs also strongly expressed MIP-1α and MIP-2. These CXC chemokines recruit neutrophils through the surface receptor CXCR2 (Mantovani, Sica et al. 2004). Within 1 day of BMM delivery, there was increased hepatic production of the neutrophil chemoattractants MIP-1α, MIP-2 and KC with subsequently increased hepatic neutrophil numbers. This is in keeping with the role of macrophage mediated neutrophil recruitment in fibrosis resolution following cessation of injury (Harty, Papa et al. 2008). During ongoing hepatic damage in the experiments described in this results chapter, BMM therapy induced neutrophil recruitment. Host neutrophils produced MMP-9 in this model. During the recovery phase after liver injury, endogenous BM derived neutrophils have been shown to home to the hepatic scar and produce MMP-9 (Higashiyama, Inagaki et al. 2007). Separately, supra-physiological MMP-9 over-expression reduces myofibroblast number and fibrogenesis during experimental liver injury (Roderfeld, Weiskirchen et al. 2006). This suggests that BMM therapy may recapitulate certain features of the resolution process despite ongoing injury. The concurrent trend of increased MMP-12 (macrophage metalloelastase) and MMP-8 (neutrophil collagenase) expression reinforces a fibrolytic role for recruited macrophages and neutrophils.

In addition to MMPs, both IGF-1 (Sobrevals, Rodriguez et al. 2010) and IL-10 (Thompson, Maltby et al. 1998; Huang, Shi et al. 2006) have been shown to reduce myofibroblast number and fibrosis. The delivery of exogenous recombinant CSF-1 limits scar formation in murine models of myocardial infarction (Morimoto, Takahashi et al. 2007). The magnitude of hepatic IL-10 protein upregulation was considerable (346%) and may modify the behaviour of both resident and incoming cells as well as limiting the degree of injury. This suggests that the chemokine mediated recruitment of host effector cells to the injured liver, critically at a time when the prevailing hepatic cytokine environment is anti-inflammatory, could represent a novel and realistic mechanism for the therapeutic actions of comparatively few donor cells on the whole liver.

The improved liver function following BMM therapy is multifactorial in origin. Elevated levels of cytokines such as CSF-1 (Menke, Iwata et al. 2009), VEGF (Nakamura, Torimura et al. 2007) and IGF-1 (Sobrevals, Rodriguez et al. 2010) have individually been shown to have powerful reparative properties. All of these factors were significantly upregulated following BMM delivery. Though statistically significant hepatocyte proliferation was not detected, there was a consistent trend at each time point. Ki67 is a marker of cellular proliferation; Ki67 positive hepatocyte number has been shown to correlate with restoration of liver mass after partial hepatectomy. (Zou, Bao et al. 2012) Whilst this antigen is present throughout the active phases of the cell cycle, quantification of mitotic hepatocytes may have provided more specific information regarding hepatocyte mediated regeneration following BMM therapy. (Marshall, Rushbrook et al. 2005) It is plausible that the improvement in hepatic milieu in addition to trophic signalling (e.g. by HGF) contribute to this regenerative compartment. BMM induced activation of the LPC compartment is compatible with the clinical observation that BM infusion transiently stimulated LPCs and improved serum albumin in a series of cirrhotic patients (Kim, Park et al. 2010). Given the close spatial relationship between LPCs and endogenous macrophages *in vivo* during disease (Lorenzini, Bird et al. 2010), it was predicted that BMM delivered signals could support LPC activation. Exogenous TWEAK delivery results in LPC activation (Tirnitz-Parker, Viebahn et al. 2010) which parallels the observed macrophage mediated delivery of this mitogen to the site of action followed by LPC proliferation. Intriguingly, BMMs even activate LPCs in healthy, normal mice. The functional effects of the BMM – TWEAK axis in the uninjured liver have since been explored providing a clear role for TWEAK acting via the Fn14 receptor to stimulate LPCs resulting in proliferation, liver growth and supra-physiological serum albumin levels.(Bird, Lu et al. 2013). In the context of liver disease, hepatic scar degradation itself supports LPC activation (Kallis, Robson et al. 2011). Therefore LPC proliferation is also indirectly enhanced by the macrophage mediated hepatic scar reduction. This highlights the multiple, overlapping effector pathways initiated by cell therapy.

The donor BMMs used here expressed high levels of TWEAK and recruited additional host macrophages to the injured liver. This supports the paradigm of donor cell derived paracrine signals having downstream actions on host cell populations. This could permit a numerically small number of injected (and even fewer engrafted) cells to exert whole organ changes.

CHAPTER FIVE

The importance of the route of BMM therapy

Introduction

The routes of administration of cells in human studies have included peripheral veins, the hepatic portal vein (HPV) and hepatic artery (HA). The most concerning report from the literature to date relates to complications following use of the hepatic artery (Mohamadnejad, Namiri et al. 2007). The safety, acceptability and costs of peripheral cell infusions are considerably more favourable than with the HPV or HA route. However, determining the efficacy of different routes of cell delivery is crucial in addition to assessing the associated risks.

Chapters 3 and 4 report results following the HPV delivery of BM derived cells. In this chapter, I compare the outcomes from HPV and tail vein BMM administration. This was further examined by delivering a greater number of BMMs repeatedly by the peripheral route. The fate of donor BMMs was studied by *in vivo* tracking experiments using a transgenic GFP reporter, which provided insights into the reasons behind the lack of effect from peripheral vein macrophage delivery.

A single dose of BMMs delivered via the tail vein does not produce therapeutic effect

In contrast to the injection of 1 x 10^6 BMMs into the HPV having therapeutic effect (figures 3.4, 3.5 and 3.6), 1 x 10^6 BMMs injected into the tail vein did not improve the measured parameters (figure 5.2A, B and C). The schematic below (figure 5.1) illustrates the time course of his experiment.

Figure 5.1 Schematic of CCl_4 experimental protocol testing alternative routes of BMM delivery

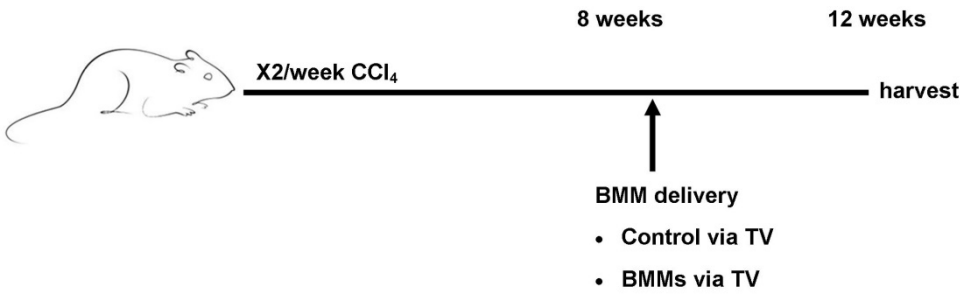

Figure 5.2 Tail vein administered BMMs do not have therapeutic effect

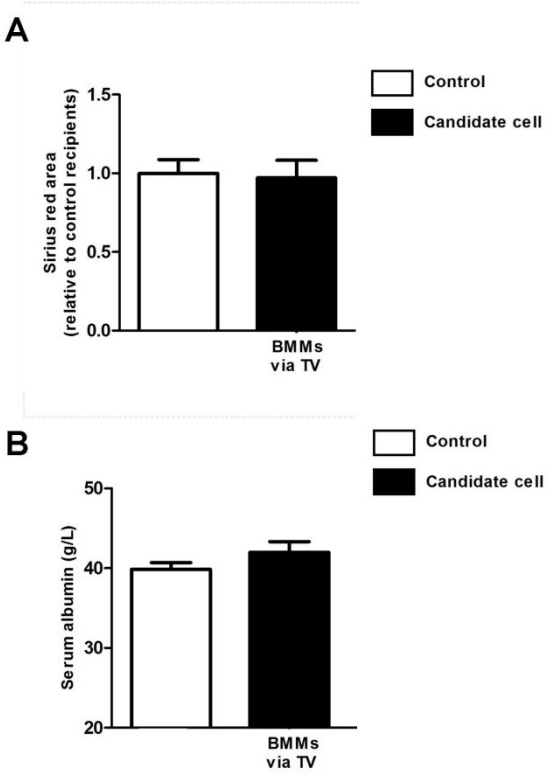

Figure 5.2 Tail vein administered BMMs do not have therapeutic effect

Advanced liver fibrosis was induced in adult female C57Bl/6 mice by the chronic administration of twice weekly IP CCl_4. These mice received 1 x 10^6 syngeneic BMMs or an equal volume of control medium injected by the tail vein (TV).

(**A**) Morphometric analysis of PSR staining was performed to detect hepatic collagen 4 weeks after BMMs were delivered to syngeneic fibrotic mice by the TV. There was no significant reduction in liver fibrosis. This histogram is derived from the data in table 5.1 below; all values are expressed as a ratio of the mean of the internal control group. This allows relative comparison of BMM effect between experiments at different time points.

(**B**) Serum albumin levels were also unchanged following BMM delivery via the TV (n=7-8 per group).

Table 5.1 Tail vein administered BMMs do not have therapeutic effect

Sample	Control	BMMs
PSR % Mean +/- SEM	3.7 +/- 0.3	3.6 +/- 0.4
PSR % N	8	8
P value (Student's t test)	0.83	
albumin g/L Mean +/- SEM	39.9 +/- 0.9	42.0 +/- 1.3
albumin g/L N	7	7
P value (Student's t test)	0.20	

Repeated peripheral vein administration of BMMs does not recapitulate the effect of the intraportal route

Given the lack of improvement in liver fibrosis or serum albumin following the single injection of 1 x 10^6 BMMs via the tail vein, I next tested the effects of 5 x 10^6 BMMs delivered on 4 occasions at weekly intervals.

The schematic below (figure 5.3) illustrates the time course.

Figure 5.3 Schematic of CCl4 experimental protocol testing repeated delivery of BMMs via the tail vein

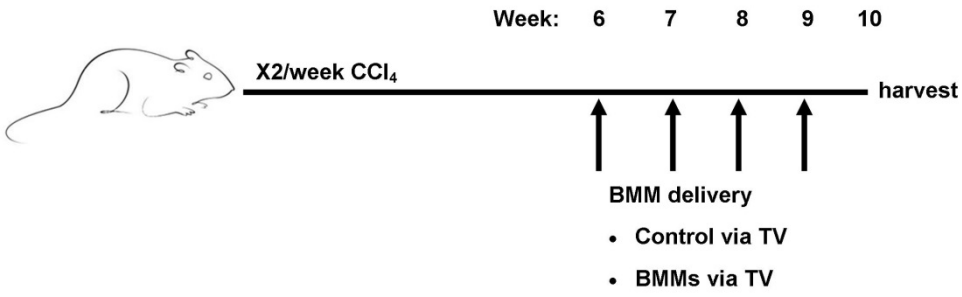

The application of 5 x 10^6 BMMs four times over the last month of CCl_4 did not change the amount of fibrosis, number of LPCs or serum albumin (figure 5.4). Therefore, further experiments were undertaken to investigate the anatomical distribution of BMMs early after infusion via the HPV and TV.

Figure 5.4 Repeated applications of BMMs via the tail vein do not have therapeutic effect

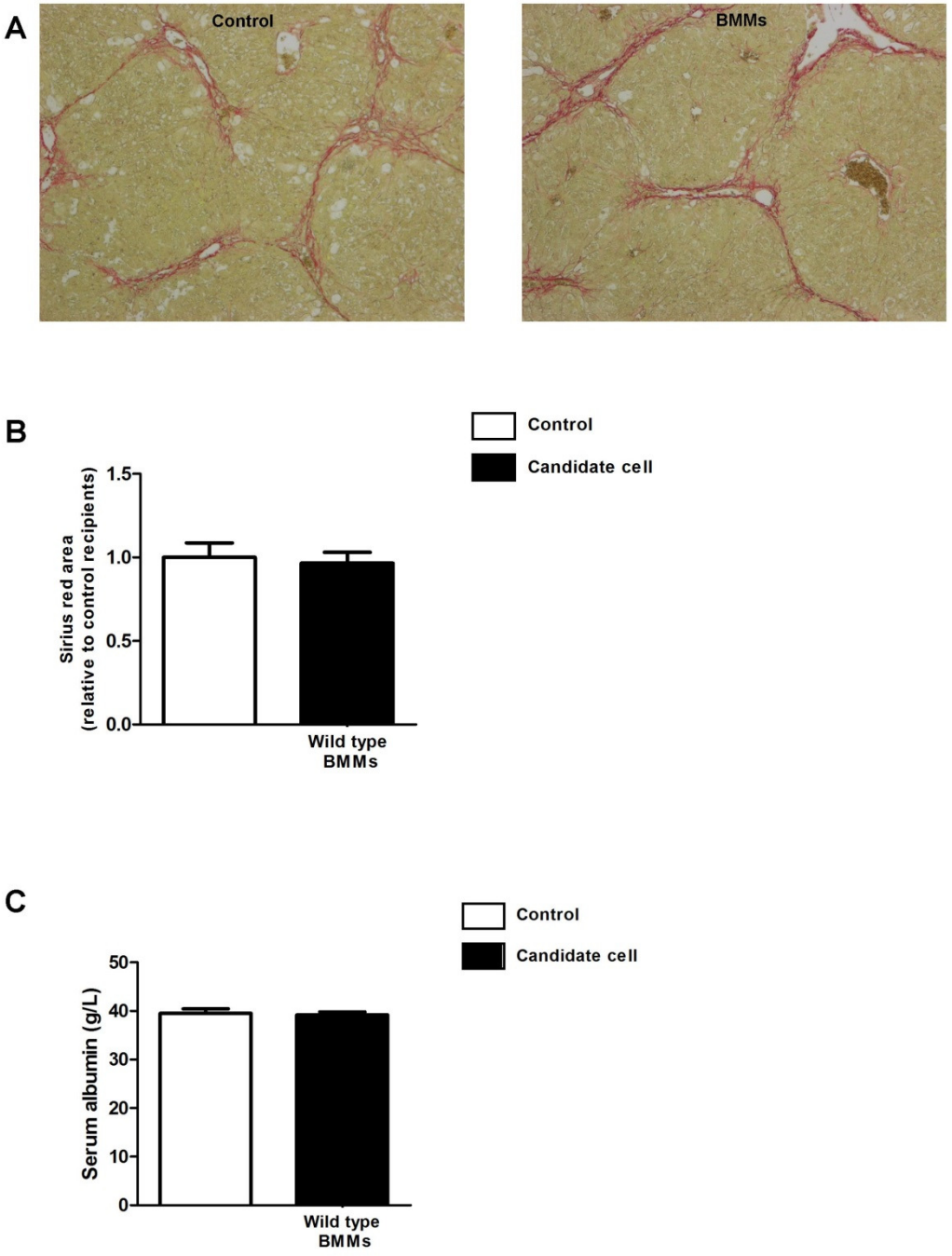

Figure 5.4 Repeated applications of BMMs via the tail vein do not have therapeutic effect

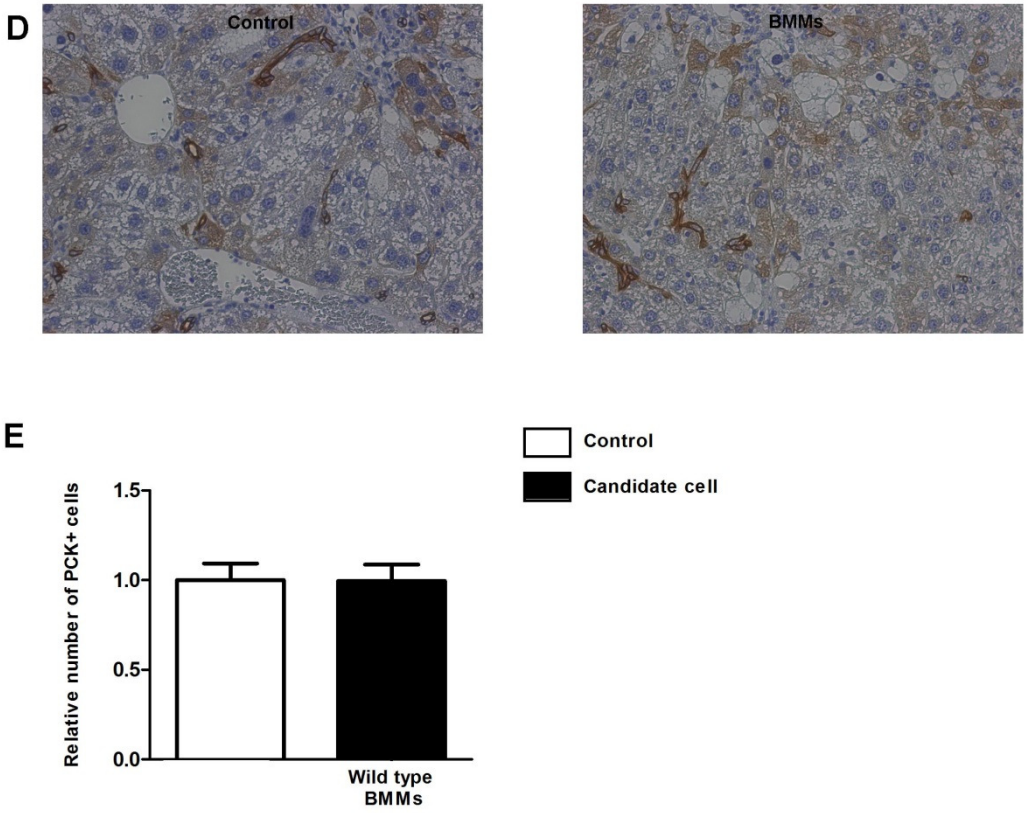

Figure 5.4 Repeated applications of BMMs via the tail vein do not have therapeutic effect

Advanced liver fibrosis was induced in adult female C57Bl/6 mice by the chronic administration of twice weekly IP CCl_4. The injection of four doses of 5 x 10^6 syngeneic BMMs at 1 week intervals into the TV did not lead to apparent improvements in disease phenotype.

(**A**) Photomicrographs show PSR staining for hepatic collagens after BMMs were delivered to syngeneic fibrotic mice (right sided image). Age and strain-matched mice from the same cohort received an equal volume of control medium (left image). Original magnification, x200.

(**B**) Morphometric analysis did not show any difference in liver fibrosis.

(**C**) Serum albumin levels were not changed by the repeated peripheral administration of BMMs.

(**D**) Photomicrographs show PCK immunostaining of LPCs. Original magnification, x200.

(**E**) Quantification of LPC number did not show any difference following repeated BMM delivery via the tail vein (n=8-11 per group).

These histograms are derived from the data in table 5.2 below; all values are expressed as a ratio of the mean of the internal control group. This allows relative comparison of BMM effect between experiments at different time points.

Table 5.2 Repeated applications of BMMs via the tail vein do not have therapeutic effect

Sample	Control	BMMs
PSR % Mean +/- SEM	10.1 +/- 0.9	9.7 +/- 0.7
PSR % N	8	11
P value (Student's t test)	0.75	
PCK+ LPCs/ x200 field Mean +/- SEM	9.7 +/- 0.9	9.7 +/- 0.9
PCK+ LPCs/ x200 field N	8	11
P value (Student's t test)	0.98	
serum albumin (g/L) Mean +/- SEM	39.5 +/- 0.9	39.2 +/- 0.6
serum albumin (g/L) N	8	11
P value (Mann-Whitney test)	0.59	

Constitutive GFP expression does not affect the biology of donor BMMs

Differentiated donor BMMs that constitutively express GFP (Pratt, Sharp et al. 2000) were used to allow *in vivo* tracking of these cells as they pass through the recipient circulation and organs. Firstly, experiments were performed to confirm that the reporter did not compromise the phenotype of these cells in terms of the therapeutic effects on liver fibrosis and albumin. As previously, the area of fibrosis significantly decreased whilst the serum albumin level was higher in the treatment group (43.3 ±0.6 g/L v 40.4 ±1.0 g/L) following BMM delivery via the HPV (figure 5.5).

Figure 5.5 GFP positive BMMs delivered via the HPV improve liver fibrosis and serum albumin

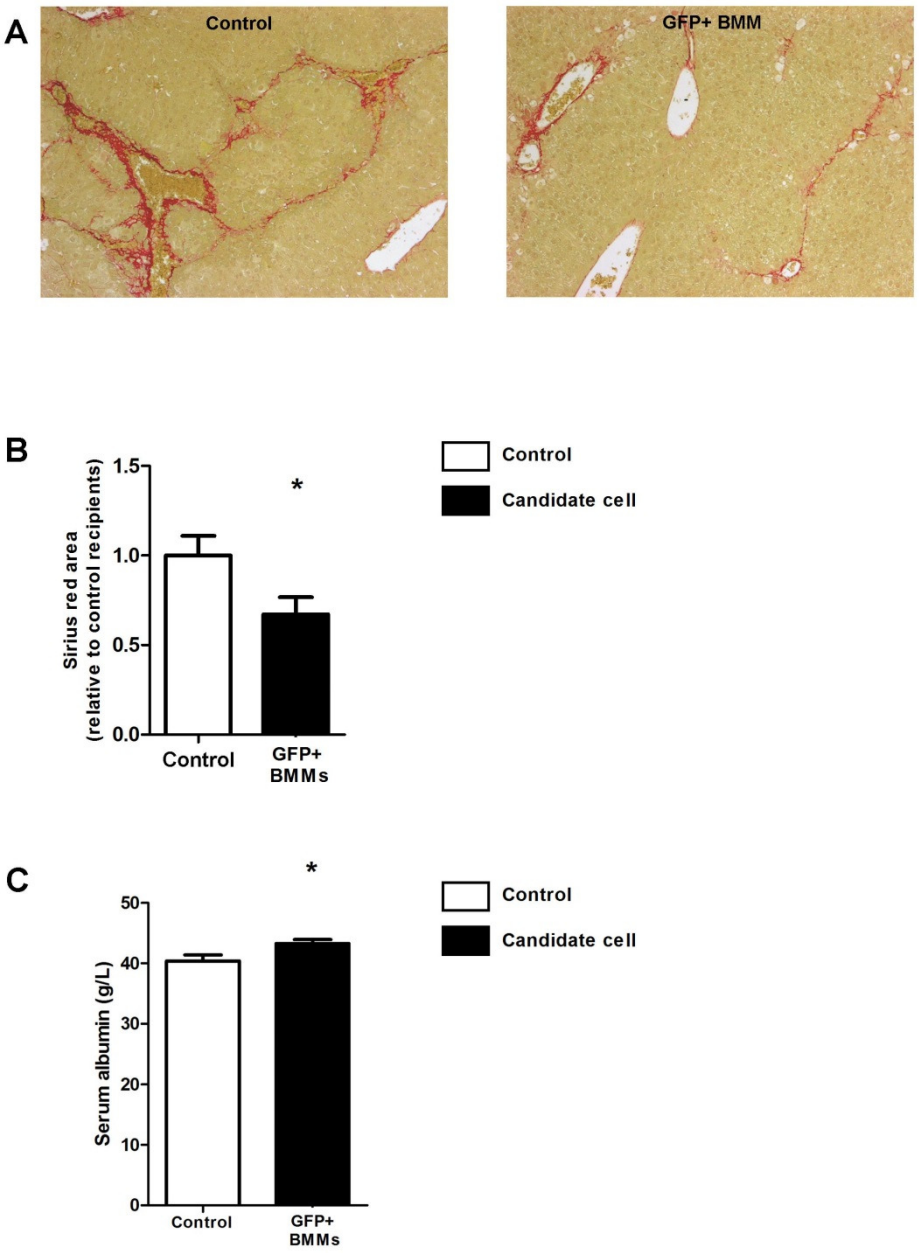

Figure 5.5 GFP positive BMMs delivered via the HPV improve liver fibrosis and serum albumin

Advanced liver fibrosis was induced in adult female wild type CBA mice by the chronic administration of twice weekly IP CCl_4. BMMs were cultured from the BM of transgenic constitutively GFP expressing mice on a CBA background. BMMs were cultured as described in Chapter 2, fluorescence based selection was therefore not required. 5 x 10^6 GFP positive BMMs were injected into the HPV of wild type CBA mice 6 weeks into a 10 week CCl_4 injury protocol.

(**A**) Photomicrographs show PSR staining for hepatic collagens after BMMs were delivered to syngeneic fibrotic mice (right sided image). Age and strain-matched mice from the same cohort received an equal volume of control medium (left image). Original magnification, x200.

(**B**) Morphometric analysis shows a reduction in liver fibrosis. This histogram is derived from the data in table 5.3 below; all values are expressed as a ratio of the mean of the internal control group. This allows relative comparison of BMM effect between experiments at different time points.

(**C**) Serum albumin levels increased following administration of GFP positive BMMs. (* $P < .05$ compared with control recipients per time point; n=7-8 per group).

Table 5.3 GFP positive BMMs delivered via the HPV improve liver fibrosis and serum albumin

Sample	Control	BMMs
PSR % Mean +/- SEM	1.0 +/- 0.1	0.7 +/- 0.1
PSR % N	8	7
P value (Student's t test)	0.04	
albumin g/L Mean +/- SEM	40.4 +/- 1.0	43.3 +/- 0.6
albumin g/L N	8	7
P value (Student's t test)	0.04	

Peripheral vein BMM delivery affects cell destination and hepatic engraftment

To determine why the tail vein route of BMM administration did not cause the improvements seen after the HPV delivery of the same cells, a series of early time course experiments were conducted in collaboration with Dr Caroline Pope using BMMs expressing the stable GFP reporter (Pratt, Sharp et al. 2000). 1 x 10^6 GFP positive BMMs were delivered via the HPV or tail vein. BMM recipients were harvested 10 minutes and 1, 6, 12 and 24 hours after BMM delivery. In particular, the liver, spleen, kidneys and lungs were examined for the presence of GFP positive BMMs by immunohistochemistry which was then quantified (figure 5.6).

Shortly after injection of BMMs via the tail vein, these cells had predominantly accumulated in the lungs (figure 5.6B). In contrast, few BMMs injected via the HPV were detectable in the lungs at this time point (figure 5.6B). The peak rate of hepatic engraftment was detected 6 hours after BMM delivery by the HPV (figure 5.6A). Interestingly, between the first hour and 1 day time points there was evidence of BMM migration from the vessel wall (figure 5.7C) into the parenchyma and towards the scar (figure 5.7D). The cells also seemed to change morphology, appearing more compressed (in 2 dimensions) during ingress into the solid organ. The TV delivered BMMs achieved less than 30% of the hepatic engraftment of HPV injected cells (figure 5.6A). The number of BMMs in the spleen was similar in both groups (figure 5.6C). Few cells were found in the kidney (figure 5.7E).

Figure 5.6 In vivo tracking of donor BMMs during the first 24 hours after injection

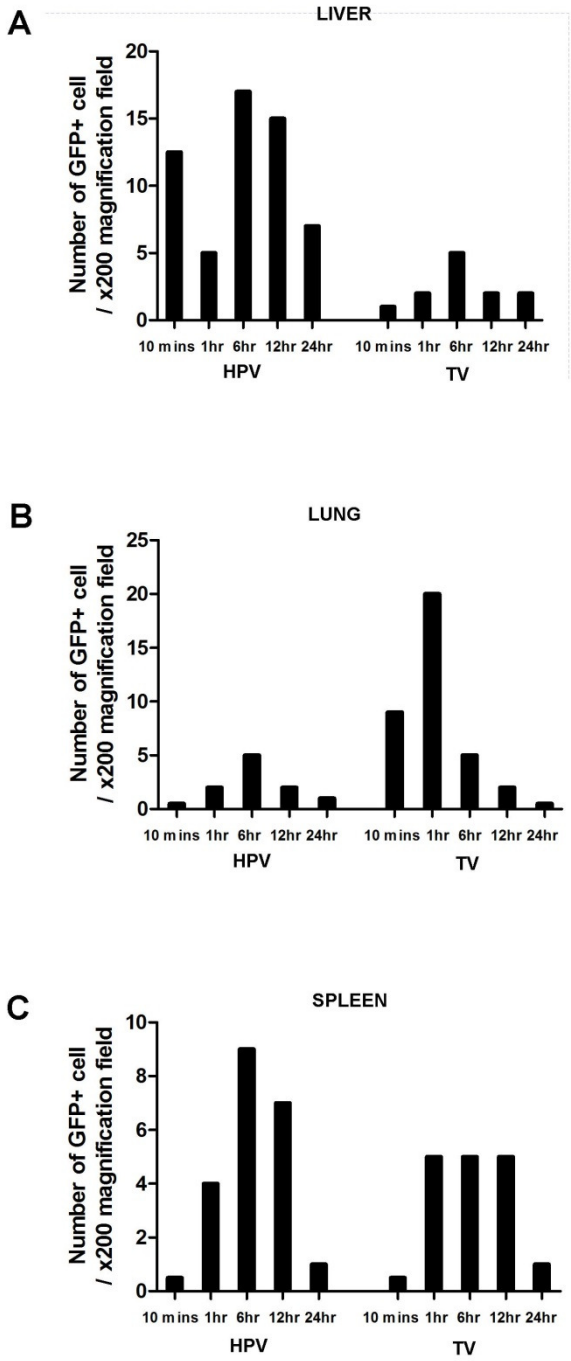

Figure 5.6 In vivo tracking of donor BMMs during the first 24 hours after injection

Advanced liver fibrosis was induced in adult female wild type CBA mice by the chronic administration of twice weekly IP CCl_4. 1 x 10^6 GFP positive BMMs were injected into wild type fibrotic CBA recipients. Mice were then harvested at time points over the first day. This allowed immunohistochemical detection of the donor BMMs and their quantification in the (**A**) liver, (**B**) lungs and (**C**) spleen. This is graphically represented to demonstrate the kinetics of donor BMM in the host. Data in collaboration with Dr Caroline Pope (n=1-2 per group per time point).

Figure 5.7 Visualisation of donor BMMs in recipient tissue

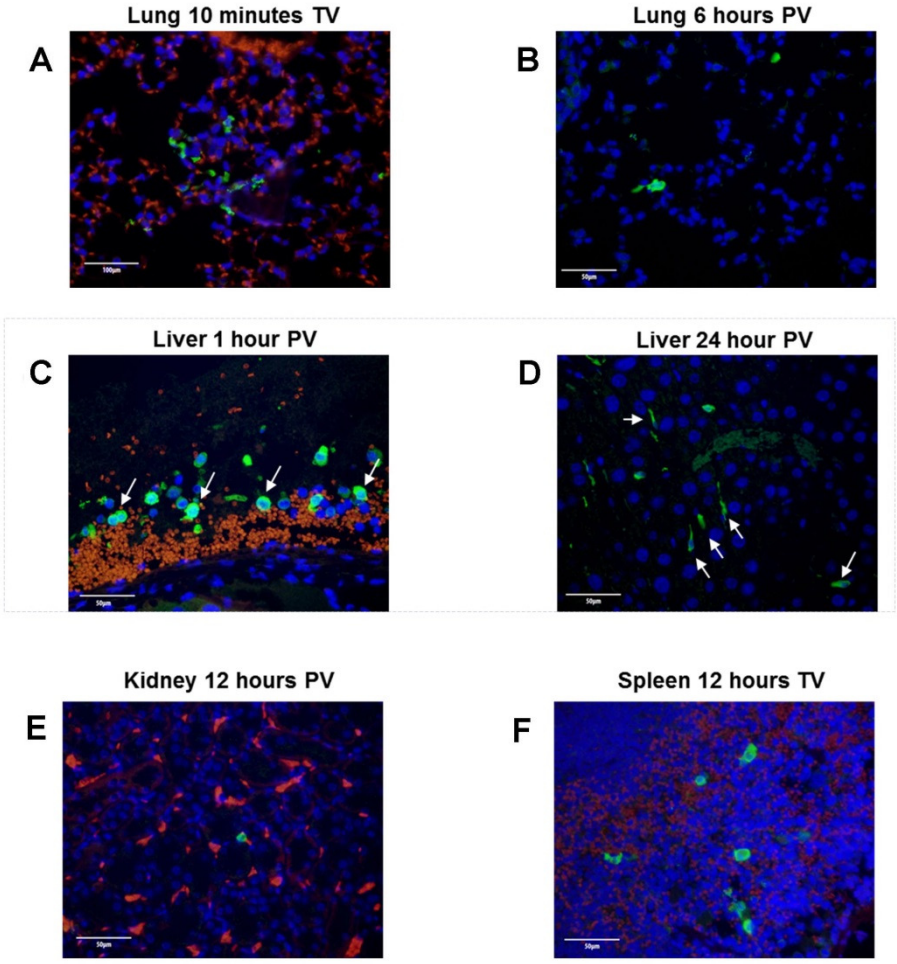

Figure 5.7 Visualisation of donor BMMs in recipient tissue

Donor GFP positive BMMs were injected into wild type fibrotic CBA mice. Sections of liver, lung, spleen and kidney were immunostained for GFP which was visualised fluorescently.

(A) Tracked BMMs were detected in lung from 10 minutes after infusion by the tail vein (TV).

(B) Few cells were detected in the lungs 6 hours after HPV delivery.

(C) Hepatic BMMs (arrows) were noted to be near the vessel wall within an hour of HPV delivery.

By 24 hours **(D)**, HPV delivered BMMs (arrows) appeared to have ingressed into the liver parenchyma.

(E) BMMs were only detected infrequently in the kidney; this is a representative image 12 hours after the HPV injection of BMMs.

(F) The numbers of BMMs in the spleen were fairly constant, this image is from 12 hours after the TV administration of BMMs. Data in collaboration with Dr Caroline Pope. Scale bars present in images (n=1-2 per group per time point).

Discussion

These data confirm that the TV delivery of BMMs resulted in markedly fewer donor cells engrafting in the liver. Therefore the lack of response to cells by this route may in part be dose related. However, the experiments outlined in figures 5.3 and 5.4 used significantly greater numbers of BMMs delivered repeatedly to address this issue. A limiting factor could potentially be insufficient numbers of donor BMMs in the liver to trigger the threshold required to initiate the cascade of events resulting in the amplification of effects already discussed in chapter 4. Another issue could be that the TV route requires BMMs to pass through the pulmonary vasculature at least once before having the opportunity to engraft in the injured liver. Some of these cells may remain in the lungs for a number of hours before transiting to the liver. This could result in phenotypic change of these donor BMMs by the host pulmonary micro-environment. It is plausible that this could affect the subsequent behaviour of donor BMMs in the liver and introduce functional heterogeneity to this cell population.

Route related differences on the effects of cell therapy have since been reported by Wang and colleagues (Wang, Lian et al. 2012). Though MSCs and macrophages have different biological actions, the donor cell dose and route to the liver could also explain why they found that MSCs had similarly therapeutic effects on mouse liver only when delivered via the HPV, and not when injected into the TV.

CHAPTER SIX

Conclusions and future directions

Key findings and their integration with the literature

Liver fibrosis and regeneration are intrinsically linked processes which are both in part directed by host macrophages. The effects of HPV delivered exogenous BMMs on these pathways are summarised in figure 6.1. Following hepatic engraftment of donor BMMs, there is upregulation of chemotactic mediators and increased scar cellularity particularly comprising host macrophages and neutrophils. This is accompanied by a significant early increase in hepatic levels of the anti-inflammatory mediator IL-10. Host hepatic macrophages and neutrophils express scar degrading MMPs. There is a subsequent reduction in fibrogenic myofibroblasts and liver scarring. Donor BMMs also expressed the LPC mitogen TWEAK and caused expansion of the stem cell compartment with elevated serum albumin levels.

The potentially harmful effects of unfractionated (whole) BM represent an important caveat for human studies. Following publication of these findings (Thomas, Pope et al. 2011), a Japanese group have reported data with a number of similarities (Iwamoto, Terai et al. 2013). Though the culture of donor BM cells was by a different protocol, a significant proportion of infused (and engrafted) cells were F4/80 positive macrophages. Cell injection caused upregulation of hepatic MMP-9 with a reduction in fibrosis. A fraction of the infused cells was considered to contain MSCs; consistent with this, vimentin positive cells of donor origin were identified. This indicates the possibility of supplying cells with the potential to have myofibroblast-like actions, highlighting the benefits of using a defined and committed cell population.

Subsequently published data from our group has shown that during fibrosis regression following the cessation of CCl_4 injury, circulating macrophages are recruited to the liver and switch phenotype to upregulate MMP expression and exert anti-fibrotic actions (Ramachandran, Pellicoro et al. 2012). Though a distinct process from this study of *ex vivo* cultured cells delivered as therapy in the context of ongoing injury, there are parallels in terms of mode of action.

In addition to the literature concerning cell therapy for liver disease, these findings can also be viewed in the context of macrophage cell therapy in diabetes and renal and pulmonary disease models. The ability of macrophages to home to sites of inflammation has been utilised to target these cells to the injured organ in question. In a rat model of nephrotoxic nephritis, macrophages transfected with adenovirus expressing IL-4 reduced albuminuria (Kluth, Ainslie et al. 2001), whilst transfection with adenovirus expressing IL-10 also produced anti-inflammatory effects and improved albuminuria (Wilson, Stewart et al. 2002). Distinct from the specific over-expression of a reparative cytokine, the delivery of wild type macrophages in a transgenic murine model of pulmonary alveolar proteinosis (GM-CSF receptor β subunit -/-) corrects the host deficiency thereby treating the lung disease (Suzuki, Arumugam et al. 2014).

In contrast to direct genetic modification of or by macrophages, *ex vivo* direction of macrophages towards the stereotypical M2 phenotype prior to injection has been successful in preventing type 1 diabetes in NOD mice (Parsa, Andresen et al. 2012). Macrophages influenced towards the M2 phenotype also ameliorated renal injury in severe combined immunodeficient (SCID) mice with adriamycin nephropathy (Wang, Wang et al. 2007). Though a useful construct, the M1 M2 paradigm is considered a simplification that does not reflect the biological spectrum of macrophage phenotypes (Mosser and Edwards 2008). The BMMs given as therapy in this thesis were not polarised *ex vivo* to express the typical M1 or M2 profiles. Similarly, unstimulated macrophages have also been shown to have anti-fibrotic effects in a murine model of renal fibrosis caused by cyclophosphamide exposure and unilateral ureteral obstruction (Nishida, Okumura et al. 2005).

Figure 6.1 The effects of HPV delivered BMMs on key processes in liver fibrosis and regeneration during chronic liver injury

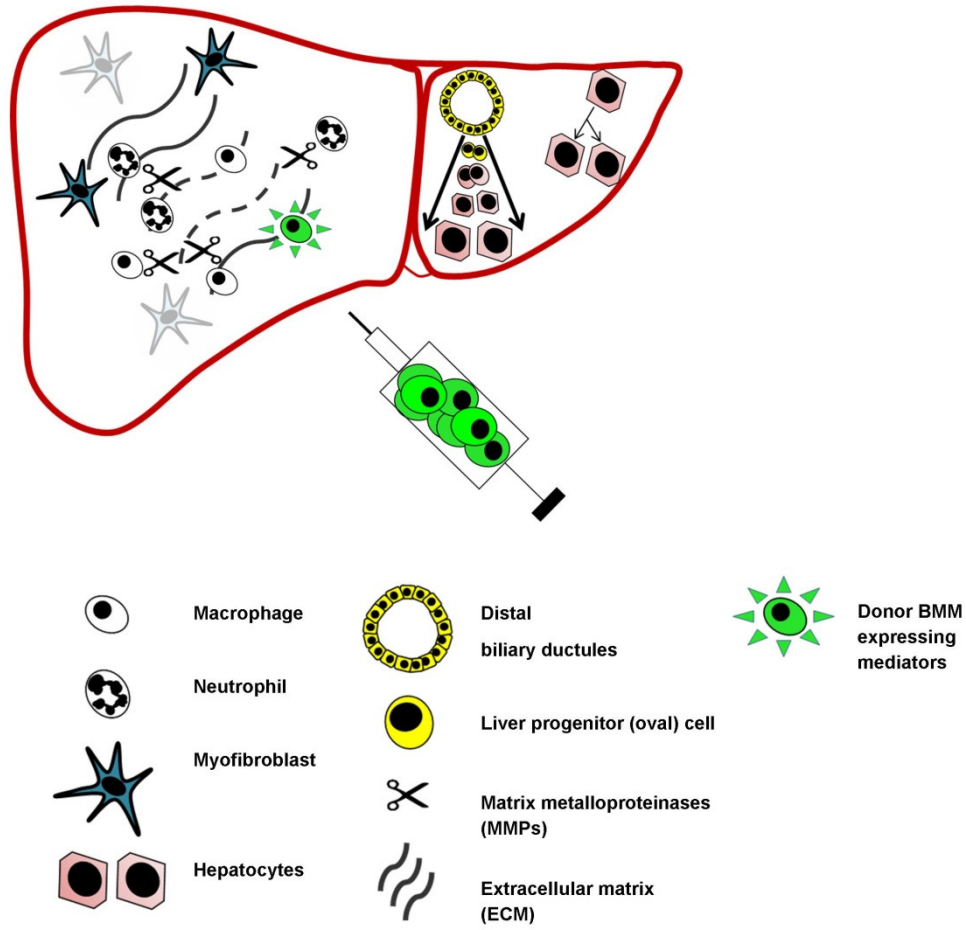

Figure 6.1 The effects of HPV delivered BMMs on key processes in liver fibrosis and regeneration during chronic liver injury

This figure illustrates the consequences of donor BMM injection via the HPV on mediators of liver fibrosis and regeneration in the context of ongoing liver injury. There is an increase in host macrophages and neutrophils within the hepatic scar. These cells produce scar degrading MMPs. The amount of hepatic myofibroblasts decreases and there is a reduction in liver fibrosis. Concurrently, there is increased expression of regenerative mediators such as TWEAK and activation of the progenitor cell compartment of the liver with subsequent elevated serum albumin levels. Thus BMM delivery causes structural and functional improvements in this model of chronic CCl_4 injury.

Route and timing of BMM therapy

Selection of the optimal route of cell delivery is a critical issue for translation. Peripheral injection has the significant advantages of safety, technical ease, reduced costs and greater acceptability to patients. Radiologically guided techniques to deliver cells into the HPV and HA are well established and have been used in preliminary human studies (e.g. (Lyra, Soares et al. 2010), (Nikeghbalian, Pournasr et al. 2011)). There are several positive reports of cell therapy delivered via peripheral veins (e.g. (Kim, Park et al. 2010), (Terai, Ishikawa et al. 2006) however the precise cell type used would likely affect its relative success. Despite increasing the BMM cell dose and delivering multiple injections, peripherally delivered BMMs did not demonstrate beneficial effects in the setting of murine CCl_4 induced liver fibrosis. In contrast, peripherally delivered BMMs do cause LPC activation in uninjured mice (Bird, Lu et al. 2013). This difference in effect could relate to circulatory changes associated with advanced fibrosis or the inflammatory milieu in chronic injury. The results in Chapter 5 demonstrate that significantly fewer cells engrafted within the host liver following peripheral as opposed to HPV delivery during liver injury. Furthermore, these tracking studies also showed that peripherally administered BMMs passed through the pulmonary circulation and so may undergo phenotypic changes that could affect their subsequent actions in the liver.

Further work in this area could examine the specific phenotype of BMMs in these different contexts. Delivering GFP positive BMMs to wild type fibrotic mice either peripherally or via the HPV would permit fluorescence based BMM extraction from selected organs at specific time points. The retrieved BMMs could then be characterised to determine phenotypic changes that may have arisen as a consequence of their passage in the host.

Given the significantly longer duration of human chronic liver disease, it is possible that small changes from each treatment could accumulate over time to yield meaningful clinical improvement. Clinical studies of *in vivo* tracking of donor cells

(Couto, Goldenberg et al. 2011) will improve our understanding of the kinetics of cell traffic. Technological improvements in vascular interventional radiology may also allow safer and more convenient access to the hepatic vessels.

The timing and need for multiple treatments would depend on the aetiology of cirrhosis and precise clinical circumstances. In the setting of ongoing liver damage without complete control of inflammation (e.g. non-alcoholic steatohepatitis, autoimmune hepatitis) with a clinical course usually measured in years, maintaining significant improvements in disease would likely need repeated intervention. Resolution of the chronic hepatic insult (e.g. successful antiviral therapy, abstinence from alcohol) can lead to sufficient regression to allow recompensation of cirrhosis and obviate the need for transplantation in some patients. An application for shorter term cell therapy might be to consolidate this process and increase the proportion of patients achieving this outcome.

Patient selection and disease models

The majority of chronic liver disease worldwide is the result of predominantly parenchymal injury. Current therapies for the less common cholestatic liver diseases, PBC and PSC, are of limited effectiveness. The DDC model of murine biliary injury was used to test whether BMM therapy could confer benefit in this setting. The positive effects of BMMs in the CCl_4 model of hepatitic type liver disease but not in the DDC model of biliary disease is compatible with subsequently published work from our group (Boulter, Govaere et al. 2012). This showed that infiltrating macrophages have restricted access to key non-parenchymal cells in biliary disease. Furthermore, macrophages were identified as critical determinants of LPC differentiation down the hepatocyte lineage in the setting of predominantly hepatitic injury. The negative results of BMM therapy in this cholestatic model are potentially attributable to a number of factors in addition to this mechanistic explanation. As previously described, experience in our group found the DDC model to be highly

toxic with a substantial mortality at higher doses. Such considerations led to restrictions on experimental design with pragmatic decisions made regarding the duration of injury and timing of therapy.

Future work to interrogate this further would include delivering BMMs at different time points during biliary injury and also using alternative cholangiopathic models such as bile duct ligation or alpha-naphthylisothiocyanate (ANIT). The possibility that BMM therapy may not be of utility in biliary disease has important implications for patient selection in clinical studies. It is plausible that patients with cirrhosis due to viral hepatitis and alcohol excess will be more likely to benefit than cirrhotic patients with chronic cholestatic disease.

Other limitations of this work

The CCl_4 model exhibits a high degree of reversibility upon cessation of injury in the experimental setting. This has made it a useful and popular tool to examine the mechanisms underlying fibrolysis and the experimental potential of candidate therapies. Fibrosis resolution is seen in clinical practice, a notable example being the successful treatment of HCV followed by histological regression of cirrhosis (Poynard, McHutchison et al. 2002). An important difference however, is that human disease has a significantly longer timeframe than experimental models. Mature fibrosis is characterised by a less cellular scar with increased elastin (Pellicoro, Aucott et al. 2012) and is less amenable to resolution (Issa, Zhou et al. 2004). Also of importance is the fact that a significant proportion of patients with cirrhosis are aged. Cellular senescence has consequences on regenerative pathways (Marshall, Rushbrook et al. 2005) and also fibrogenesis and its regression (Casado, Quereda et al. 2013). The physiology underlying this is not well characterised at present however the clinical relevance of therapies in the elderly is of increasing importance.

Further work would therefore test the effects of BMM therapy in models of significantly advanced fibrosis and also in aged mice. The magnitude of effect seen in the rodent models may not ultimately be reflected in humans. Even so, clinically meaningful improvement e.g. from decompensated to compensated cirrhosis, may be achievable with relatively limited structural change.

Donor BMMs have multiple actions, some direct and others mediated indirectly through the recruitment of host effector cells. The multiple, overlapping pathways demonstrate the multi-faceted effects of cell therapy. This contrasts with studies of single molecules or genes where the effects of the single pathway can be shown. With regard to clinical translation, the use of a readily available, differentiated, single cell type increases the predictability of effect. These findings will inform the rational design of clinical studies to determine the efficacy of autologous macrophage therapy in chronic liver disease (Thomas, Pope et al. 2011).

REFERENCES

Albilllos, A. and Garcia-Tsao, G. (2011). "Classification of cirrhosis: the clinical use of HVPG measurements." Dis Markers **31**(3): 121-128.

Alison, M. R., Poulsom, R., Jeffery, R., Dhillon, A. P., Quaglia, A., Jacob, J., Novelli, M., Prentice, G., Williamson, J. and Wright, N. A. (2000). "Hepatocytes from non-hepatic adult stem cells." Nature **406**(6793): 257.

Araki, H., Katayama, N., Yamashita, Y., Mano, H., Fujieda, A., Usui, E., Mitani, H., Ohishi, K., Nishii, K., Masuya, M., Minami, N., Nobori, T. and Shiku, H. (2004). "Reprogramming of human postmitotic neutrophils into macrophages by growth factors." Blood **103**(8): 2973-2980.

Benyon, R. C., Hovell, C. J., Da Gaca, M., Jones, E. H., Iredale, J. P. and Arthur, M. J. (1999). "Progelatinase A is produced and activated by rat hepatic stellate cells and promotes their proliferation." Hepatology **30**(4): 977-986.

Bird, T. G., Lorenzini, S. and Forbes, S. J. (2008). "Activation of stem cells in hepatic diseases." Cell Tissue Res **331**(1): 283-300.

Bird, T. G., Lu, W. Y., Boulter, L., Gordon-Keylock, S., Ridgway, R. A., Williams, M. J., Taube, J., Thomas, J. A., Wojtacha, D., Gambardella, A., Sansom, O. J., Iredale, J. P. and Forbes, S. J. (2013). "Bone marrow injection stimulates hepatic ductular reactions in the absence of injury via macrophage-mediated TWEAK signaling." Proc Natl Acad Sci U S A **110**(16): 6542-6547.

Boulter, L., Govaere, O., Bird, T. G., Radulescu, S., Ramachandran, P., Pellicoro, A., Ridgway, R. A., Seo, S. S., Spee, B., Van Rooijen, N., Sansom, O. J., Iredale, J. P., Lowell, S., Roskams, T. and Forbes, S. J. (2012). "Macrophage-derived Wnt opposes Notch signaling to specify hepatic progenitor cell fate in chronic liver disease." Nat Med **18**(4): 572-579.

Bradford, M. M. (1976). "A rapid and sensitive method for the quantitation of microgram quantities of protein utilizing the principle of protein-dye binding." Anal Biochem **72**: 248-254.

Carvalho, A. B., Quintanilha, L. F., Dias, J. V., Paredes, B. D., Mannheimer, E. G., Carvalho, F. G., Asensi, K. D., Gutfilen, B., Fonseca, L. M., Resende, C. M., Rezende, G. F., Takiya, C. M., de Carvalho, A. C. and Goldenberg, R. C. (2008). "Bone marrow multipotent mesenchymal stromal cells do not reduce fibrosis or improve function in a rat model of severe chronic liver injury." Stem Cells **26**(5): 1307-1314.

Casado, J. L., Quereda, C., Moreno, A., Perez-Elias, M. J., Marti-Belda, P. and Moreno, S. (2013). "Regression of liver fibrosis is progressive after sustained virological response to HCV therapy in patients with hepatitis C and HIV coinfection." J Viral Hepat **20**(12): 829-837.

Connolly, M. K., Bedrosian, A. S., Malhotra, A., Henning, J. R., Ibrahim, J., Vera, V., Cieza-Rubio, N. E., Hassan, B. U., Pachter, H. L., Cohen, S., Frey, A. B. and Miller, G. (2010). "In Hepatic Fibrosis, Liver Sinusoidal Endothelial Cells Acquire Enhanced Immunogenicity." J Immunol **185**(4): 2200-2208.

Constandinou, C., Henderson, N. and Iredale, J. P. (2005). "Modeling liver fibrosis in rodents." Methods Mol Med **117**: 237-250.

Couto, B. G., Goldenberg, R. C., da Fonseca, L. M., Thomas, J., Gutfilen, B., Resende, C. M., Azevedo, F., Mercante, D. R., Torres, A. L., Coelho, H. S., Maiolino, A., Alves, A. L., Dias, J. V., Moreira, M. C., Sampaio, A. L., Sousa, M. A., Kasai-Brunswick, T. H., Souza, S. A., Campos-de-Carvalho, A. C. and Rezende, G. F. (2011). "Bone marrow mononuclear cell therapy for patients with cirrhosis: a Phase 1 study." Liver Int **31**(3): 391-400.

Crofton, R. W., Diesselhoff-den Dulk, M. M. and van Furth, R. (1978). "The origin, kinetics, and characteristics of the Kupffer cells in the normal steady state." J Exp Med **148**(1): 1-17.

D'Amico, G., Garcia-Tsao, G. and Pagliaro, L. (2006). "Natural history and prognostic indicators of survival in cirrhosis: a systematic review of 118 studies." J Hepatol **44**(1): 217-231.

de Wynter, E. A., Buck, D., Hart, C., Heywood, R., Coutinho, L. H., Clayton, A., Rafferty, J. A., Burt, D., Guenechea, G., Bueren, J. A., Gagen, D., Fairbairn, L. J., Lord, B. I. and Testa, N. G. (1998). "CD34+AC133+ cells isolated from cord blood are highly enriched in long-term culture-initiating cells, NOD/SCID-repopulating cells and dendritic cell progenitors." Stem Cells **16**(6): 387-396.

di Bonzo, L. V., Ferrero, I., Cravanzola, C., Mareschi, K., Rustichell, D., Novo, E., Sanavio, F., Cannito, S., Zamara, E., Bertero, M., Davit, A., Francica, S., Novelli, F., Colombatto, S., Fagioli, F. and Parola, M. (2008). "Human mesenchymal stem cells as a two-edged sword in hepatic regenerative medicine: engraftment and hepatocyte differentiation versus profibrogenic potential." Gut **57**(2): 223-231.

Dienstag, J. L., Goldin, R. D., Heathcote, E. J., Hann, H. W., Woessner, M., Stephenson, S. L., Gardner, S., Gray, D. F. and Schiff, E. R. (2003). "Histological outcome during long-term lamivudine therapy." Gastroenterology **124**(1): 105-117.

Duan, X. Z., Liu, F. F., Tong, J. J., Yang, H. Z., Chen, J., Liu, X. Y., Mao, Y. L., Xin, S. J. and Hu, J. H. (2013). "Granulocyte-colony stimulating factor therapy improves survival in patients with hepatitis B virus-associated acute-on-chronic liver failure." World J Gastroenterol **19**(7): 1104-1110.

Duffield, J. S., Erwig, L. P., Wei, X., Liew, F. Y., Rees, A. J. and Savill, J. S. (2000). "Activated macrophages direct apoptosis and suppress mitosis of mesangial cells." J Immunol **164**(4): 2110-2119.

Duffield, J. S., Forbes, S. J., Constandinou, C. M., Clay, S., Partolina, M., Vuthoori, S., Wu, S., Lang, R. and Iredale, J. P. (2005). "Selective depletion of macrophages reveals distinct, opposing roles during liver injury and repair." J Clin Invest **115**(1): 56-65.

Fallowfield, J. A., Mizuno, M., Kendall, T. J., Constandinou, C. M., Benyon, R. C., Duffield, J. S. and Iredale, J. P. (2007). "Scar-associated macrophages are a major source of hepatic matrix metalloproteinase-13 and facilitate the resolution of murine hepatic fibrosis." J Immunol **178**(8): 5288-5295.

Fausto, N., Campbell, J. S. and Riehle, K. J. (2006). "Liver regeneration." Hepatology **43**(2 Suppl 1): S45-53.

Fernandez, I., Pena, A., Del Teso, N., Perez, V. and Rodriguez-Cuesta, J. (2010). "Clinical biochemistry parameters in C57BL/6J mice after blood collection from the submandibular vein and retroorbital plexus." J Am Assoc Lab Anim Sci **49**(2): 202-206.

Fickert, P., Stoger, U., Fuchsbichler, A., Moustafa, T., Marschall, H. U., Weiglein, A. H., Tsybrovskyy, O., Jaeschke, H., Zatloukal, K., Denk, H. and Trauner, M. (2007). "A new xenobiotic-induced mouse model of sclerosing cholangitis and biliary fibrosis." Am J Pathol **171**(2): 525-536.

Forbes, S. J., Russo, F. P., Rey, V., Burra, P., Rugge, M., Wright, N. A. and Alison, M. R. (2004). "A significant proportion of myofibroblasts are of bone marrow origin in human liver fibrosis." Gastroenterology **126**(4): 955-963.

Friedman, S. L. (1993). "Seminars in medicine of the Beth Israel Hospital, Boston. The cellular basis of hepatic fibrosis. Mechanisms and treatment strategies." N Engl J Med **328**(25): 1828-1835.

Friedman, S. L., Rockey, D. C., McGuire, R. F., Maher, J. J., Boyles, J. K. and Yamasaki, G. (1992). "Isolated hepatic lipocytes and Kupffer cells from normal human liver: morphological and functional characteristics in primary culture." Hepatology **15**(2): 234-243.

Friedman, S. L., Roll, F. J., Boyles, J. and Bissell, D. M. (1985). "Hepatic lipocytes: the principal collagen-producing cells of normal rat liver." Proc Natl Acad Sci U S A **82**(24): 8681-8685.

Friedrich, E. B., Walenta, K., Scharlau, J., Nickenig, G. and Werner, N. (2006). "CD34-/CD133+/VEGFR-2+ endothelial progenitor cell subpopulation with potent vasoregenerative capacities." Circ Res **98**(3): e20-25.

Furst, G., Schulte am Esch, J., Poll, L. W., Hosch, S. B., Fritz, L. B., Klein, M., Godehardt, E., Krieg, A., Wecker, B., Stoldt, V., Stockschlader, M., Eisenberger, C. F., Modder, U. and Knoefel, W. T. (2007). "Portal vein embolization and autologous CD133+ bone marrow stem cells for liver regeneration: initial experience." Radiology **243**(1): 171-179.

Gabele, E., Brenner, D. A. and Rippe, R. A. (2003). "Liver fibrosis: signals leading to the amplification of the fibrogenic hepatic stellate cell." Front Biosci **8**: d69-77.

Gerlach, C., Sakkab, D. Y., Scholzen, T., Dassler, R., Alison, M. R. and Gerdes, J. (1997). "Ki-67 expression during rat liver regeneration after partial hepatectomy." Hepatology **26**(3): 573-578.

Gordon, M. Y., Levicar, N., Pai, M., Bachellier, P., Dimarakis, I., Al-Allaf, F., M'Hamdi, H., Thalji, T., Welsh, J. P., Marley, S. B., Davies, J., Dazzi, F., Marelli-Berg, F., Tait, P., Playford, R., Jiao, L., Jensen, S., Nicholls, J. P., Ayav, A., Nohandani, M., Farzaneh, F., Gaken, J., Dodge, R., Alison, M., Apperley, J. F., Lechler, R. and Habib, N. A. (2006). "Characterization and clinical application of human CD34+ stem/progenitor cell populations mobilized into the blood by granulocyte colony-stimulating factor." Stem Cells **24**(7): 1822-1830.

Gressner, A. M., Weiskirchen, R., Breitkopf, K. and Dooley, S. (2002). "Roles of TGF-beta in hepatic fibrosis." Front Biosci **7**: d793-807.

Harty, M. W., Huddleston, H. M., Papa, E. F., Puthawala, T., Tracy, A. P., Ramm, G. A., Gehring, S., Gregory, S. H. and Tracy, T. F., Jr. (2005). "Repair after cholestatic liver injury correlates with neutrophil infiltration and matrix metalloproteinase 8 activity." Surgery **138**(2): 313-320.

Harty, M. W., Muratore, C. S., Papa, E. F., Gart, M. S., Ramm, G. A., Gregory, S. H. and Tracy, T. F., Jr. (2010). "Neutrophil depletion blocks early collagen degradation in repairing cholestatic rat livers." Am J Pathol **176**(3): 1271-1281.

Harty, M. W., Papa, E. F., Huddleston, H. M., Young, E., Nazareth, S., Riley, C. A., Ramm, G. A., Gregory, S. H. and Tracy, T. F., Jr. (2008). "Hepatic macrophages promote the neutrophil-dependent resolution of fibrosis in repairing cholestatic rat livers." Surgery **143**(5): 667-678.

Higashiyama, R., Inagaki, Y., Hong, Y. Y., Kushida, M., Nakao, S., Niioka, M., Watanabe, T., Okano, H., Matsuzaki, Y., Shiota, G. and Okazaki, I. (2007). "Bone marrow-derived cells express matrix metalloproteinases and contribute to regression of liver fibrosis in mice." Hepatology **45**(1): 213-222.

Hosaka, T., Suzuki, F., Kobayashi, M., Seko, Y., Kawamura, Y., Sezaki, H., Akuta, N., Suzuki, Y., Saitoh, S., Arase, Y., Ikeda, K. and Kumada, H. (2013). "Long-term entecavir treatment reduces hepatocellular carcinoma incidence in patients with hepatitis B virus infection." Hepatology **58**(1): 98-107.

Houlihan, D. D. and Newsome, P. N. (2008). "Critical review of clinical trials of bone marrow stem cells in liver disease." Gastroenterology **135**(2): 438-450.

http://www.statistics.gov.uk/, O. f. N. S.

Huang, Y. H., Shi, M. N., Zheng, W. D., Zhang, L. J., Chen, Z. X. and Wang, X. Z. (2006). "Therapeutic effect of interleukin-10 on CCl4-induced hepatic fibrosis in rats." World J Gastroenterol **12**(9): 1386-1391.

Hume, D. A. (2006). "The mononuclear phagocyte system." Curr Opin Immunol **18**(1): 49-53.

Iredale, J. P. (1997). "Tissue inhibitors of metalloproteinases in liver fibrosis." Int J Biochem Cell Biol **29**(1): 43-54.

Iredale, J. P. (2007). "Models of liver fibrosis: exploring the dynamic nature of inflammation and repair in a solid organ." J Clin Invest **117**(3): 539-548.

Iredale, J. P., Benyon, R. C., Pickering, J., McCullen, M., Northrop, M., Pawley, S., Hovell, C. and Arthur, M. J. (1998). "Mechanisms of spontaneous resolution of rat liver fibrosis. Hepatic stellate cell apoptosis and reduced hepatic expression of metalloproteinase inhibitors." J Clin Invest **102**(3): 538-549.

Iredale, J. P., Thompson, A. and Henderson, N. C. (2013). "Extracellular matrix degradation in liver fibrosis: Biochemistry and regulation." Biochim Biophys Acta **1832**(7): 876-883.

Issa, R., Zhou, X., Constandinou, C. M., Fallowfield, J., Millward-Sadler, H., Gaca, M. D., Sands, E., Suliman, I., Trim, N., Knorr, A., Arthur, M. J., Benyon, R. C. and Iredale, J. P. (2004). "Spontaneous recovery from micronodular cirrhosis: evidence for incomplete resolution associated with matrix cross-linking." Gastroenterology **126**(7): 1795-1808.

Issa, R., Zhou, X., Trim, N., Millward-Sadler, H., Krane, S., Benyon, C. and Iredale, J. (2003). "Mutation in collagen-1 that confers resistance to the action of collagenase results in failure of recovery from CCl4-induced liver fibrosis, persistence of activated hepatic stellate cells, and diminished hepatocyte regeneration." Faseb J **17**(1): 47-49.

Iwamoto, T., Terai, S., Hisanaga, T., Takami, T., Yamamoto, N., Watanabe, S. and Sakaida, I. (2013). "Bone-marrow-derived cells cultured in serum-free medium reduce liver fibrosis and improve liver function in carbon-tetrachloride-treated cirrhotic mice." Cell Tissue Res **351**(3): 487-495.

Jakubowski, A., Ambrose, C., Parr, M., Lincecum, J. M., Wang, M. Z., Zheng, T. S., Browning, B., Michaelson, J. S., Baetscher, M., Wang, B., Bissell, D. M. and Burkly, L. C. (2005). "TWEAK induces liver progenitor cell proliferation." J Clin Invest **115**(9): 2330-2340.

Jiao, J., Sastre, D., Fiel, M. I., Lee, U. E., Ghiassi-Nejad, Z., Ginhoux, F., Vivier, E., Friedman, S. L., Merad, M. and Aloman, C. (2012). "Dendritic cell regulation of carbon tetrachloride-induced murine liver fibrosis regression." Hepatology **55**(1): 244-255.

Kallis, Y. N., Robson, A. J., Fallowfield, J. A., Thomas, H. C., Alison, M. R., Wright, N. A., Goldin, R. D., Iredale, J. P. and Forbes, S. J. (2011). "Remodelling of extracellular matrix is a requirement for the hepatic progenitor cell response." Gut.

Karlmark, K. R., Weiskirchen, R., Zimmermann, H. W., Gassler, N., Ginhoux, F., Weber, C., Merad, M., Luedde, T., Trautwein, C. and Tacke, F. (2009). "Hepatic recruitment of the inflammatory Gr1+ monocyte subset upon liver injury promotes hepatic fibrosis." Hepatology **50**(1): 261-274.

Kharaziha, P., Hellstrom, P. M., Noorinayer, B., Farzaneh, F., Aghajani, K., Jafari, F., Telkabadi, M., Atashi, A., Honardoost, M., Zali, M. R. and Soleimani, M. (2009). "Improvement of liver function in liver cirrhosis patients after autologous mesenchymal stem cell injection: a phase I-II clinical trial." Eur J Gastroenterol Hepatol **21**(10): 1199-1205.

Kim, J. K., Park, Y. N., Kim, J. S., Park, M. S., Paik, Y. H., Seok, J. Y., Chung, Y. E., Kim, H. O., Kim, K. S., Ahn, S. H., Kim do, Y., Kim, M. J., Lee, K. S., Chon, C. Y., Kim, S. J., Terai, S., Sakaida, I. and Han, K. H. (2010). "Autologous bone marrow infusion activates the progenitor cell compartment in patients with advanced liver cirrhosis." Cell Transplant **19**(10): 1237-1246.

Kinnman, N. and Housset, C. (2002). "Peribiliary myofibroblasts in biliary type liver fibrosis." Front Biosci **7**: d496-503.

Kisseleva, T., Uchinami, H., Feirt, N., Quintana-Bustamante, O., Segovia, J. C., Schwabe, R. F. and Brenner, D. A. (2006). "Bone marrow-derived fibrocytes participate in pathogenesis of liver fibrosis." J Hepatol **45**(3): 429-438.

Klein, I., Cornejo, J. C., Polakos, N. K., John, B., Wuensch, S. A., Topham, D. J., Pierce, R. H. and Crispe, I. N. (2007). "Kupffer cell heterogeneity: functional properties of bone marrow derived and sessile hepatic macrophages." Blood **110**(12): 4077-4085.

Kluth, D. C., Ainslie, C. V., Pearce, W. P., Finlay, S., Clarke, D., Anegon, I. and Rees, A. J. (2001). "Macrophages transfected with adenovirus to

express IL-4 reduce inflammation in experimental glomerulonephritis." J Immunol **166**(7): 4728-4736.

Knight, B., Matthews, V. B., Akhurst, B., Croager, E. J., Klinken, E., Abraham, L. J., Olynyk, J. K. and Yeoh, G. (2005). "Liver inflammation and cytokine production, but not acute phase protein synthesis, accompany the adult liver progenitor (oval) cell response to chronic liver injury." Immunol Cell Biol **83**(4): 364-374.

Knittel, T., Mehde, M., Kobold, D., Saile, B., Dinter, C. and Ramadori, G. (1999). "Expression patterns of matrix metalloproteinases and their inhibitors in parenchymal and non-parenchymal cells of rat liver: regulation by TNF-alpha and TGF-beta1." J Hepatol **30**(1): 48-60.

Kofman, A. V., Morgan, G., Kirschenbaum, A., Osbeck, J., Hussain, M., Swenson, S. and Theise, N. D. (2005). "Dose- and time-dependent oval cell reaction in acetaminophen-induced murine liver injury." Hepatology **41**(6): 1252-1261.

Kolf, C. M., Cho, E. and Tuan, R. S. (2007). "Mesenchymal stromal cells. Biology of adult mesenchymal stem cells: regulation of niche, self-renewal and differentiation." Arthritis Res Ther **9**(1): 204.

Lagasse, E., Connors, H., Al-Dhalimy, M., Reitsma, M., Dohse, M., Osborne, L., Wang, X., Finegold, M., Weissman, I. L. and Grompe, M. (2000). "Purified hematopoietic stem cells can differentiate into hepatocytes in vivo." Nat Med **6**(11): 1229-1234.

Levicar, N., Pai, M., Habib, N. A., Tait, P., Jiao, L. R., Marley, S. B., Davis, J., Dazzi, F., Smadja, C., Jensen, S. L., Nicholls, J. P., Apperley, J. F. and Gordon, M. Y. (2008). "Long-term clinical results of autologous infusion of mobilized adult bone marrow derived CD34+ cells in patients with chronic liver disease." Cell Prolif **41 Suppl 1**: 115-125.

Lim, A. K., Patel, N., Hamilton, G., Hajnal, J. V., Goldin, R. D. and Taylor-Robinson, S. D. (2003). "The relationship of in vivo 31P MR spectroscopy to histology in chronic hepatitis C." Hepatology **37**(4): 788-794.

Lorenzini, S., Bird, T. G., Boulter, L., Bellamy, C., Samuel, K., Aucott, R., Clayton, E., Andreone, P., Bernardi, M., Golding, M., Alison, M. R., Iredale, J. P. and Forbes, S. J. (2010). "Characterisation of a stereotypical cellular and extracellular adult liver progenitor cell niche in rodents and diseased human liver." Gut **59**(5): 645-654.

Lorenzini, S., Isidori, A., Catani, L., Gramenzi, A., Talarico, S., Bonifazi, F., Giudice, V., Conte, R., Baccarani, M., Bernardi, M., Forbes, S. J., Lemoli, R. M. and Andreone, P. (2008). "Stem cell mobilization and collection in patients with liver cirrhosis." Aliment Pharmacol Ther **27**(10): 932-939.

Lyra, A. C., Soares, M. B., da Silva, L. F., Braga, E. L., Oliveira, S. A., Fortes, M. F., Silva, A. G., Brustolim, D., Genser, B., Dos Santos, R. R. and Lyra, L. G. (2010). "Infusion of autologous bone marrow mononuclear cells through hepatic artery results in a short-term improvement of liver function in patients with chronic liver disease: a pilot randomized controlled study." Eur J Gastroenterol Hepatol **22**(1): 33-42.

Maeda, M., Takami, T., Terai, S. and Sakaida, I. (2012). "Autologous bone marrow cell infusions suppress tumor initiation in hepatocarcinogenic mice with liver cirrhosis." J Gastroenterol Hepatol **27 Suppl 2**: 104-111.

Maher, J. J. and McGuire, R. F. (1990). "Extracellular matrix gene expression increases preferentially in rat lipocytes and sinusoidal endothelial cells during hepatic fibrosis in vivo." J Clin Invest **86**(5): 1641-1648.

Mantovani, A., Sica, A., Sozzani, S., Allavena, P., Vecchi, A. and Locati, M. (2004). "The chemokine system in diverse forms of macrophage activation and polarization." Trends Immunol **25**(12): 677-686.

Marshall, A., Rushbrook, S., Davies, S. E., Morris, L. S., Scott, I. S., Vowler, S. L., Coleman, N. and Alexander, G. (2005). "Relation between hepatocyte G1 arrest, impaired hepatic regeneration, and fibrosis in chronic hepatitis C virus infection." Gastroenterology **128**(1): 33-42.

Menke, J., Iwata, Y., Rabacal, W. A., Basu, R., Yeung, Y. G., Humphreys, B. D., Wada, T., Schwarting, A., Stanley, E. R. and Kelley, V. R. (2009). "CSF-1 signals directly to renal tubular epithelial cells to mediate repair in mice." J Clin Invest **119**(8): 2330-2342.

Mohamadnejad, M., Alimoghaddam, K., Mohyeddin-Bonab, M., Bagheri, M., Bashtar, M., Ghanaati, H., Baharvand, H., Ghavamzadeh, A. and Malekzadeh, R. (2007). "Phase 1 trial of autologous bone marrow mesenchymal stem cell transplantation in patients with decompensated liver cirrhosis." Arch Iran Med **10**(4): 459-466.

Mohamadnejad, M., Namiri, M., Bagheri, M., Hashemi, S. M., Ghanaati, H., Zare Mehrjardi, N., Kazemi Ashtiani, S., Malekzadeh, R. and Baharvand, H. (2007). "Phase 1 human trial of autologous bone marrow-hematopoietic stem cell transplantation in patients with decompensated cirrhosis." World J Gastroenterol **13**(24): 3359-3363.

Morimoto, H., Takahashi, M., Shiba, Y., Izawa, A., Ise, H., Hongo, M., Hatake, K., Motoyoshi, K. and Ikeda, U. (2007). "Bone marrow-derived CXCR4+ cells mobilized by macrophage colony-stimulating factor participate in the reduction of infarct area and improvement of cardiac remodeling after myocardial infarction in mice." Am J Pathol **171**(3): 755-766.

Mosser, D. M. and Edwards, J. P. (2008). "Exploring the full spectrum of macrophage activation." Nat Rev Immunol **8**(12): 958-969.

Nakamura, T., Torimura, T., Sakamoto, M., Hashimoto, O., Taniguchi, E., Inoue, K., Sakata, R., Kumashiro, R., Murohara, T., Ueno, T. and Sata, M. (2007). "Significance and therapeutic potential of endothelial progenitor cell transplantation in a cirrhotic liver rat model." Gastroenterology **133**(1): 91-107 e101.

Nakamura, T., Tsutsumi, V., Torimura, T., Naitou, M., Iwamoto, H., Masuda, H., Hashimoto, O., Koga, H., Abe, M., Ii, M., Kawamoto, A., Asahara, T., Ueno, T. and Sata, M. (2012). "Human peripheral blood CD34-positive cells enhance therapeutic regeneration of chronically injured liver in nude rats." J Cell Physiol **227**(4): 1538-1552.

Nikeghbalian, S., Pournasr, B., Aghdami, N., Rasekhi, A., Geramizadeh, B., Hosseini Asl, S. M., Ramzi, M., Kakaei, F., Namiri, M., Malekzadeh, R., Vosough Dizaj, A., Malek-Hosseini, S. A. and Baharvand, H. (2011).

"Autologous transplantation of bone marrow-derived mononuclear and CD133(+) cells in patients with decompensated cirrhosis." Arch Iran Med **14**(1): 12-17.

Nishida, M., Okumura, Y., Fujimoto, S., Shiraishi, I., Itoi, T. and Hamaoka, K. (2005). "Adoptive transfer of macrophages ameliorates renal fibrosis in mice." Biochem Biophys Res Commun **332**(1): 11-16.

Oben, J. A., Roskams, T., Yang, S., Lin, H., Sinelli, N., Li, Z., Torbenson, M., Huang, J., Guarino, P., Kafrouni, M. and Diehl, A. M. (2003). "Sympathetic nervous system inhibition increases hepatic progenitors and reduces liver injury." Hepatology **38**(3): 664-673.

Olynyk, J. K., Yeoh, G. C., Ramm, G. A., Clarke, S. L., Hall, P. M., Britton, R. S., Bacon, B. R. and Tracy, T. F. (1998). "Gadolinium chloride suppresses hepatic oval cell proliferation in rats with biliary obstruction." Am J Pathol **152**(2): 347-352.

Pai, M., Zacharoulis, D., Milicevic, M. N., Helmy, S., Jiao, L. R., Levicar, N., Tait, P., Scott, M., Marley, S. B., Jestice, K., Glibetic, M., Bansi, D., Khan, S. A., Kyriakou, D., Rountas, C., Thillainayagam, A., Nicholls, J. P., Jensen, S., Apperley, J. F., Gordon, M. Y. and Habib, N. A. (2008). "Autologous infusion of expanded mobilized adult bone marrow-derived CD34+ cells into patients with alcoholic liver cirrhosis." Am J Gastroenterol **103**(8): 1952-1958.

Parsa, R., Andresen, P., Gillett, A., Mia, S., Zhang, X. M., Mayans, S., Holmberg, D. and Harris, R. A. (2012). "Adoptive transfer of immunomodulatory M2 macrophages prevents type 1 diabetes in NOD mice." Diabetes **61**(11): 2881-2892.

Pellicoro, A., Aucott, R. L., Ramachandran, P., Robson, A. J., Fallowfield, J. A., Snowdon, V. K., Hartland, S. N., Vernon, M., Duffield, J. S., Benyon, R. C., Forbes, S. J. and Iredale, J. P. (2012). "Elastin accumulation is regulated at the level of degradation by macrophage metalloelastase (MMP-12) during experimental liver fibrosis." Hepatology **55**(6): 1965-1975.

Peng, L., Xie, D. Y., Lin, B. L., Liu, J., Zhu, H. P., Xie, C., Zheng, Y. B. and Gao, Z. L. (2011). "Autologous bone marrow mesenchymal stem cell transplantation in liver failure patients caused by hepatitis B: short-term and long-term outcomes." Hepatology **54**(3): 820-828.

Petersen, B. E., Bowen, W. C., Patrene, K. D., Mars, W. M., Sullivan, A. K., Murase, N., Boggs, S. S., Greenberger, J. S. and Goff, J. P. (1999). "Bone marrow as a potential source of hepatic oval cells." Science **284**(5417): 1168-1170.

Pinzani, M., Gesualdo, L., Sabbah, G. M. and Abboud, H. E. (1989). "Effects of platelet-derived growth factor and other polypeptide mitogens on DNA synthesis and growth of cultured rat liver fat-storing cells." J Clin Invest **84**(6): 1786-1793.

Piscaglia, A. C., Shupe, T. D., Oh, S. H., Gasbarrini, A. and Petersen, B. E. (2007). "Granulocyte-colony stimulating factor promotes liver repair and induces oval cell migration and proliferation in rats." Gastroenterology **133**(2): 619-631.

Pollard, J. W. (2009). "Trophic macrophages in development and disease." Nat Rev Immunol **9**(4): 259-270.

Poynard, T., McHutchison, J., Manns, M., Trepo, C., Lindsay, K., Goodman, Z., Ling, M. H. and Albrecht, J. (2002). "Impact of pegylated interferon alfa-2b and ribavirin on liver fibrosis in patients with chronic hepatitis C." Gastroenterology **122**(5): 1303-1313.

Pratt, T., Sharp, L., Nichols, J., Price, D. J. and Mason, J. O. (2000). "Embryonic stem cells and transgenic mice ubiquitously expressing a tau-tagged green fluorescent protein." Dev Biol **228**(1): 19-28.

Preaux, A. M., Mallat, A., Nhieu, J. T., D'Ortho, M. P., Hembry, R. M. and Mavier, P. (1999). "Matrix metalloproteinase-2 activation in human hepatic fibrosis regulation by cell-matrix interactions." Hepatology **30**(4): 944-950.

Ramachandran, P., Pellicoro, A., Vernon, M. A., Boulter, L., Aucott, R. L., Ali, A., Hartland, S. N., Snowdon, V. K., Cappon, A., Gordon-Walker, T. T., Williams, M. J., Dunbar, D. R., Manning, J. R., van Rooijen, N., Fallowfield, J. A., Forbes, S. J. and Iredale, J. P. (2012). "Differential Ly-6C expression identifies the recruited macrophage phenotype, which orchestrates the regression of murine liver fibrosis." Proc Natl Acad Sci U S A **109**(46): E3186-3195.

Reddy, G. K. and Enwemeka, C. S. (1996). "A simplified method for the analysis of hydroxyproline in biological tissues." Clin Biochem **29**(3): 225-229.

Rockey, D. C. (2001). "Hepatic blood flow regulation by stellate cells in normal and injured liver." Semin Liver Dis **21**(3): 337-349.

Roderfeld, M., Weiskirchen, R., Wagner, S., Berres, M. L., Henkel, C., Grotzinger, J., Gressner, A. M., Matern, S. and Roeb, E. (2006). "Inhibition of hepatic fibrogenesis by matrix metalloproteinase-9 mutants in mice." Faseb J **20**(3): 444-454.

Rosenberg, W. M., Voelker, M., Thiel, R., Becka, M., Burt, A., Schuppan, D., Hubscher, S., Roskams, T., Pinzani, M., Arthur, M. J. and European Liver Fibrosis, G. (2004). "Serum markers detect the presence of liver fibrosis: a cohort study." Gastroenterology **127**(6): 1704-1713.

Russo, F. P., Alison, M. R., Bigger, B. W., Amofah, E., Florou, A., Amin, F., Bou-Gharios, G., Jeffery, R., Iredale, J. P. and Forbes, S. J. (2006). "The bone marrow functionally contributes to liver fibrosis." Gastroenterology **130**(6): 1807-1821.

Ryan, J. M., Barry, F., Murphy, J. M. and Mahon, B. P. (2007). "Interferon-gamma does not break, but promotes the immunosuppressive capacity of adult human mesenchymal stem cells." Clin Exp Immunol **149**(2): 353-363.

Sakaida, I., Terai, S., Yamamoto, N., Aoyama, K., Ishikawa, T., Nishina, H. and Okita, K. (2004). "Transplantation of bone marrow cells reduces CCl4-induced liver fibrosis in mice." Hepatology **40**(6): 1304-1311.

Salama, H., Zekri, A. R., Bahnassy, A. A., Medhat, E., Halim, H. A., Ahmed, O. S., Mohamed, G., Al Alim, S. A. and Sherif, G. M. (2010). "Autologous CD34+ and CD133+ stem cells transplantation in patients

with end stage liver disease." World J Gastroenterol **16**(42): 5297-5305.

Salama, H., Zekri, A. R., Zern, M., Bahnassy, A., Loutfy, S., Shalaby, S., Vigen, C., Burke, W., Mostafa, M., Medhat, E., Alfi, O. and Huttinger, E. (2010). "Autologous hematopoietic stem cell transplantation in 48 patients with end-stage chronic liver diseases." Cell Transplant **19**(11): 1475-1486.

Sasmono, R. T., Ehrnsperger, A., Cronau, S. L., Ravasi, T., Kandane, R., Hickey, M. J., Cook, A. D., Himes, S. R., Hamilton, J. A. and Hume, D. A. (2007). "Mouse neutrophilic granulocytes express mRNA encoding the macrophage colony-stimulating factor receptor (CSF-1R) as well as many other macrophage-specific transcripts and can transdifferentiate into macrophages in vitro in response to CSF-1." J Leukoc Biol **82**(1): 111-123.

Sasmono, R. T., Oceandy, D., Pollard, J. W., Tong, W., Pavli, P., Wainwright, B. J., Ostrowski, M. C., Himes, S. R. and Hume, D. A. (2003). "A macrophage colony-stimulating factor receptor-green fluorescent protein transgene is expressed throughout the mononuclear phagocyte system of the mouse." Blood **101**(3): 1155-1163.

Sellers, E. A., Lucas, C. C. and Best, C. H. (1948). "The lipotropic factors in experimental cirrhosis." Br Med J **1**(4561): 1061-1065.

Sharma, S., Kumar, L., Mohanty, S., Kumar, R., Datta Gupta, S. and Gupta, D. K. (2011). "Bone marrow mononuclear stem cell infusion improves biochemical parameters and scintigraphy in infants with biliary atresia." Pediatr Surg Int **27**(1): 81-89.

Shi, M., Zhang, Z., Xu, R., Lin, H., Fu, J., Zou, Z., Zhang, A., Shi, J., Chen, L., Lv, S., He, W., Geng, H., Jin, L., Liu, Z. and Wang, F. S. (2012). "Human mesenchymal stem cell transfusion is safe and improves liver function in acute-on-chronic liver failure patients." Stem Cells Transl Med **1**(10): 725-731.

Siller-Lopez, F., Sandoval, A., Salgado, S., Salazar, A., Bueno, M., Garcia, J., Vera, J., Galvez, J., Hernandez, I., Ramos, M., Aguilar-Cordova, E. and Armendariz-Borunda, J. (2004). "Treatment with human metalloproteinase-8 gene delivery ameliorates experimental rat liver cirrhosis." Gastroenterology **126**(4): 1122-1133; discussion 1949.

Sobrevals, L., Rodriguez, C., Romero-Trevejo, J. L., Gondi, G., Monreal, I., Paneda, A., Juanarena, N., Arcelus, S., Razquin, N., Guembe, L., Gonzalez-Aseguinolaza, G., Prieto, J. and Fortes, P. (2010). "Insulin-like growth factor I gene transfer to cirrhotic liver induces fibrolysis and reduces fibrogenesis leading to cirrhosis reversion in rats." Hepatology **51**(3): 912-921.

Spahr, L., Chalandon, Y., Terraz, S., Kindler, V., Rubbia-Brandt, L., Frossard, J. L., Breguet, R., Lanthier, N., Farina, A., Passweg, J., Becker, C. D. and Hadengue, A. (2013). "Autologous bone marrow mononuclear cell transplantation in patients with decompensated alcoholic liver disease: a randomized controlled trial." PLoS One **8**(1): e53719.

Spahr, L., Lambert, J. F., Rubbia-Brandt, L., Chalandon, Y., Frossard, J. L., Giostra, E. and Hadengue, A. (2008). "Granulocyte-colony stimulating

factor induces proliferation of hepatic progenitors in alcoholic steatohepatitis: a randomized trial." Hepatology **48**(1): 221-229.

Steen, R., Morkrid, L., Tjonnfjord, G. E. and Egeland, T. (1994). "c-kit ligand combined with GM-CSF and/or IL-3 can expand CD34+ hematopoietic progenitor subsets for several weeks in vitro." Stem Cells **12**(2): 214-224.

Suh, Y. G., Kim, J. K., Byun, J. S., Yi, H. S., Lee, Y. S., Eun, H. S., Kim, S. Y., Han, K. H., Lee, K. S., Duester, G., Friedman, S. L. and Jeong, W. I. (2012). "CD11b(+) Gr1(+) bone marrow cells ameliorate liver fibrosis by producing interleukin-10 in mice." Hepatology **56**(5): 1902-1912.

Suzuki, T., Arumugam, P., Sakagami, T., Lachmann, N., Chalk, C., Sallese, A., Abe, S., Trapnell, C., Carey, B., Moritz, T., Malik, P., Lutzko, C., Wood, R. E. and Trapnell, B. C. (2014). "Pulmonary macrophage transplantation therapy." Nature **514**(7523): 450-454.

Terai, S., Ishikawa, T., Omori, K., Aoyama, K., Marumoto, Y., Urata, Y., Yokoyama, Y., Uchida, K., Yamasaki, T., Fujii, Y., Okita, K. and Sakaida, I. (2006). "Improved liver function in patients with liver cirrhosis after autologous bone marrow cell infusion therapy." Stem Cells **24**(10): 2292-2298.

Theise, N. D., Badve, S., Saxena, R., Henegariu, O., Sell, S., Crawford, J. M. and Krause, D. S. (2000). "Derivation of hepatocytes from bone marrow cells in mice after radiation-induced myeloablation." Hepatology **31**(1): 235-240.

Theise, N. D., Nimmakayalu, M., Gardner, R., Illei, P. B., Morgan, G., Teperman, L., Henegariu, O. and Krause, D. S. (2000). "Liver from bone marrow in humans." Hepatology **32**(1): 11-16.

Thomas, J. A., Forbes, S. J. (2009). Cell Therapy in Liver Disease. Treatment of Liver Diseases. A. V., Ars Medica**:** 445-455.

Thomas, J. A., Forbes, S. J. (2013). Clinical Studies of Cell Therapy for Liver Cirrhosis. Regenerative Medicine and Cell Therapy. H. Baharvand, Aghdami, N., Springer**:** 233-243.

Thomas, J. A., Pope, C., Wojtacha, D., Robson, A. J., Gordon-Walker, T. T., Hartland, S., Ramachandran, P., Van Deemter, M., Hume, D. A., Iredale, J. P. and Forbes, S. J. (2011). "Macrophage therapy for murine liver fibrosis recruits host effector cells improving fibrosis, regeneration, and function." Hepatology **53**(6): 2003-2015.

Thompson, K., Maltby, J., Fallowfield, J., McAulay, M., Millward-Sadler, H. and Sheron, N. (1998). "Interleukin-10 expression and function in experimental murine liver inflammation and fibrosis." Hepatology **28**(6): 1597-1606.

Thorgeirsson, S. S. and Grisham, J. W. (2006). "Hematopoietic cells as hepatocyte stem cells: a critical review of the evidence." Hepatology **43**(1): 2-8.

Tirnitz-Parker, J. E., Viebahn, C. S., Jakubowski, A., Klopcic, B. R., Olynyk, J. K., Yeoh, G. C. and Knight, B. (2010). "Tumor necrosis factor-like weak inducer of apoptosis is a mitogen for liver progenitor cells." Hepatology **52**(1): 291-302.

Van Hul, N., Lanthier, N., Espanol Suner, R., Abarca Quinones, J., van Rooijen, N. and Leclercq, I. (2011). "Kupffer cells influence parenchymal invasion and phenotypic orientation, but not the proliferation, of liver progenitor cells in a murine model of liver injury." Am J Pathol **179**(4): 1839-1850.

Vig, P., Russo, F. P., Edwards, R. J., Tadrous, P. J., Wright, N. A., Thomas, H. C., Alison, M. R. and Forbes, S. J. (2006). "The sources of parenchymal regeneration after chronic hepatocellular liver injury in mice." Hepatology **43**(2): 316-324.

Wang, X., Willenbring, H., Akkari, Y., Torimaru, Y., Foster, M., Al-Dhalimy, M., Lagasse, E., Finegold, M., Olson, S. and Grompe, M. (2003). "Cell fusion is the principal source of bone-marrow-derived hepatocytes." Nature **422**(6934): 897-901.

Wang, Y., Lian, F., Li, J., Fan, W., Xu, H., Yang, X., Liang, L., Chen, W. and Yang, J. (2012). "Adipose derived mesenchymal stem cells transplantation via portal vein improves microcirculation and ameliorates liver fibrosis induced by CCl4 in rats." J Transl Med **10**: 133.

Wang, Y., Wang, Y. P., Zheng, G., Lee, V. W., Ouyang, L., Chang, D. H., Mahajan, D., Coombs, J., Wang, Y. M., Alexander, S. I. and Harris, D. C. (2007). "Ex vivo programmed macrophages ameliorate experimental chronic inflammatory renal disease." Kidney Int **72**(3): 290-299.

Wells, R. G., Kruglov, E. and Dranoff, J. A. (2004). "Autocrine release of TGF-beta by portal fibroblasts regulates cell growth." FEBS Lett **559**(1-3): 107-110.

Willenbring, H., Bailey, A. S., Foster, M., Akkari, Y., Dorrell, C., Olson, S., Finegold, M., Fleming, W. H. and Grompe, M. (2004). "Myelomonocytic cells are sufficient for therapeutic cell fusion in liver." Nat Med **10**(7): 744-748.

Wilson, H. M., Stewart, K. N., Brown, P. A., Anegon, I., Chettibi, S., Rees, A. J. and Kluth, D. C. (2002). "Bone-marrow-derived macrophages genetically modified to produce IL-10 reduce injury in experimental glomerulonephritis." Mol Ther **6**(6): 710-717.

Yang, C., Zeisberg, M., Mosterman, B., Sudhakar, A., Yerramalla, U., Holthaus, K., Xu, L., Eng, F., Afdhal, N. and Kalluri, R. (2003). "Liver fibrosis: insights into migration of hepatic stellate cells in response to extracellular matrix and growth factors." Gastroenterology **124**(1): 147-159.

Yang, M., Busche, G., Ganser, A. and Li, Z. (2013). "Morphology and quantitative composition of hematopoietic cells in murine bone marrow and spleen of healthy subjects." Ann Hematol **92**(5): 587-594.

Yannaki, E., Anagnostopoulos, A., Kapetanos, D., Xagorari, A., Iordanidis, F., Batsis, I., Kaloyannidis, P., Athanasiou, E., Dourvas, G., Kitis, G. and Fassas, A. (2006). "Lasting amelioration in the clinical course of decompensated alcoholic cirrhosis with boost infusions of mobilized peripheral blood stem cells." Exp Hematol **34**(11): 1583-1587.

Yovchev, M. I., Grozdanov, P. N., Zhou, H., Racherla, H., Guha, C. and Dabeva, M. D. (2008). "Identification of adult hepatic progenitor cells capable of repopulating injured rat liver." Hepatology **47**(2): 636-647.

Zhang, D. Y. and Friedman, S. L. (2012). "Fibrosis-dependent mechanisms of hepatocarcinogenesis." Hepatology **56**(2): 769-775.

Zhao, D. C., Lei, J. X., Chen, R., Yu, W. H., Zhang, X. M., Li, S. N. and Xiang, P. (2005). "Bone marrow-derived mesenchymal stem cells protect against experimental liver fibrosis in rats." World J Gastroenterol **11**(22): 3431-3440.

Zhou, X., Murphy, F. R., Gehdu, N., Zhang, J., Iredale, J. P. and Benyon, R. C. (2004). "Engagement of alphavbeta3 integrin regulates proliferation and apoptosis of hepatic stellate cells." J Biol Chem **279**(23): 23996-24006.

Zou, Y., Bao, Q., Kumar, S., Hu, M., Wang, G. Y. and Dai, G. (2012). "Four waves of hepatocyte proliferation linked with three waves of hepatic fat accumulation during partial hepatectomy-induced liver regeneration." PLoS One **7**(2): e30675.

Appendix One

CCl4 induces liver fibrosis in rats

Since the first description of experimental liver fibrosis induced by CCl_4 in 1926, this model has been particularly attractive due to its relative consistency, rapidity and similarity to human disease. (Sellers, Lucas et al. 1948) The repeated administration of CCl_4 results in probably the most used and best characterised experimental model of rodent liver fibrosis.(Constandinou, Henderson et al. 2005) In addition to the substantial literature, there was considerable experience of its use in our research group and animal facility. To confirm its safe administration and reliability, I undertook preliminary work in collaboration with Dr Caroline Pope who was examining rat liver fibrosis. Twice weekly IP injection of CCl_4 was performed safely in adult female rats.

Rats were harvested at 8 (n=4), 10 (n=3) and 12 (n=4) weeks of injury. PSR staining of liver sections was compared to control subjects (n=8) that had not received CCl_4. Appendix One figure 1 demonstrates that repeated CCl_4 injections caused liver fibrosis. The degree of variation can partly be explained by the small size of these preliminary groups. Subsequent work focused on murine models in line with the majority of the recent literature on experimental liver fibrosis and regeneration. This work informed subsequent experiments; larger groups were used and intergroup comparison of treatment effect was only made in the context of controls from the same batch that had undergone the same conditions including duration of injury.

Appendix 1 figure 1 CCl_4 causes liver fibrosis in rats

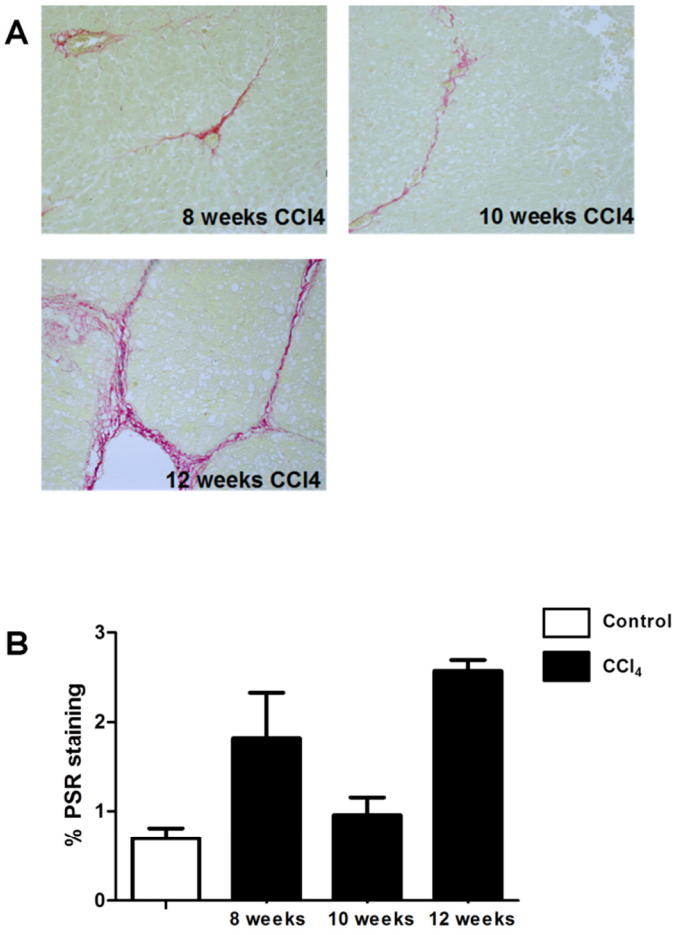

Appendix 1 figure 1 CCl_4 causes liver fibrosis in rats

(**A**) PSR staining was performed to detect hepatic collagen after I.P. CCl_4 administration to adult female rats. Representative images show the increased staining following repeated CCl_4 delivery. Original magnification, x200.

(**B**) Morphometric analysis shows the relationship between duration of injury and area of PSR staining.

Appendix 1 table 1 CCl_4 causes liver fibrosis in rats

Sample	Control (PSR %)	8 weeks CCl_4 (PSR %)	10 weeks CCl_4 (PSR %)	12 weeks CCl_4 (PSR %)
Mean +/- SEM	0.69 +/- 0.12	1.82 +/- 0.50	0.96 +/- 0.2	2.56 +/- 0.12
N	8	4	3	4

Appendix Two

Publication

Macrophage Therapy for Murine Liver Fibrosis Recruits Host Effector Cells Improving Fibrosis, Regeneration, and Function

James A. Thomas,[1,2] Caroline Pope,[1,2] Davina Wojtacha,[1,2] Andrew J. Robson,[1,2] Timothy T. Gordon-Walker,[1] Stephen Hartland,[1] Prakash Ramachandran,[1,2] Marielle Van Deemter,[1] David A. Hume,[3] John P. Iredale,[1] and Stuart J. Forbes[1,2]

Clinical studies of bone marrow (BM) cell therapy for liver cirrhosis are under way but the mechanisms of benefit remain undefined. Cells of the monocyte-macrophage lineage have key roles in the development and resolution of liver fibrosis. Therefore, we tested the therapeutic effects of these cells on murine liver fibrosis. Advanced liver fibrosis was induced in female mice by chronic administration of carbon tetrachloride. Unmanipulated, syngeneic macrophages, their specific BM precursors, or unfractionated BM cells were delivered during liver injury. Mediators of inflammation, fibrosis, and regeneration were measured. Donor cells were tracked by sex-mismatch and green fluorescent protein expression. BM-derived macrophage (BMM) delivery resulted in early chemokine up-regulation with hepatic recruitment of endogenous macrophages and neutrophils. These cells delivered matrix metalloproteinases-13 and -9, respectively, into the hepatic scar. The effector cell infiltrate was accompanied by increased levels of the antiinflammatory cytokine interleukin 10. A reduction in hepatic myofibroblasts was followed by reduced fibrosis detected 4 weeks after macrophage infusion. Serum albumin levels were elevated at this time. Up-regulation of the liver progenitor cell mitogen tumor necrosis factor-like weak inducer of apoptosis (TWEAK) preceded expansion of the progenitor cell compartment. Increased expression of colony stimulating factor-1, insulin-like growth factor-1, and vascular endothelial growth factor also followed BMM delivery. In contrast to the effects of differentiated macrophages, liver fibrosis was not significantly altered by the application of macrophage precursors and was exacerbated by whole BM. *Conclusion:* Macrophage cell therapy improves clinically relevant parameters in experimental chronic liver injury. Paracrine signaling to endogenous cells amplifies the effect. The benefits from this single, defined cell type suggest clinical potential. (HEPATOLOGY 2011;53:2003-2015)

Abbreviations: ALT, alanine aminotransferase; α-SMA, α-smooth muscle actin; BM, bone marrow; BMM, bone marrow derived macrophage; CCl_4, carbon tetrachloride; CSF-1/M-CSF, colony stimulating factor-1/macrophage colony stimulating factor; CSF-1R, colony stimulating factor-1 receptor; DMEM, Dulbecco's Modified Eagle Medium; EGFP, enhanced green fluorescent protein; FACS, fluorescence-activated cell sorting; FISH, fluorescent in situ hybridization; HGF, hepatocyte growth factor; HPV, hepatic portal vein; IGF-1, insulin-like growth factor 1; IL, interleukin; IP, intraperitoneal; LPC, liver progenitor cell; MCP-1, macrophage chemoattractant protein-1; MIP, macrophage inflammatory protein; MMP, matrix metalloproteinase; NOS, nitric oxide synthase; PBS, phosphate buffered saline; PCK, pancytokeratin; SAM, scar associated macrophage; SC, subcutaneous; TNF, tumor necrosis factor; TWEAK, tumor necrosis factor-like weak inducer of apoptosis; VEGF, vascular endothelial growth factor.

From the [1]MRC Centre for Inflammation Research, University of Edinburgh, Edinburgh, UK; [2]MRC Centre for Regenerative Medicine, University of Edinburgh, Edinburgh, UK; and [3]Roslin Institute and Royal (Dick) School of Veterinary Studies, University of Edinburgh, Roslin, UK.

Received August 25, 2010; accepted March 12, 2011.

Supported by the Sir Jules Thorn Charitable Trust. Also supported by EASL Sheila Sherlock Entry LevelFellowship (to van Deemter).

Address reprint requests to: Stuart J. Forbes, Queen's Medical Research Institute, 47 Little France Crescent, Edinburgh EH16 4TJ, UK. E-mail: stuart.forbes@ed.ac.uk; fax: +44 131 2426379.

View this article online at wileyonlinelibrary.com.

DOI 10.1002/hep.24315

Potential conflict of interest: Nothing to report.

Additional Supporting Information may be found in the online version of this article.

Chronic liver injury results in scar deposition, hepatocyte loss, and ultimately cirrhosis. The only effective treatment for endstage liver disease is liver transplantation; however, organ demand exceeds available supply. There is, therefore, an urgent need to develop alternative therapies for cirrhosis. BM (bone marrow)-derived cell populations influence the progression and recovery phases of liver fibrosis.[1-3] Clinical studies of BM cell therapy for cirrhosis are under way. However, the use of mixed cell populations limits the understanding of mechanisms of action.[4] The identification of defined single cell types with beneficial effects will enable rational and predictable therapy.

Macrophages have a broad repertoire of context-dependent immune, inflammatory, trophic, and regulatory actions.[5] We have previously shown that upon cessation of chronic liver injury, endogenous macrophages mediate hepatic scar remodeling through local matrix metalloproteinase (MMP) expression.[2,6] BM precursors differentiate into macrophages under the control of colony stimulating factor-1 (CSF-1) via its receptor (CSF-1R). CSF-1 also regulates macrophage proliferation, viability, and phenotypic fate.[7] Furthermore, exogenous CSF-1 stimulates macrophage infiltration, improving fibrosis and function in models of renal[8] and cardiac[9] injury. Developing therapy using cells from the monocyte-macrophage lineage therefore holds promise. In chronic liver injury, hepatocyte proliferation is impaired and liver progenitor cells (LPCs) become activated to supply hepatocytes.[10] LPCs are not of BM origin[11,12]; however, their activation is influenced by a number of paracrine signals that represent potential targets for BM-derived cell therapy.[10,13]

We examined the therapeutic potential of exogenous unmanipulated BM cells, in particular those of the monocyte-macrophage lineage, delivered during chronic liver injury. The intraportal application of differentiated BM-derived macrophages (BMMs) improved liver fibrosis, regeneration, and function. Distinct from our current understanding of endogenous macrophages in postinjury scar resolution, the application of these *ex vivo* cultured and expanded cells activates a wide range of reparative pathways during ongoing injury, with therapeutic benefit. Importantly, we observed paracrine signaling from the exogenous cells to larger populations of endogenous cells, which amplified their effects. This allowed comparatively modest numbers of donor BMMs to exert whole organ changes—encouraging from a translational perspective.

Materials and Methods

Preparation and Characterization of Donor Cells. Femurs and tibias were removed from age-matched, syngeneic male mice. BM cells were extracted and a single-cell suspension prepared by passing the cells through a 40-μm filter (BD Falcon). The Tg(Csf1r-Gfp)Hume (MacGreen) mouse has been characterized.[14] Briefly, this transgenic model uses the promoter region of the CSF-1R gene to direct expression of an enhanced green fluorescent protein (EGFP). Flow cytometric analysis of MacGreen mouse BM shows that EGFP colocalizes with CD11b, indicating that transgene expression is confined to myeloid cells. Approximately 50% of EGFP+ BM cells express F4/80.[14] EGFP+ BM cells expressing the Gr-1 antigen include Ly-6C+ monocytes and Ly-6G+ granulocytes. Monocytes are physiological precursors of macrophages. Culture with CSF-1 converts Ly-6G+ granulocytes into F4/80+ macrophages.[15] Therefore, all macrophage precursor cells within the BM with the potential to respond to CSF-1 (and differentiate into macrophages) express the EGFP reporter, allowing their selection by fluorescence-activated cell sorting (FACS, FACSVantage, Becton and Dickinson). BM-derived macrophages were prepared as described[16] by BM culture for 7 days in Teflon pots using Dulbecco's Modified Eagle Medium (DMEM)/F12 medium conditioned with CSF-1 from L929 cells. Diff-Quik staining was performed on cytospin samples. BMM marker expression was analyzed by flow cytometry (FACSCalibur, Becton and Dickinson). Cells were stained using the following preconjugated antibodies: F4/80, CD11b (eBiosciences), Ly-6G (Biolegend), Ly-6C, CD3 and CD19 (BD Pharmingen) with appropriate isotype controls. For phenotypic comparison, naïve BMMs were classically activated (M1) by overnight stimulation with lipopolysaccharide (Sigma, 50 ng/mL) and interferon-γ (Peprotech, 20 ng/mL) or alternatively activated (M2) with interleukin (IL)-4 and IL-13 (both Peprotech, 20 ng/mL).[5]

Disease Models and Cell Delivery. Wildtype mice were supplied by Harlan (UK) and housed in a sterile animal facility with a 12-hour dark/light cycle and free access to food and water. All animal experiments were carried out under procedural and ethical guidelines of the British Home Office. Advanced liver fibrosis was induced in adult female mice over a 10- week period by twice weekly intraperitoneal (IP) injection of 0.75 mL/kg carbon tetrachloride (CCl_4) dissolved in sterile olive oil. One day after the 12th CCl_4 injection (6 weeks), mice from the same cohort were randomly

allocated to receive either cell or control medium injections via the hepatic portal vein (HPV). Candidate cells from age- and strain-matched mice were suspended in 0.1 mL of DMEM. CCl_4 administration continued for a further 4 weeks. The HPV was accessed by midline laparotomy using aseptic technique. Anesthesia was induced using 1 mg/kg medetomidine and 76 mg/kg ketamine intraperitoneally (IP) and reversed with 1 mg/kg atipamezole subcutaneously (SC). Then 22.5 μg/kg buprenorphine (SC) was given as analgesia.

The following candidate cell types were tested: (1) 1×10^6 unfractionated whole BM cells were given to syngeneic fibrotic C57Bl/6 mice (n = 6, control n = 6). (2) 1×10^6 differentiated BMMs physically disrupted by sonication were given to syngeneic fibrotic C57Bl/6 mice (n = 7, control n = 6) to test whether intact, live BMMs were required for therapeutic effect. BMMs were sonicated twice for 10 seconds at 50% power using a Bandelin sonicator (Bandelin). (3) 1×10^6 macrophage precursor cells sorted from the BM of MacGreen mice[14] on a Balb-c background were given to fibrotic Balb-c mice (n = 7, control n = 6). (4) 1×10^6 differentiated wildtype BMMs were given to syngeneic fibrotic C57Bl/6 mice (n = 7, control n = 6). As no male donor BMMs were detected 4 weeks after BMM delivery, donor cells were also tracked by an independent method. BMMs were derived from the BM of constitutively GFP+ mice (TgTP6.3 tau-GFP mice on a CBA/Ca background[17]) using the same 7-day macrophage differentiation protocol as for wildtype BMMs. The 7×10^6 GFP+ BMMs were given to fibrotic wildtype CBA mice (n = 7, control n = 8).

BMM engraftment was transient; therefore, we examined the early effects of BMMs on fibrotic C57Bl/6 mice. 1×10^6 wildtype BMMs were given after 6 weeks of CCl_4 (n = 17, control n = 17). These mice were euthanized 1, 3, or 7 days after BMM delivery.

Additionally, 1×10^6 differentiated BMMs were delivered to mice 8 weeks into a longer schedule of 12 weeks 0.4 mL/kg CCl_4 (n = 8, control n = 8). Mice were venesected when euthanized. Harvested livers were split and pieces were snap-frozen in Tissue-Tek OCT Compound (Sakura Finetek) or fixed in formalin.

Immunohistochemistry. Collagen (Sirius red) and immunostaining were carried out as described.[1] Three-μm sections of formalin-fixed tissue were used for single immunostains. MMP-9, collagen 1, Dlk, and α-smooth muscle actin (α-SMA) detection required antigen retrieval with 0.01M sodium citrate pH 6.0; pancytokeratin (PCK) staining additionally required proteinase K solution (125 μg/mL). For Ki67, MMP-13, and GFP detection, slides were treated with Tris-EDTA pH 9.0. Primary antibodies were used at the following dilutions: 1:50 for F4/80 (Abcam), 1:100 for Ly-6G (BD Pharmingen) and collagen 1 (Southern Biotech), 1:150 for Dlk (Abcam), 1:200 for PCK (Dako), 1:500 for Ki67 (Novo Castro), GFP and MMP-9 (both Abcam), 1:800 for MMP-13 (Abcam), and 1:2,000 for α-SMA (Sigma). Secondary antibody was applied at a 1:400 dilution. Appropriate isotype controls were used for each primary antibody. Sections were developed using 3,3′-diaminobenzidine (Dako) then counterstained with Harris' hematoxylin. Frozen sections were used for dual staining with MMP-9 and F4/80 or Ly-6G. Detection was performed with Alexa Fluor 488, 546, and 555 (Invitrogen) followed by mounting using Vectashield with DAPI (Vector Laboratories). TUNEL staining (Promega) was performed on formalin-fixed tissue as per the manufacturer's instructions; dual staining with α-SMA was detected with streptavidin-Alexa Fluor 555 (Invitrogen). Male cells were detected by Y chromosome fluorescent *in situ* hybridization (FISH) using FITC-labeled Y-chromosome paint (Star-FISH; Cambio) as described.[1]

Assessment of Tissue Sections. Stained slides were blinded and a minimum of 20 serial, nonoverlapping fields were photographed at $\times$200 magnification. Male donor BMMs were detected by Y chromosome FISH. Not all male BMMs in a tissue section will exhibit the nucleus, and therefore permit binding of the Y chromosome probe. Male liver was used to establish the proportion of nonparenchymal cells that bound the probe (54%) and adjust subsequent counts to determine the total number of male donor cells present. For assessment of F4/80, Ly-6G, MMP-9, and MMP-13 staining, positive cells were counted in each field. PCK is a sensitive and validated marker of murine LPCs.[18] LPCs were defined as PCK+ cells with typical LPC morphology not directly abutting a lumen (thereby excluding biliary epithelia) as described.[18] For α-SMA, collagen I and Sirius red assessment, the percentage staining of the total field was measured using image analysis software (Adobe Photoshop). Measurements are expressed relative to matched control recipient samples from the same timepoint.

Quantification of Protein Levels. Whole liver protein extracts were quantified by Bradford assay. Samples were used at a concentration of 10 mg/mL. Cytokine concentrations were measured in duplicate using the Bioplex Protein Array System (Bio-Rad) according

to the manufacturer's instructions. Data were analyzed using Bio-Plex Manager 3.0 software (Bio-Rad). Protein levels are expressed relative to matched control samples from the same timepoint. Commercial kits were used to measure serum albumin (Randox Laboratories) and alanine aminotransferase (ALT) (Alpha Laboratories).

Hydroxyproline Assay. Snap-frozen liver samples (≈200 mg) were weighed, hydrolyzed in NaOH, and hydroxyproline content determined as described.[19] Absorbance was measured at 550 nm and hydroxyproline content expressed as μg/g liver.

Quantification of Messenger RNA (mRNA) Levels by Real-Time Reverse-Transcription Polymerase Chain Reaction (PCR). RNA was extracted from whole liver tissue using RNA extraction kits (Qiagen) according to the manufacturer's instructions. Complementary DNA was generated from 1 μg of RNA using the Superscript II kit (Invitrogen). Primers for MMPs-2, 9, 12, and 13, Fizz-1, IL-10, inducible nitric oxide synthase (iNOS), macrophage chemoattractant protein (MCP)-1, mannose receptor, tumor necrosis factor (TNF)-α, and Ym-1 were designed using primer express software (sequences supplied in the Supporting material). Predesigned, validated primer sets for macrophage inflammatory protein (MIP)-1α, MIP-2, KC, MMP-8, hepatocyte growth factor (HGF), insulin-like growth factor-1 (IGF-1), CK-19, and TNF-like weak inducer of apoptosis (TWEAK) were purchased from Qiagen (UK). A predesigned, validated eukaryotic 18S primer/probe set (Applied Biosystems) was used for internal control. Quantitative real-time PCR (qPCR) was performed using Express SYBR Green or TaqMan Express qPCR Supermix (Invitrogen). All reactions were performed in triplicate. Levels are expressed relative to matched control samples from the same timepoint.

Statistics. Data are presented as mean ± standard error of the mean. Two-tailed Student's t and Mann-Whitney U tests were used to analyze parametric and nonparametric data, respectively using Prism (GraphPad Software) unless otherwise stated.

Results

BMM Cell Therapy Improves Murine Liver Fibrosis. A hierarchical approach to candidate donor cell selection from the monocyte-macrophage lineage was taken. The effects of delivering differentiated macrophages (Fig. 1A-E), macrophage precursors from the BM (Fig. 1F), and unfractionated whole BM were tested. Macrophages were generated by 7 days of BM culture with CSF-1 conditioned medium. Diff-Quik staining confirmed that the injected cells were a morphologically homogenous population of macrophages (Fig. 1A). BMMs possessed the characteristic macrophage cell surface markers F4/80 and CD11b.[20] Flow cytometric analysis demonstrated that markers of other leukocyte populations (monocytes, neutrophils, and T and B cells) were not present in significant numbers (Fig. 1B). Donor BMMs were not manipulated and did not conform to either the traditional classically (M1) or alternatively activated (M2) macrophage phenotype (Fig. 1C,D). BMMs expressed antiinflammatory (IL-10), antifibrotic (MMP-13), proregenerative (TWEAK), and chemotactic (MCP-1, MIP-1α, MIP-2) mediators (Fig. 1E) that were subsequently found to be elevated in BMM recipient livers (Figs. 5C, 6C, 7E,F). The 1×10^6 wildtype BMMs delivered to recipient mice resulted in a significant reduction in fibrosis measured by Sirius red quantification (66% of control, $P < 0.05$, Fig. 2A,B). This effect was confirmed by reduced hydroxyproline content (368.2 ± 41.0 versus 558.8 ± 94.6 μg/g liver, $P = 0.05$, Fig. 2C) and collagen I staining (73% of control, $P < 0.01$, Fig. 2D,E). Experiments with GFP+ donor BMMs in an independent strain of wildtype recipients also demonstrated this reduction in fibrosis (Sirius red staining 67% of control, $P < 0.05$, Fig. 2B, Supporting Fig. 1A). Furthermore, in a 12-week CCl_4 injury model, BMMs injected at 8 weeks also reduced fibrosis to 69% of control (n = 8 versus n = 8 controls, $P < 0.05$).

In contrast to the effects of 7-day differentiated macrophages, injecting 1×10^6 BM macrophage precursor cells did not significantly reduce fibrosis ($P = 0.21$, Fig. 2A,B). The 1×10^6 unfractionated whole BM cells increased liver fibrosis to 161% of control ($P < 0.05$, Fig. 2A,B) and 1×10^6 sonically disrupted BMMs led to a trend of increased liver fibrosis ($P = 0.08$, Fig. 2B, Supporting Fig. 1B). Therefore, liver fibrosis was exacerbated by unfractionated BM and did not significantly improve following the delivery of BM macrophage precursors. Differentiated BMMs consistently reduced hepatic scar and cell viability was required; the underlying processes are examined in the following experiments.

Transient Engraftment of BMMs in the Fibrotic Liver. Engraftment of donor BMMs was confirmed using two independent cell tracking techniques. GFP+ BMMs were located by immunostaining sections of wildtype recipient liver for GFP. Male donor BMMs in the female recipient liver were identified by Y chromosome FISH. The majority of identified donor

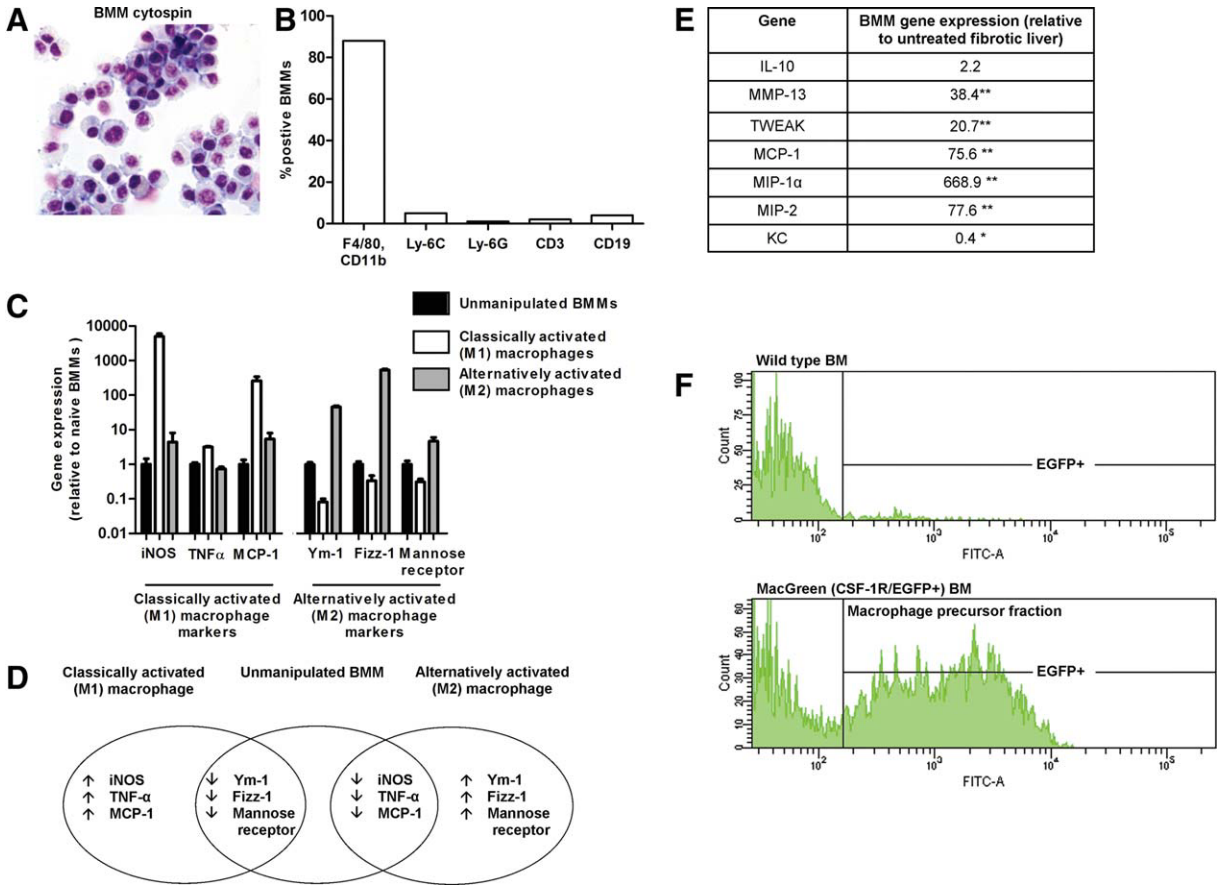

Gene	BMM gene expression (relative to untreated fibrotic liver)
IL-10	2.2
MMP-13	38.4**
TWEAK	20.7**
MCP-1	75.6 **
MIP-1α	668.9 **
MIP-2	77.6 **
KC	0.4 *

Fig. 1. The derivation and characterization of candidate donor cells. Macrophages were differentiated from whole BM cultured for 1 week in CSF-1 conditioned media. (A) Diff-Quik staining of these BMMs demonstrates a uniform morphology and staining profile. Original magnification ×200. (B) Flow cytometric analysis revealed that BMMs possessed the typical macrophage markers F4/80 and CD11b. Markers of other leukocyte populations (monocytes, neutrophils, and T and B cells) were minimally detected. (C,D) Gene expression analysis of classical (M1) and alternative (M2) macrophage activation markers revealed that BMMs have a naive phenotype in this regard. (E) qPCR analysis showed that BMMs, prior to delivery, expressed specific antiinflammatory, antifibrotic, proregenerative, and chemotactic mediators compared to untreated fibrotic liver. (F) BM cells expressing the CSF-1 receptor/EGFP transgene in the MacGreen mouse[14] represent a population of potential macrophage precursors. These cells were positively selected by FACS (denoted "EGFP+").

BMMs were located within or closely apposed to the hepatic scar (Fig. 3A). One day after the delivery of 1×10^6 BMMs, the mean number of engrafted donor BMMs was 6.9 per ×200 magnification field by GFP immunostaining. Y chromosome FISH revealed 6.5 donor BMMs (per ×200 field) at day 1, which decreased to 5.3 within the first week. In keeping with the known rapid turnover of hepatic macrophages,[21] donor BMMs were not detected 1 month after BMM delivery (Fig. 3B).

Early Reduction in Myofibroblasts Following BMM Delivery. A reduction in the number of α-SMA+ myofibroblasts through apoptosis is a key early event during fibrosis resolution.[22] The amount of α-SMA staining in the BMM treatment group decreased within the first week (Fig. 4A), falling to 40% of control 7 days after macrophage therapy ($P < 0.05$, Fig. 4B). Apoptotic myofibroblasts were detected during this reduction (Supporting Fig. 2). The decrease in myofibroblasts was no longer statistically significant 1 month after intervention ($P = 0.29$), suggesting that the peak antifibrotic effect on the myofibroblast population occurs soon after BMM delivery.

Up-regulation of Hepatic MMP-Expressing Cells in BMM Recipients. A critical component of fibrosis resolution is the degradation of extracellular matrix mediated by the MMP family of enzymes. Prior to the reduction in myofibroblasts 7 days after BMM delivery, there were increases in the numbers of cells producing MMP-13 and -9 protein ($P < 0.01$ and < 0.05, respectively, Fig. 5A,B). These MMP-expressing cells were predominantly located in the hepatic scar. Within 1 day of BMM therapy, whole liver gene expression of MMP-9 was markedly elevated ($P < 0.05$) alongside trends toward increases in MMP-13 ($P = 0.21$), MMP-8 (neutrophil collagenase, $P = 0.17$),

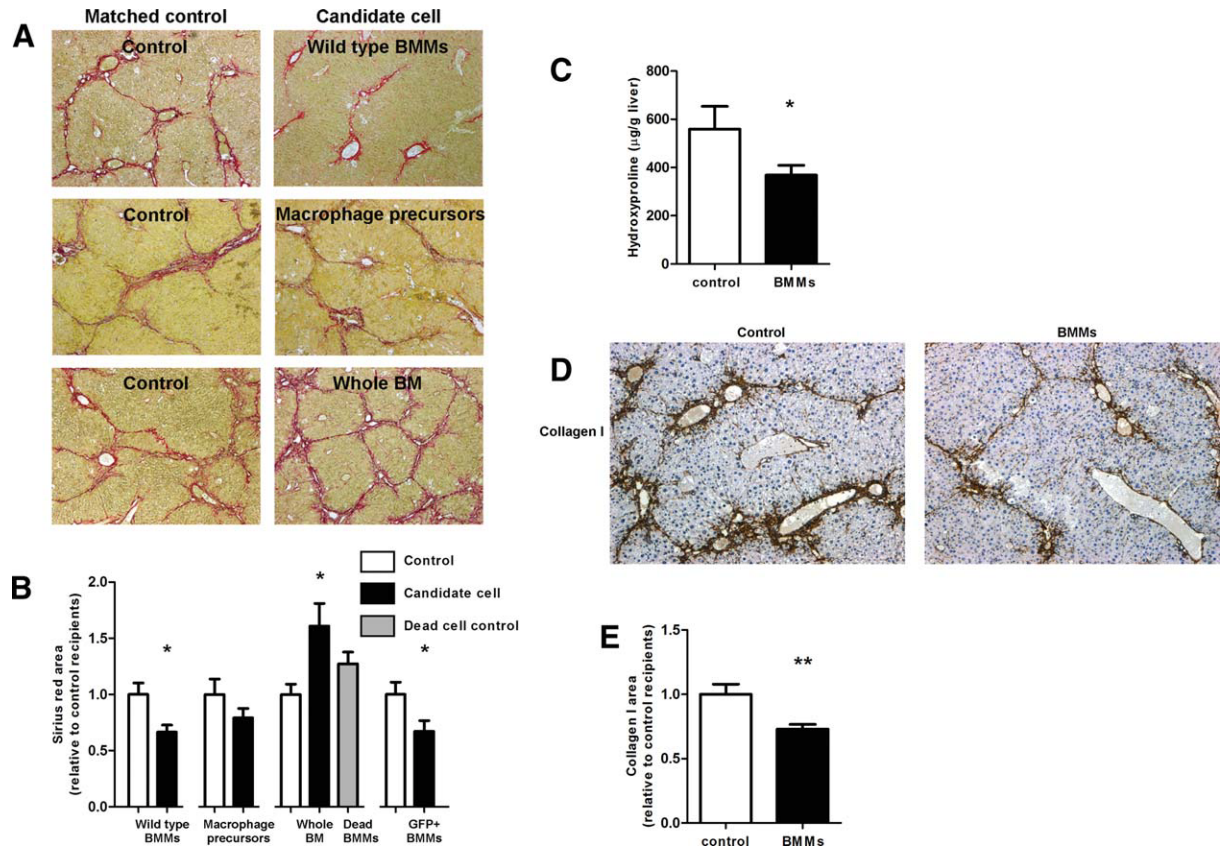

Fig. 2. Cells of the monocyte-macrophage lineage have differential therapeutic effects on liver fibrosis. Advanced liver fibrosis was induced in adult female mice by chronic administration of IP CCl_4. (A) Photomicrographs show Sirius red staining for hepatic collagens 4 weeks after wild-type BMMs, macrophage precursor cells, or unfractionated BM cells were delivered to syngeneic fibrotic mice (right-side column). Age- and strain-matched control mice within each cohort received an equal volume of control medium (left column). Original magnification, ×80. (B) Morphometric analysis of Sirius red staining revealed that the delivery of differentiated BMMs (both wildtype and GFP+) caused a reduction in the amount of fibrosis. BM macrophage precursor cells did not significantly reduce the amount of fibrosis. Unfractionated whole BM increased liver fibrosis, whereas dead BMMs lead to a trend towards this. The reduced fibrosis following BMM delivery was confirmed (1-tailed analysis) by (C) hydroxyproline assay and (D) collagen I immunostaining (original magnification ×80) with (E) morphometric analysis (*$P \leq 0.05$, **$P < 0.01$ compared with control recipients; n = 6-8 per group).

and MMP-12 (macrophage metalloelastase, $P = 0.08$) (Fig. 5C). Serial section analysis indicated that a subset of predominantly scar associated macrophages (SAMs) produced MMP-13 (Fig. 5D). We have previously shown that SAMs are an important cellular source of MMP-13 contributing to scar resolution after liver injury.[6] Dual immunostaining revealed the MMP-9 producing cells to be neither donor nor endogenous macrophages (Fig. 5Ei) but endogenous Ly-6G+ neutrophils (Fig. 5Eii). Therefore, the initial donor

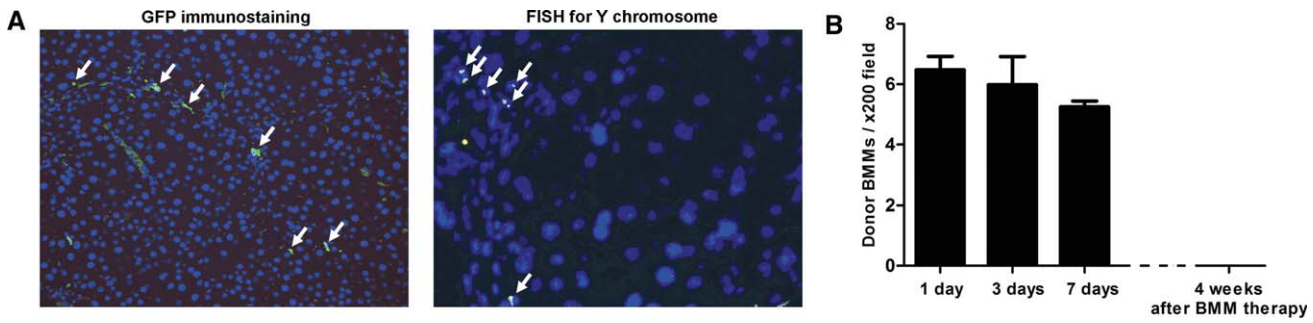

Fig. 3. Donor BMMs engraft transiently in the liver. (A) Donor cells were tracked by treating wildtype fibrotic mice with GFP+ BMMs (arrowed). Original magnification ×200. In addition, male donor cells (arrowed) were detected within injured female liver using FISH for the Y chromosome. Original magnification ×320. (B) Quantification of donor cell engraftment by Y chromosome FISH revealed a reduction in number during the first 7 days after BMM delivery. No donor cells were present 4 weeks after infusion (n = 3 per timepoint).

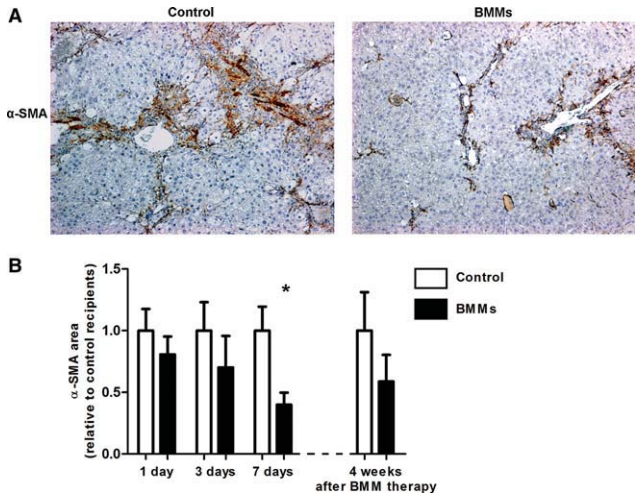

Fig. 4. BMM delivery causes a reduction in hepatic myofibroblasts. (A) Photomicrographs demonstrate the reduction in α-SMA+ myofibroblasts 7 days after BMM delivery. Original magnification ×80. (B) Quantification of α-SMA immunostaining revealed that myofibroblast numbers declined within 7 days of BMM treatment; this effect did not persist 1 month after infusion (*$P < 0.05$ compared with control recipients per timepoint; n = 5-8 per group).

BMMs caused an increase in the numbers of MMP-producing leukocytes in the hepatic scar.

BMMs Initiate the Hepatic Recruitment of Circulating Macrophages and Neutrophils. Within 1 day of BMM infusion, there was a marked change in the cellular composition of the fibrotic liver. F4/80 immunostaining demonstrated a 44% increase in macrophages ($P < 0.05$, Fig. 6A,B). The absolute increase in macrophage number in BMM-treated mice (from 53 to 76, i.e., an additional 23 per ×200 field) is greater than the number of donor BMMs (mean <7) in the same area of tissue, indicating that the majority of these macrophages were recruited. Ly-6G immunostaining revealed a 242% increase in hepatic neutrophils ($P < 0.01$, Fig. 6A,B).

Analysis of whole liver protein from this timepoint revealed that BMM recipients had significantly higher levels of several chemokines expressed by the donor BMMs (Figs. 1E, 6C). The macrophage chemoattractant MCP-1 (CCL2) was increased to 160% ($P < 0.001$), whereas MIP-1α (CCL3) was 137% of control ($P < 0.05$). The neutrophil chemoattractants KC (CXCL1) and MIP-2 (CXCL2) were also strongly up-regulated (242%, $P < 0.001$ and 842%, $P < 0.01$, respectively). Whole liver protein levels of the antiinflammatory cytokine IL-10 were elevated to 346% in BMM recipients ($P < 0.05$), whereas proinflammatory mediators such as IL-6 and TNF-α were unchanged (Fig. 7F). Four weeks after BMM delivery, serum ALT levels were not significantly reduced in recipient mice (399.2 ± 120.7) compared to controls (505.7 ± 91.7 u/l, $P = 0.5$).

Therefore, BMM therapy switches the hepatic milieu towards an antiinflammatory cytokine environment while recruiting host macrophages and neutrophils into this altered setting.

BMM Cell Therapy Stimulates Regeneration of the Injured Liver. Serum albumin was increased in BMM recipients 4 weeks after cell delivery (46.0 ± 2.6 g/l versus 39.9 ± 0.9 g/l, $P = 0.05$, Fig. 7A). The elevated serum albumin was confirmed in mice receiving GFP+ BMMs (43.3 ± 0.6 g/l versus 40.4 ± 1.0 g/l, $P < 0.05$, Fig. 7A), suggesting improved regeneration. Hepatocyte proliferation (Ki67+) was not significantly increased after BMM therapy ($P = 0.21$, Fig. 7B,C). Expression of the hepatocyte mitogen HGF also did not change (Fig. 7E). In keeping with human chronic liver disease, increased numbers of LPCs were present in CCl_4-injured mice. Three days after BMM delivery, whole tissue mRNA levels of the LPC marker CK-19 were increased by 55% over control recipients (1.55 ± 0.1 versus 1.00 ± 0.2, $P = 0.05$). By day 7, there was a periportal expansion of PCK and Dlk+ LPCs in BMM recipients. The number of LPCs increased by 40% over control ($P < 0.05$, Fig. 7B,D). There was no increase in the level of the cytokines IL-6 and TNF-α which are associated with LPC proliferation[10] (Fig. 7F). Donor BMMs used here express high levels of the LPC mitogen TWEAK relative to recipient liver (Fig. 1E). Three days after BMM therapy, at a time when hepatic macrophage numbers were increased, whole liver TWEAK mRNA levels were significantly elevated to 216% of control ($P < 0.05$, Fig. 7E).

IGF-1 mRNA levels were increased 3 and 7 days after BMM delivery ($P < 0.05$ and 0.001, respectively, Fig. 7E). CSF-1 protein levels increased to 165% 1 day after BMM delivery ($P < 0.01$, Fig. 7F) before decreasing over the first week. Vascular endothelial growth factor (VEGF) protein levels increased over this period in BMM recipients, reaching 127% of control at day 7 ($P < 0.05$, Fig. 7F). In addition to the up-regulation of these reparative factors, the increased TWEAK expression and expanded LPC compartment are also implicated in the improved hepatic function in BMM-treated mice.

Discussion

Cell therapy based on a defined, homogenous cell population adds clarity to the cause-effect relationship. Importantly for clinical translation, our data reveal that unfractionated BM had a deleterious effect on liver fibrosis. Interestingly, exogenous macrophage precursors

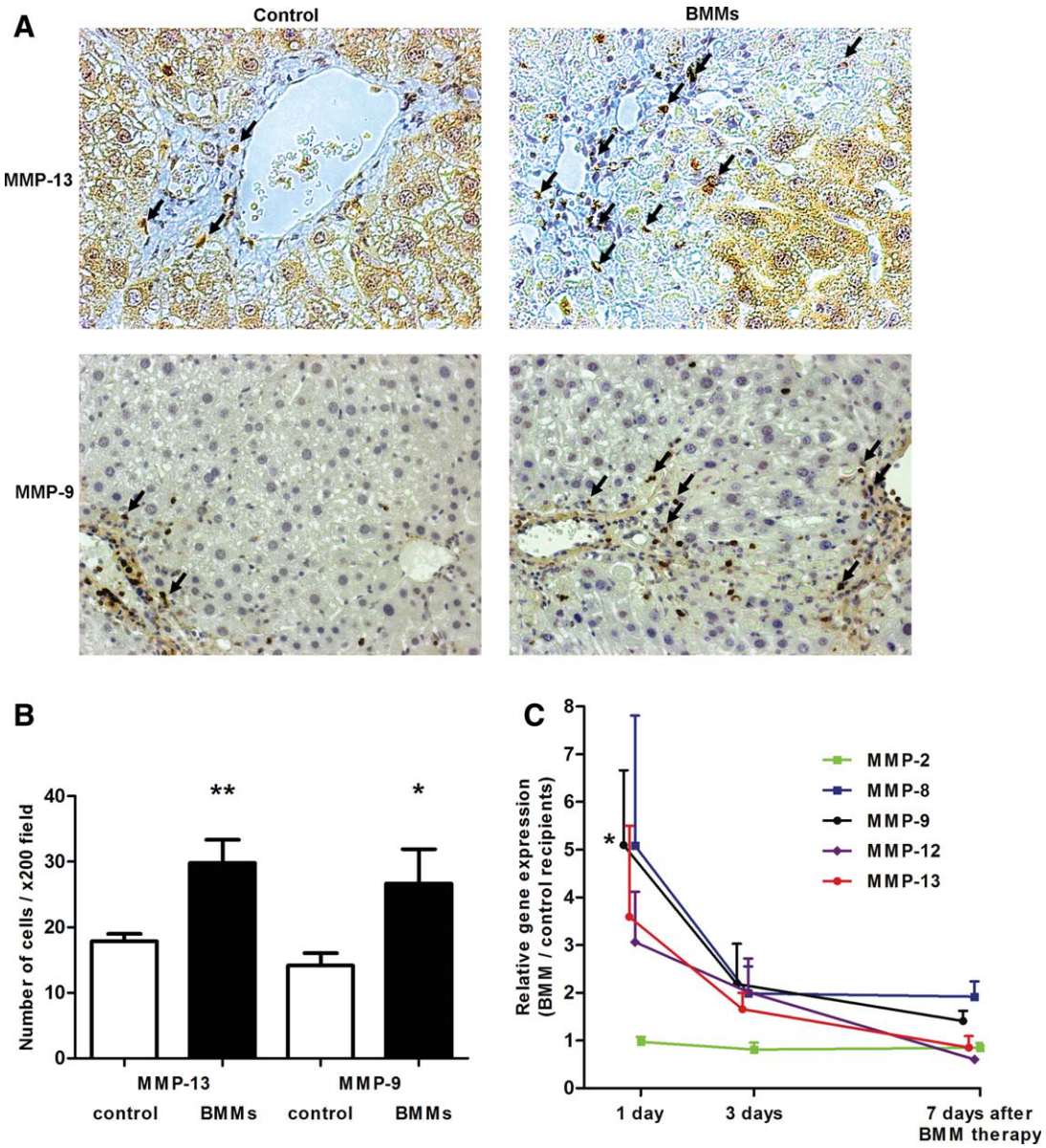

Fig. 5. BMM delivery causes the hepatic up-regulation of MMPs-13 and -9. (A) Immunohistochemical analysis of livers 1 day after BMM delivery revealed infiltration of MMP-13 and MMP-9+ cells (arrowed). Original magnification ×320 and ×200, respectively. (B) The numbers of MMP-13 and -9-expressing cells were greater than in control recipients. (C) Whole liver gene expression of MMP-9 was significantly elevated in BMM recipients at this timepoint. Gene expression levels of MMPs-8, -12, and -13 were not significantly increased. By day 3, these levels had decreased (*$P < 0.05$, **$P < 0.01$ compared with control recipients per timepoint; n = 5-6 per group). (D) Immunostaining of serial liver sections indicates that a subset of scar associated F4/80+ macrophages produced MMP-13 (arrowed). Original magnifications ×80 and ×320. (E i) Dual staining for MMP-9 (red) and F4/80 (green) demonstrates that hepatic macrophages (arrowheads) did not express MMP-9 (arrows) in BMM recipients. Original magnification ×1000. (E ii) Colocalization (arrows) of the neutrophil marker Ly-6G (red) with MMP-9 staining (green) indicates that scar associated hepatic neutrophils were expressing MMP-9 in BMM recipients. Original magnification ×200.

did not significantly improve liver fibrosis. Of note, this population contains Gr-1^{hi} (Ly-6C^{hi}) monocytes[15] that have profibrogenic actions during liver injury.[23] Following culture in CSF-1 conditioned medium, CSF-1R+ macrophage precursors within BM differentiate into macrophages.[15] The BMMs used here are a relatively homogenous population of cells without significant contamination from other cell types such as monocytes, granulocytes, and stem cells. The differentiated macrophages generated by this process are antifibrotic and proregenerative in this model. Unmanipulated BMMs cultured in these nonadherent conditions possess neither the typical classically (M1) nor alternatively activated (M2) profiles. Donor BMM engraftment was transient; however, their effects persisted and were amplified by paracrine signaling to host cell

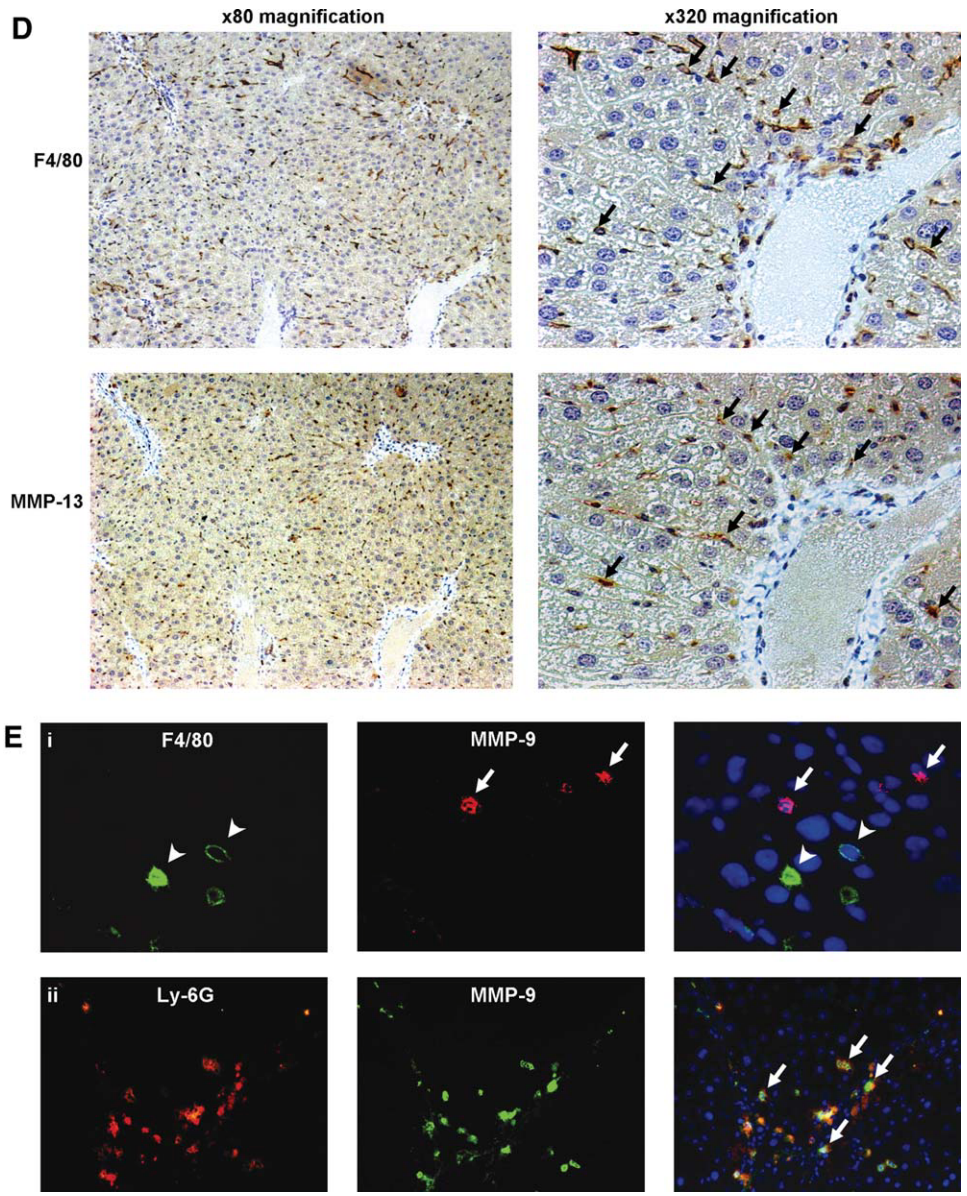

Fig. 5. (Continued)

populations. The net effect was a reduction in fibrosis and improved regeneration of the injured liver.

BMM therapy caused the recruitment of MMP producing host cells into the hepatic scar. MCP-1 and MIP-1α are members of the CC chemokine subfamily that bind to the CCR2 and CCR1/5 receptors of monocytes, respectively. These interactions contribute to the navigation of monocytes into target tissues during their maturation into macrophages.[5] The delivery of MCP-1 and MIP-1α-expressing BMMs to injured mice caused up-regulation of hepatic MCP-1 and MIP-1α and the recruitment of endogenous macrophages. These macrophages produced MMP-13, whose actions include the degradation of fibrillar collagens and gelatin as well activation of other MMPs (such as MMP-9).[6] Donor BMMs also express MIP-2 and KC, which are examples of CXC chemokines that recruit neutrophils through the surface receptor CXCR2.[5] One day after BMM delivery, hepatic expression of these neutrophil chemoattractants was markedly up-regulated, with elevated hepatic neutrophil numbers. This is in keeping with the role of macrophage-mediated neutrophil recruitment in fibrosis resolution following cessation of cholestatic injury.[24] In our model, recruited neutrophils produce MMP-9. MMP-9 overexpression reduces myofibroblast number and inhibits

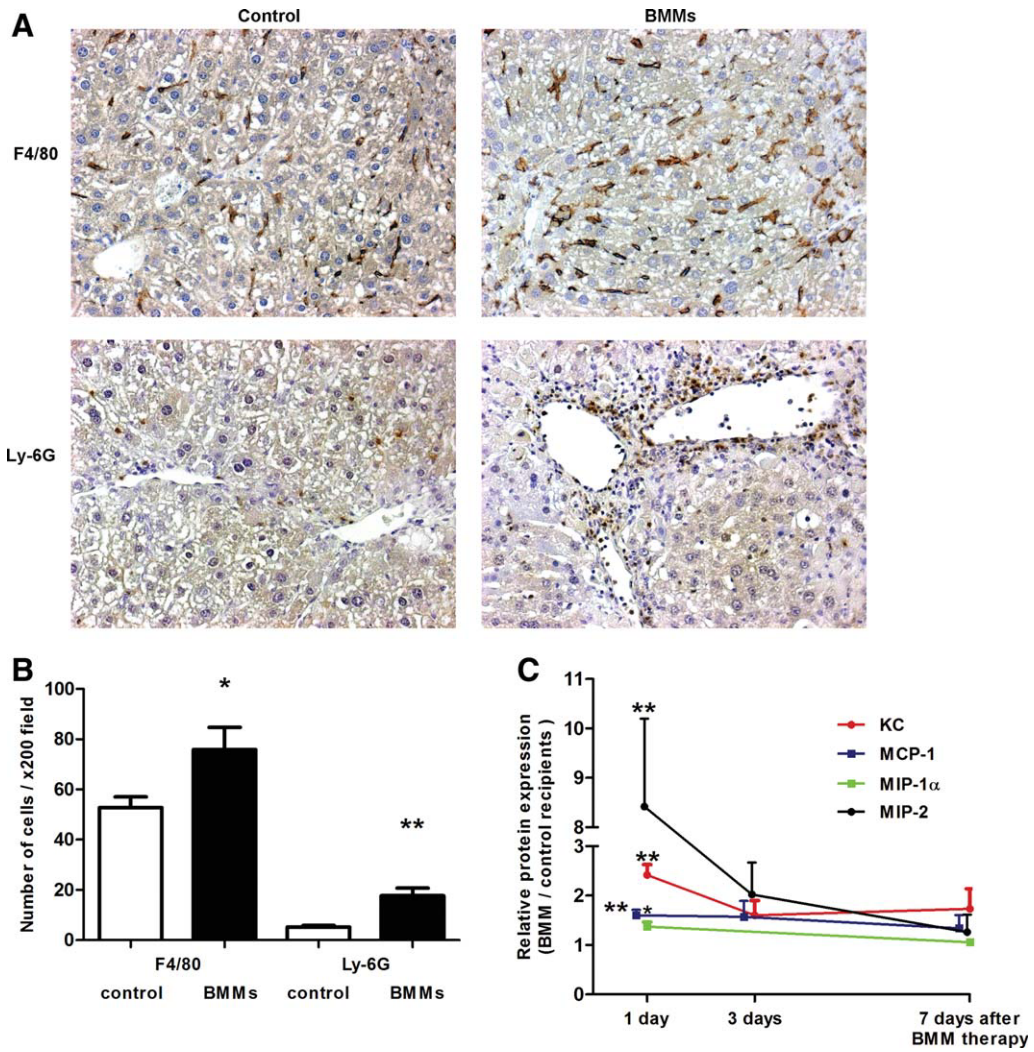

Fig. 6. Host leukocytes are recruited to the liver following BMM delivery. (A) Immunohistochemical analysis of livers 1 day after BMM delivery revealed that macrophages and neutrophils were recruited to the injured liver. Original magnification ×200. (B) The degree of cell influx was greater than in control tissue. (C) Whole liver protein expression of macrophage and neutrophil chemokines (MCP-1, MIP-1α, MIP-2, and KC) was significantly up-regulated 1 day after BMM delivery. By day 3 these levels returned toward baseline (*$P < 0.05$, **$P < 0.01$ compared with control recipients per timepoint; n = 5-6 per group).

fibrogenesis during experimental liver injury.[25] The simultaneous trend of increased MMP-12 (macrophage metalloelastase) and MMP-8 (neutrophil collagenase) expression following BMM therapy reinforces the fibrolytic role of recruited leukocytes. The markedly elevated hepatic IL-10 levels in BMM recipients may modify the behavior of resident and incoming leukocytes and the degree of injury.[26] Simultaneous up-regulation of IL-10 and MMPs following BMM therapy may reduce myofibroblast activation[26] and promote apoptosis.[27] The chemokine-mediated recruitment of host effector cells to the injured liver, importantly at a time when the prevailing hepatic environment is antiinflammatory, represents a novel and realistic mechanism for the therapeutic actions of comparatively few donor cells in the context of the whole organ.

The improved liver function following BMM therapy is multifactorial. There is a less fibrotic cellular milieu, a proregenerative stimulus to LPCs, and elevated levels of cytokines such as CSF-1, VEGF, and IGF-1 that are involved in reparative processes during tissue injury.[9,28,29] Hepatocyte proliferation was not significantly increased following BMM therapy. There was significant activation of the LPC compartment, compatible with the recent observation that BM infusion transiently stimulated LPCs and improved serum albumin in a series of cirrhotic patients.[30] We have previously noted the close spatial relationship between LPCs and endogenous macrophages *in vivo*.[12] The cytokine TWEAK is a member of the TNF superfamily and is currently the only known mitogen that is selective for LPCs but not

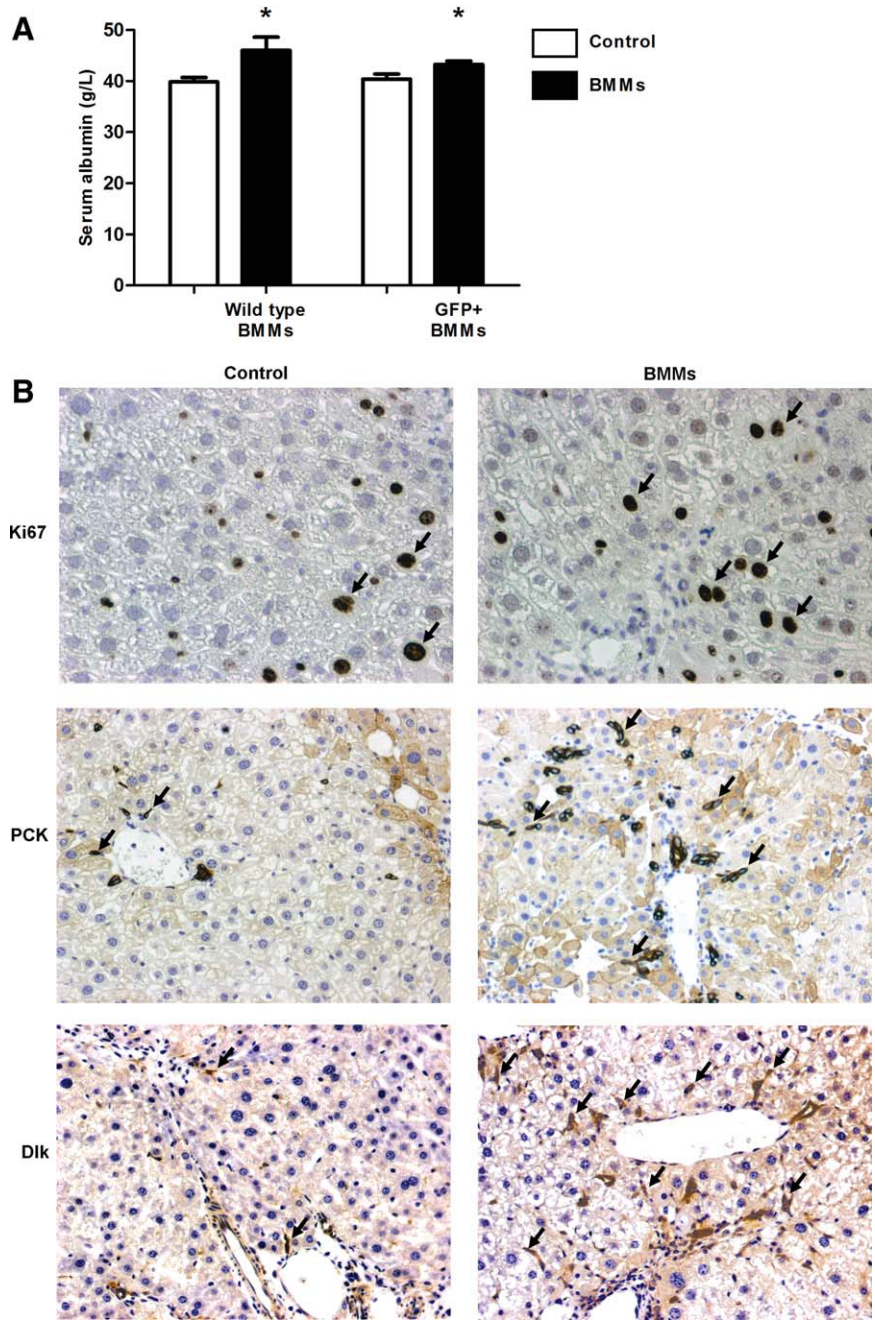

Fig. 7. BMM therapy activates regenerative pathways. (A) Serum albumin was increased 4 weeks after the delivery of wildtype or GFP+ BMMs to fibrotic mice. (B) Photomicrographs show Ki67, PCK, and Dlk staining of liver tissue 7 days after BMM therapy. Original magnification ×200. (C) The number of Ki67+ hepatocytes did not increase significantly after BMM therapy. (D) Increased numbers of pancytokeratin-positive liver progenitor cells were detected 7 days after BMM infusion. This expansion was not maintained at 4 weeks. (E) Gene expression of HGF was not significantly elevated in BMM recipients. The liver progenitor cell mitogen TWEAK was up-regulated 3 days after BMM delivery. IGF-1 mRNA was increased 3 and 7 days after BMM treatment. (F) Whole liver protein levels of IL-10 and CSF-1 were elevated 1 day after BMM delivery, whereas IL-6 and TNF-α were unchanged. VEGF protein levels increased after BMM therapy, reaching significance at day 7 (*$P \leq 0.05$, **$P < 0.01$ compared with control recipients per timepoint; n = 5-8 per group).

mature hepatocytes.[13] TWEAK acts through its cognate receptor Fn14 to stimulate LPC proliferation. Interestingly, endogenous hepatic macrophages have recently been identified as a cellular source of TWEAK during chronic liver injury.[31] Donor BMMs used in our studies expressed high levels of TWEAK and recruited additional host macrophages to the injured liver, supporting the paradigm of donor cell-derived paracrine signals having downstream actions on host cell populations. In addition, we

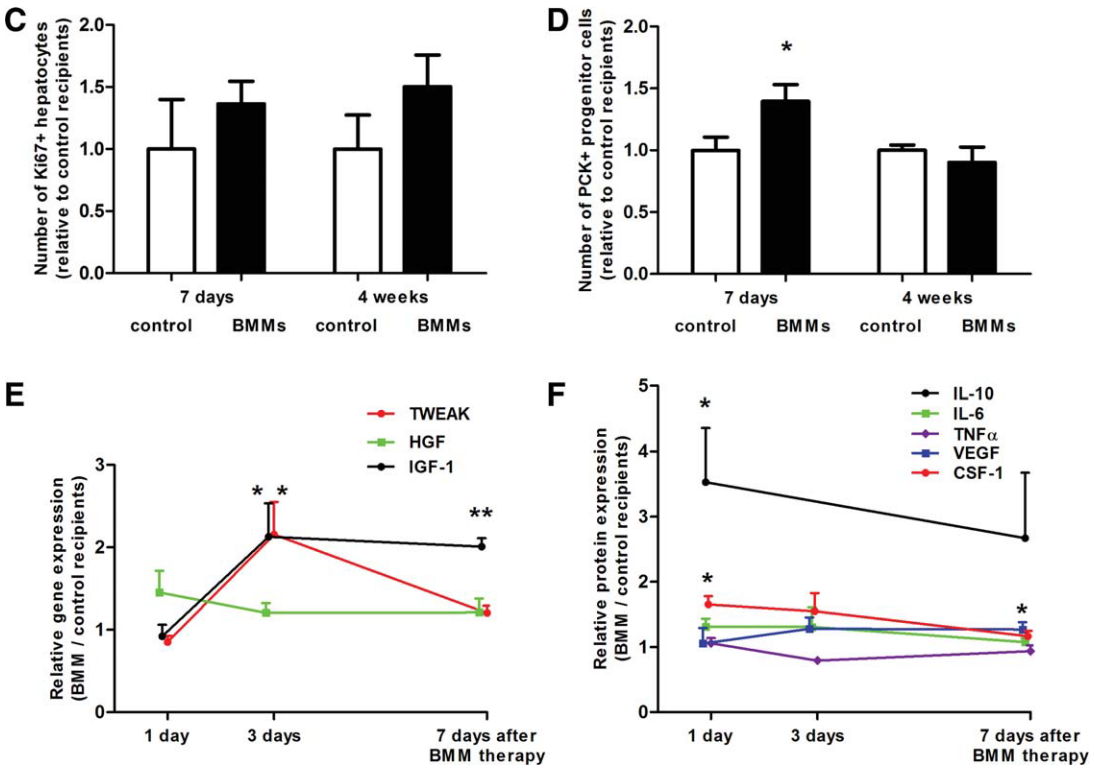

Fig. 7. (Continued)

have recently found that hepatic scar degradation promotes LPC activation,[32] suggesting that LPC proliferation is also indirectly enhanced by the macrophage-mediated hepatic scar reduction.

In conclusion, we have demonstrated the benefit of BMM therapy upon structural and functional parameters of chronic liver injury. BMMs clearly have multiple actions, some direct and others mediated indirectly through recruitment of host effector cells with antiinflammatory, antifibrotic, and proregenerative results. A number of the mediators reported here have previously been shown to determine the course of experimental liver injury. When overexpressed in isolation, MMP-9,[25] IGF-1,[29] and IL-10[26] have each been shown to reduce myofibroblast numbers and fibrosis in injured liver. CSF-1 also reduces organ fibrosis while improving function.[8,9] MMP-13 knockout impairs fibrosis resolution[6] and MMPs-8 and -12 mediate hepatic scar degradation. Overexpression of TWEAK and IL-10 improve LPC proliferation[13,31] and hepatic regeneration,[26] respectively. The simultaneous up-regulation of these factors demonstrates the multifaceted effects of cell therapy. This contrasts with studies of single molecules or genes where the effects of the single pathway can be shown. Future work will examine the cellular events underpinning leukocyte recruitment and also activation of progenitor cells within the injured liver following BMM therapy. With regard to clinical translation, the use of a differentiated, readily available, single cell type increases the predictability of effect. The data reported here will inform the rational design of clinical studies to determine the efficacy of autologous cell therapy in chronic liver disease.

References

1. Russo FP, Alison MR, Bigger BW, Amofah E, Florou A, Amin F, et al. The bone marrow functionally contributes to liver fibrosis. Gastroenterology 2006;130:1807-1821.
2. Duffield JS, Forbes SJ, Constandinou CM, Clay S, Partolina M, Vuthoori S, et al. Selective depletion of macrophages reveals distinct, opposing roles during liver injury and repair. J Clin Invest 2005;115:56-65.
3. Forbes SJ, Russo FP, Rey V, Burra P, Rugge M, Wright NA, et al. A significant proportion of myofibroblasts are of bone marrow origin in human liver fibrosis. Gastroenterology 2004;126:955-963.
4. Houlihan DD, Newsome PN. Critical review of clinical trials of bone marrow stem cells in liver disease. Gastroenterology 2008;135:438-450.
5. Mantovani A, Sica A, Sozzani S, Allavena P, Vecchi A, Locati M. The chemokine system in diverse forms of macrophage activation and polarization. Trends Immunol 2004;25:677-686.
6. Fallowfield JA, Mizuno M, Kendall TJ, Constandinou CM, Benyon RC, Duffield JS, et al. Scar-associated macrophages are a major source of hepatic matrix metalloproteinase-13 and facilitate the resolution of murine hepatic fibrosis. J Immunol 2007;178:5288-5295.

7. Pollard JW. Trophic macrophages in development and disease. Nat Rev Immunol 2009;9:259-270.
8. Menke J, Iwata Y, Rabacal WA, Basu R, Yeung YG, et al. CSF-1 signals directly to renal tubular epithelial cells to mediate repair in mice. J Clin Invest 2009;119:2330-2342.
9. Morimoto H, Takahashi M, Shiba Y, Izawa A, Ise H, Hongo M, et al. Bone marrow-derived CXCR4+ cells mobilized by macrophage colony-stimulating factor participate in the reduction of infarct area and improvement of cardiac remodeling after myocardial infarction in mice. Am J Pathol 2007;171:755-766.
10. Bird TG, Lorenzini S, Forbes SJ. Activation of stem cells in hepatic diseases. Cell Tissue Res 2008;331:283-300.
11. Vig P, Russo FP, Edwards RJ, Tadrous PJ, Wright NA, Thomas HC, et al. The sources of parenchymal regeneration after chronic hepatocellular liver injury in mice. HEPATOLOGY 2006;43:316-324.
12. Lorenzini S, Bird TG, Boulter L, Bellamy C, Samuel K, Aucott R, et al. Characterisation of a stereotypical cellular and extracellular adult liver progenitor cell niche in rodents and diseased human liver. Gut 2010;59:645-654.
13. Jakubowski A, Ambrose C, Parr M, Lincecum JM, Wang MZ, Zheng TS, et al. TWEAK induces liver progenitor cell proliferation. J Clin Invest 2005;115:2330-2340.
14. Sasmono RT, Oceandy D, Pollard JW, Tong W, Pavli P, Wainwright BJ, et al. A macrophage colony-stimulating factor receptor-green fluorescent protein transgene is expressed throughout the mononuclear phagocyte system of the mouse. Blood 2003;101:1155-1163.
15. Sasmono RT, Ehrnsperger A, Cronau SL, Ravasi T, Kandane R, Hickey MJ, et al. Mouse neutrophilic granulocytes express mRNA encoding the macrophage colony-stimulating factor receptor (CSF-1R) as well as many other macrophage-specific transcripts and can transdifferentiate into macrophages in vitro in response to CSF-1. J Leukoc Biol 2007;82:111-123.
16. Duffield JS, Erwig LP, Wei X, Liew FY, Rees AJ, Savill JS. Activated macrophages direct apoptosis and suppress mitosis of mesangial cells. J Immunol 2000;164:2110-2119.
17. Pratt T, Sharp L, Nichols J, Price DJ, Mason JO. Embryonic stem cells and transgenic mice ubiquitously expressing a tau-tagged green fluorescent protein. Dev Biol 2000;228:19-28.
18. Kofman AV, Morgan G, Kirschenbaum A, Osbeck J, Hussain M, Swenson S, et al. Dose- and time-dependent oval cell reaction in acetaminophen-induced murine liver injury. HEPATOLOGY 2005;41:1252-1261.
19. Reddy GK, Enwemeka CS. A simplified method for the analysis of hydroxyproline in biological tissues. Clin Biochem 1996;29:225-229.
20. Hume DA. The mononuclear phagocyte system. Curr Opin Immunol 2006;18:49-53.
21. Crofton RW, Diesselhoff-den Dulk MM, van Furth R. The origin, kinetics, and characteristics of the Kupffer cells in the normal steady state. J Exp Med 1978;148:1-17.
22. Iredale JP, Benyon RC, Pickering J, McCullen M, Northrop M, Pawley S, et al. Mechanisms of spontaneous resolution of rat liver fibrosis. Hepatic stellate cell apoptosis and reduced hepatic expression of metalloproteinase inhibitors. J Clin Invest 1998;102:538-549.
23. Karlmark KR, Weiskirchen R, Zimmermann HW, Gassler N, Ginhoux F, Weber C, et al. Hepatic recruitment of the inflammatory Gr1+ monocyte subset upon liver injury promotes hepatic fibrosis. HEPATOLOGY 2009;50:261-274.
24. Harty MW, Papa EF, Huddleston HM, Young E, Nazareth S, Riley CA, et al. Hepatic macrophages promote the neutrophil-dependent resolution of fibrosis in repairing cholestatic rat livers. Surgery 2008;143:667-678.
25. Roderfeld M, Weiskirchen R, Wagner S, Berres ML, Henkel C, Grotzinger J, et al. Inhibition of hepatic fibrogenesis by matrix metalloproteinase-9 mutants in mice. FASEB J 2006;20:444-454.
26. Lan L, Chen Y, Sun C, Sun Q, Hu J, Li D. Transplantation of bone marrow-derived hepatocyte stem cells transduced with adenovirus-mediated IL-10 gene reverses liver fibrosis in rats. Transpl Int 2008;21:581-592.
27. Zhou X, Murphy FR, Gehdu N, Zhang J, Iredale JP, Benyon RC. Engagement of alphavbeta3 integrin regulates proliferation and apoptosis of hepatic stellate cells. J Biol Chem 2004;279:23996-24006.
28. Nakamura T, Torimura T, Sakamoto M, Hashimoto O, Taniguchi E, Inoue K, et al. Significance and therapeutic potential of endothelial progenitor cell transplantation in a cirrhotic liver rat model. Gastroenterology 2007;133:91-107.
29. Sobrevals L, Rodriguez C, Romero-Trevejo JL, Gondi G, Monreal I, Paneda A, et al. Insulin-like growth factor I gene transfer to cirrhotic liver induces fibrolysis and reduces fibrogenesis leading to cirrhosis reversion in rats. HEPATOLOGY 2010;51:912-921.
30. Kim JK, Park YN, Kim JS, Park MS, Paik YH, Seok JY, et al. Autologous bone marrow infusion activates the progenitor cell compartment in patients with advanced liver cirrhosis. Cell Transplant 2010;19:1237-1246.
31. Tirnitz-Parker JE, Viebahn CS, Jakubowski A, Klopcic BR, Olynyk JK, Yeoh GC, et al. Tumor necrosis factor-like weak inducer of apoptosis is a mitogen for liver progenitor cells. HEPATOLOGY 2010;52:291-302.
32. Kallis YN, Robson AJ, Fallowfield JA, Thomas HC, Alison MR, Wright NA, et al. Remodelling of extracellular matrix is a requirement for the hepatic progenitor cell response. Gut 2011;60:525-533.